INVESTIGATION OF EXO-NEURO-MUSCULO-SKELETON

WITH NEURAL-NETWORK-BASED EVALUATION FOR

ANKLE-FOOT REHABILITATION AFTER STROKE

YE FUQIANG

PhD

The Hong Kong Polytechnic University

2023

The Hong Kong Polytechnic University

Department of Biomedical Engineering

Investigation of Exo-neuro-musculo-skeleton with Neural-network-based Evaluation for Ankle-foot Rehabilitation after Stroke

Ye Fuqiang

A thesis submitted in partial fulfilment of the requirements for the degree of Doctor of Philosophy

August 2022

CERTIFICATE OF ORIGINALITY

I hereby declare that this thesis is my own work and that, to the best of my knowledge and belief, it reproduces no material previously published or written, nor material that has been accepted for the award of any other degree or diploma, except where due acknowledgement has been made in the text.

_____(Signed)

_____Ye Fuqiang_____ (Name of student)

ABSTRACT

Stroke is one of the primary causes of adult hemiplegia globally. Conventional motor recovery of the hemiparetic limb necessitates repeated and intensive training for stroke survivors. However, the current rehabilitation service for motor restoration after discharge from the hospital is insufficient, particularly for the ambulation ability. Although 60%–80% of stroke survivors can walk independently, most of them exhibit long-term gait disturbances, including high gait asymmetry, lower walking speed, inability to walk far, and being more likely to fall, which affect their mobility and integration into the community. Thus, more effective, and readily accessible rehabilitation services or methods are required to enhance the ambulation ability of chronic stroke survivors to improve their life quality. On the other hand, the evaluation of the training effects during neurorehabilitation is also a crucial issue, which is commonly conducted by a blinded assessor (e.g., professional physiotherapists). Clinical assessment is hard to obtain owing to the shorthanded situation in the current healthcare system, e.g., professional therapists. The surface electromyography (sEMG) signals driven quantitative and objective evaluations have been used to track the training effects, e.g., the co-contraction index (CI) of muscle pairs and activation level of individual muscle. However, these quantitative metrics are not available online and cannot be robustly correlated to clinical scores. The objectives of this study were: (1) development of a data-driven model involving sEMG for facilitating an objective and automated metric of training effects for poststroke rehabilitation

assisted by robots, (2) development of an exo-neuro-musculo-skeleton ankle-foot system with balance sensing feedback (ENMS-BF) for motor recovery of the paralyzed lower extremity after stroke, and (3) investigation of the assistive capability and rehabilitation effects of the proposed ENMS-BF on chronic stroke survivors, with both face-to-face individual training and remote self-help paired training. This study was implemented in three sections as follows:

In the first part, we constructed a backpropagation neural network (BPNN) model with the sEMG signals as the driven data, which matched the mapping relationship between the sEMG characteristics and commonly utilized clinical scales, i.e., the Modified Ashworth Scale (MAS) and the Fugl–Meyer Assessment (FMA). Twenty-nine individuals with chronic stroke completed a robot-assisted upper limb rehabilitation program, with the sEMG signals collected before and after the 20-session intervention. There were significant correlations (P<0.001) between the manually assessed and mapped FMA and MAS scores, within the labelled data captured before and after the intervention. The results showed that the proposed sEMG-driven model based on BPNN enables the automated tracking of motor recovery for chronic stroke survivors and demonstrated the potential to be applied in automated assessment post-stroke.

In the second section, we developed a novel ENMS-BF driven by plantar pressures to assist gait training by dynamic correction of foot drop and foot inversion. The ENMS-BF can be worn unilaterally onto the paretic lower limb with a weight of 0.47 kg. It consists of a soft-and-rigid musculoskeletal combination, i.e., musculoskeleton, two-channel neuromuscular

electrical stimulation (NMES), and a tactile vibrator. The properties of pressure-to-torque transmission of the musculoskeleton were measured quantitatively. The results showed that the ENMS-BF could effectively correct foot drop and foot inversion in the hemiparetic gait pattern.

In the third section, the feasibility and rehabilitative effects of the ENMS-BF-assisted gait training after stroke were evaluated. Twelve stroke survivors participated in the individual gait training with close supervision. Then, another 12 individuals with chronic stroke were recruited in self-help paired training based on a cyber physical social system (CPSS) for remote social links. The results indicated that the ENMS-BF assisted gait training was feasible and effective in improving the motor function, gait pattern, and plantar pressure of the paralyzed lower limb in both groups. The developed ENMS-BF combining with CPSS could effectively facilitate self-help gait training with remote management and peer support.

In conclusion, the developed sEMG-driven model based on BPNN could facilitate the automated assessment of motor function recovery post-stroke. The developed ENMS-BF could assist in ankle dorsiflexion and self-correction of foot inversion during gait training. The ENMS-BF-assisted individual gait training was effective for improvements of lower limb motor function, gait pattern, and plantar balance in the paralyzed limb post-stroke. Based on the CPSS, the ENMS-BF-assisted paired training could support and facilitate self-help rehabilitation with professional management and social links with peers remotely.

PUBLICATIONS ARISING FROM THE THESIS

Journal Publications

(1) **<u>F.Q. Ye</u>**, B.B. Yang, C.Y. Nam, Y.N. Xie, F. Chen, and X.L. Hu. A Data-Driven Investigation on Surface Electromyography Based Clinical Assessment in Chronic Stroke. Frontiers in Neurorobotics, 2021, 15. DOI: 10.3389/fnbot.2021.648855.

(2) C.Y. Nam, B.B. Zhang, T. Chow, **<u>F.Q. Ye</u>**, Y.H. Huang, Z.Q. GUO, W.M. Li, W. Rong, X.L. Hu, W.S. Poon. Home-based Self-help Telerehabilitation of the Upper Limb Assisted by An Electromyography-driven Wrist/hand Exoneuromusculoskeleton after Stroke. Journal of NeuroEngineering and Rehabilitation, 2021, 18(1), 137. DOI: 10.1186/s12984-021-00930-3.

(3) J.N. Zhang, Y.H. Huang, **<u>F.Q. Ye</u>**, B.B. Yang, Z.Y. Li, and X.L. Hu. Evaluation of Post-Stroke Impairment in Fine Tactile Sensation by Electroencephalography (EEG)-Based Machine Learning. Applied Sciences, 2022, 12(9). DOI: 10.3390/app12094796.

(4) S. Zhou, **<u>F.Q. Ye,</u>** N. Chan, J. Song, Y.F. Han, X.L. Hu, F. Chen, and Y.P. Zheng. Integrated Sensorimotor Evaluation of Cortical Reorganization after Stroke with Sensory-/motor-level Neuromuscular Electrical Stimulation (NMES) and Electroencephalography (EEG). Computer Methods and Programs in Biomedicine, 2022, Under Review.

Conference publications and presentations

(1) **F.Q. Ye**, C.Y. Nam, W.M. Li, W. Rong, F. Chen, X.L. Hu. A Data-Driven Investigation on Surface Electromyogram based Clinical Assessment in Chronic Stroke. IEEE EMBS Hong Kong-Macau Joint Chapter Student Competition 2021.

(2) **F.Q. Ye**, Z.X. Liu, F. Chen. Non-intrusive Intelligibility Prediction of Noise-suppressed Speech Based on Neural Network. The 31st Wireless and Optimal Communication Conference 2022.

Patent

(1) X.L. Hu, **F.Q. Ye**, W.M. Li, W. Rong, K.T. Wong, T.C. Cheung, M.K. Pang, H.W. Wai, Gait Event-driven Phase-dependent and Multi-modal Foot Rehabilitation System and Use Method Thereof, WIPO/PCT, The Hong Kong Polytechnic University, Application number: WO2023/273324 A1.

ACKNOWLEDGEMENTS

TABLE OF CONTENTS

LIST OF FIGURES

LIST OF TABLES

LIST OF ABBREVIATIONS

A/D	Analog to Digital
AFO	Ankle Foot Orthoses
ANOVA	Analysis of Variance
APB	Abductor Pollicis Brevis
APP	Application
ARAT	Action Research Arm Test
BBS	Berg Balance Scale
BIC	Biceps Brachii
BPNN	Backpropagation Neural Network
CI	Co-Contraction Index
CPN	Common Peroneal Nerve
CPSS	Cyber Physical Social System
CVA	Cerebrovascular Accident
ED	Extensor Digitorum
ENMS-BF	Exo-neuro-musculo-skeleton Ankle-foot System with
FAC	Functional Ambulatory Category
FD	Flexor Digitorum
FMA	Fugl–Meyer Assessment
FMA-SE	Fugl–Meyer Assessment for Shoulder/Elbow

FMA-WH	Fugl–Meyer Assessment for Wrist/Hand
FSRs	Force Sensitive Resistors
GRFs	Ground Reaction Forces
GA	Gastrocnemius
LF	Lateral Forefoot
LM	Lateral Midfoot
LR	Lateral Rearfoot
MAS	Modified Ashworth Scale
MAV	Mean Absolute Value
MDC	Minimal Detectable Change
MF	Medial Forefoot
MM	Medial Midfoot
MR	Medial Rearfoot
MMSE	Mini-Mental State Examination
MSS	Motors Status Scale
NMES	Neuromuscular Electrical Stimulation
PVC	Polyvinyl Chloride
RMS	Root Mean Square
ROM	Range Of Motion
sEMG	Surface Electromyography

SD	Standard Deviations
SPSS	Statistical Package for Social Science
SSC	Slope Sign Change
TA	Tibialis Anterior
TRI	Triceps Brachii
WL	Wavelength
ZC	Zero Crossing

LIST OF APPENDICES

CHAPTER 1

INTRODUCTION

1.1 Background

Stroke is one of the primary causes of disability in adults [1]. By 2016, there were

approximately 300,000 stroke survivors in Hong Kong and over 8 million in Chinese mainland.

From 2009 to 2016, the population of stroke exhibited an upward trend with an annual of two

million new cases in HK and a growth of 8% per year in Mainland China [2]. Globally, by

2019, the accumulated number of survivors suffering from chronic stroke was around 102

million, with ~77 million survivors suffering from ischemic stroke and ~25 million survivors

caused by hemorrhage [3]. In contrast to the growing stroke population, resources in the

rehabilitation industry (e.g., professional therapists and the length of hospital stay) are limited

even in developed countries [4].

Upper limb deficits were present in around 80% of stroke survivors [5], limiting their

independence in daily living. Moreover, although 60%-80% of stroke survivors can walk

independently, the majority of them suffer from long-term gait problems, such as significant

gait asymmetry, walking slowly, cannot walk far, and are more prone to stumble, limiting their

mobility and integration into the community [6]. Voluntary, extensive, and repetitive practice

on paretic limbs throughout the subacute and chronic periods is required for effective

1

neurorehabilitation after stroke [7]. Although traditional rehabilitation assumed that significant motor recovery predominantly appears in the acute and subacute periods, i.e., within six months following the occurrence of stroke [6] [7], some studies have found that after the first six months, i.e., in the chronic stroke period, significant improvements of motor function can also be accomplished through rehabilitation training with the same intensity as that provided in the subacute period [8] [9]. Unfortunately, due to a shortage of professional labor in the current healthcare system, discharged stroke survivors usually find it difficult to acquire regular and intensive physical training. For public hospitals in Hong Kong, regular rehabilitative training was usually provided within the first year following a stroke, comprising physiotherapeutic services in hospital stay for 3–4 weeks and twice-weekly out-patient services [10]. In the current inpatient lower limb rehabilitation, Significant improvements in motor recovery are primarily achieved at the hip and knee (i.e., the proximal joints), which is associated with the sequence of proximal to distal joints in spontaneous motor recovery during the early phase of stroke. The motor recovery can be enhanced by voluntary physical training during the hospital stay. However, most stroke survivors do not obtain sufficient spontaneous motor recovery at the distal joints, i.e., the ankle and foot, when they are discharged from the hospital, making voluntary physical activity at these joints challenging in early rehabilitation while they are in the hospital. This results in commonly observed muscle weakness of ankle dorsiflexors and increased spasticity in the plantar flexors [11], leading to the degradation of the gait pattern

2

later, for example, high muscular co-contraction in the paralyzed limb, low balance due to asymmetry between the two limbs, high consumption of energy, and high risk of falling [12] [13].

1.2 Device-assisted Rehabilitation of Lower Limb

Due to the requirement of physical training with high intensity and repeatability, long-term physical therapy post-stroke is time-and-labor consuming and challenging for both the therapists and the stroke survivors. Thus, various rehabilitation devices have been designed to aid during hemiplegic walking. Passive ankle foot orthoses (AFO) have been commonly used in conventional ankle foot rehabilitation post-stroke to avoid foot drop and foot inversion with a preset joint angle at the ankle [11]. However, excessive usage of passive AFO could be associated with muscular disuse atrophy because that stroke survivors with the long-term wearing of AFOs could eventually rely on mechanical fixation instead of stabilizing and strengthening the joints with their own muscular efforts. Thus, for the motor restoration of the distal joint, i.e., ankle joint, advanced solutions with flexible and necessary assistance are needed to improve the muscle coordination at the ankle complex.

1.2.1 Neuromuscular Electrical Stimulation (NMES)

One of the alternative solutions to assist in the hemiplegic walking is NMES, which mimics nerve-to-muscle stimulation. Repetitive sensorimotor experiences would be generated by

cyclic stimulations from the NMES, which could enhance the impaired muscle and activate more neuroplasticity pathways [14]. In the previous studies of stroke rehabilitation, two-channel NMES on the target muscles of ankle dorsiflexion and plantarflexion have been applied in the correction of foot drop post-stroke with improved muscular coordination [15]. Moreover, it was also found that 30-min NMES on the plantar flexors could effectively release the muscular spasticity for individuals with chronic stroke [16]. However, due to a lack control of foot inversion in the frontal plane, NMES alone is hard to achieve accurate kinematic qualities post-stroke, e.g., correction of foot inversion, which has been found as a leading cause of muscular discoordination of the ankle joint [17]. Additionally, assisted by the robot, mechanical torque at the target joint could be provided with specific kinematics features using actuators to correct foot drop and foot inversion.

1.2.2 Robot-assisted Rehabilitation

Currently, various exoskeletal robots for restoration of lower limb motor function post-stroke have been developed [18], providing powerful mechanical support for the large and proximal joints, e.g., the hip and knee joints. However, these robots are mainly for patients with paraplegia, e.g., spinal cord injury, with a bilateral design [19] [20]. Thus, they are bulky for the lower limb motor recovery post-stroke, and could hardly facilitate motor relearning after stroke, which requires assistance-as-necessary for the goal to walk without external aids [13]. Later, unilateral exoskeletal robots were developed for lower limb motor relearning post-stroke

[21] [22] [23] with the necessary assistance on the affected side. However, these unilateral robots introduced extra and unbalanced weight at the paretic limb, which could generate mechanical imbalance load during the swing phase. More recently, soft robots with attempts of pneumatic muscles [24] and Bolden cable systems [25] [26] have gained more attention. However, for the pneumatic actuated and Bolden cable-powered robot [24] [25], an external cable connected to the power unit at the waist could affect the relearning of the gait pattern. Moreover, no rehabilitation effects of these robots [24] [26] have been reported in motor recovery post-stroke. Meanwhile, the exosuit [25] provides assistance for ankle dorsiflexion and plantarflexion in the sagittal plane, neglecting the correction of foot inversion in the frontal plane. Biofeedback has been found effective in the correction of foot inversion during gait training after stroke [27] [28], while biofeedback only cannot correct foot drop during the motor relearning after stroke. Thus, a more lightweight, and compact design of the robot is desirable for correction of both foot drop and foot inversion after stroke. It has been found that social interactions during the therapy of stroke training are necessary and beneficial for stroke survivors engaging in long-term rehabilitation [29]. Up to now, no attempt of integrating the robot with social interactions has been reported in the self-help motor recovery of lower limb post-stroke.

1.3 Assessment of motor function post-stroke

1.3.1 Clinical Assessment

In addition to the repetitive and intensive rehabilitation, assessments of training effects are also crucial for motor recovery post-stroke. Clinical assessments manually marked by a professional assessor are commonly adopted to evaluate training effects before and after the intervention related to robot-assisted rehabilitation. For example, the Action Research Arm Test (ARAT) [31], the Fugl–Meyer Assessment (FMA) [30], the Modified Ashworth Scale (MAS) [32], and the Motors Status Scale (MSS) [33] for upper limb assessment following stroke. Among these clinical scales, FMA was commonly used as the primary outcome for the track of motor function improvements, and MAS was widely adopted as the secondary outcome to assess the changes in muscular spasticity post-stroke [34]. FMA is deemed precise and responsive for the assessment of motor performance following stroke. The FMA scale of upper limb owns 66 points in total, which can be spilt into 42 points for the shoulder and elbow sections, and 24 points for the wrist and hand parts. Moreover, the FMA lower limb scale has a total of 34 points. The MAS is a quantified metric of the passively stretched soft tissues, which generates ranked scores at 0, 1, 1+, 2, 3, and 4. For the clinical assessment of lower limb motor function, in addition to the commonly used FMA and MAS, the 10-Meter Walk Test (10MWT) [35], the Berg Balance Scale (BBS) [36], and the Functional Ambulatory Category (FAC) [37] are also widely used clinical assessments of ambulation and balance post-stroke. Although clinical

assessments remain the "golden standard" for assessing training effects of motor recovery [38], these clinical measurements are performed manually by professional therapists, which is confined by the limited professional manpower in the current medical system. The data-driven automated assessments are desirable as the objective metrics of training effects during the long-term robot-assisted rehabilitation post-stroke.

1.3.2 Data-driven Automated Assessment

Data-driven automated assessments are the potential to track the effectiveness of long-term rehabilitation, with less time- and labor-consumption of professional therapists in comparison to the subjective clinical assessment. In the previous studies, the complex interactions between the kinematic data and clinical scales were investigated with the neural network [39] [40], which had the satisfying performance of nonlinear mapping. However, these kinematic data-based automated assessments neglected the intrinsic muscle activities, e.g., surface electromyography (sEMG) which were related to the muscular coordination in the upper extremity movements. More recently, multi-modal models combining the kinematic and sEMG data have been developed to quantitatively measure the motor rehabilitation of the impaired upper limb during long-term rehabilitation following stroke [41] [42]. However, the predicted scores produced by the model were different from manually marked scores, which could be hardly accepted by the professionals [38]. Moreover, sEMG-based quantified measurement has been attempted to track motor recovery during long-term rehabilitation. For example, previous

studies have employed sEMG to predict muscle force [43], monitor neuromuscular changes [44] [45], and detect muscle fatigue [46]. Particularly, in our previous studies, improvements in motor recovery of the upper extremity were measured based on sEMG data during the robot-assisted rehabilitation post-stroke [44] [47] [48] [49] [50]. Parameters of the co-contraction index (CI) and activation level were calculated from sEMG data to monitor the muscular spasticity and coordination throughout the long-term program of rehabilitation for individuals with chronic stroke. Nevertheless, the calculated and modified metrics from the sEMG are still not practicable and acceptable in the clinical application since the interpretation of the mathematical parameters from the sEMG data can be difficult for clinical professionals [51]. Therefore, a data-driven automated assessment directly mapping the sEMG data to manually marked scores is desirable for tracking motor recovery in the long-term poststroke rehabilitation assisted by robots.

1.4 Objectives of this study

In summary, due to the shortage of professional therapists in the current healthcare system, device-assisted rehabilitation with intensive and repetitive training is in high demand for individuals with chronic stroke to restore lower limb motor functions. However, current device/technique, e.g., AFO, NMES, and the designed robots, could not well satisfy the motor relearning of lower limb post-stroke, which required a lightweight and compact designed robot, the advanced control of muscular coordination, and necessary assistance in foot drop and foot

inversion during the dynamic ambulation training. On the other hand, even with robot-assisted rehabilitation, clinical assessments of training effects are also limited by the shortage of professional manpower. Meanwhile, clinical applications have been hindered due to the deficient interpretation of sEMG signals to clinical operators. Thus, automated assessment, which can directly map the sEMG data to manually marked scores, is of great significance in self-help robot-assisted rehabilitation. Thus, objectives of this study could be summarized as:

(1) To propose a novel data-driven model based on sEMG data during a robotic-hand-assisted training for individuals with chronic stroke, mapping sEMG data to the commonly adopted clinical scores, i.e., MAS and FMA.

(2) To develop the lightweight, and compact designed exo-neuro-musculo-skeleton ankle-foot system with balance sensing feedback (ENMS-BF) for correction of foot drop and foot inversion post-stroke, and to examine the assisting capability of the ENMS-BF.

(3) To explore the feasibility and rehabilitation effects of the developed ENMS-BF-assisted individual gait training, and to validate the viability and effectiveness of the cyber physical social system (CPSS) based self-help paired training, with assistance from the developed NMES-BF, remote monitoring, and cyber social links.

CHAPTER 2

A DATA-DRIVEN INVESTIGATION ON SURFACE ELECTROMYOGRAPHY (SEMG) BASED CLINICAL ASSESSMENT IN CHRONIC STROKE

2.1 Introduction

As one of the principal etiologies underlying impairment of upper extremity function, stroke, i.e., the cerebrovascular accident (CVA), impacts approximately 15 million people per year globally [52]. For those chronic stroke survivors, i.e., with the manifestation of 6 months following the vascular insult, 65% of them cannot use the paralyzed hand for routine daily activities [53]. Motor recovery of the impaired upper limb following a CVA could be enhanced by voluntary, reiterated, and intensive physical practice [54]. Traditional rehabilitation facilities are based on one-to-one and in-person interventions; current healthcare manpower is limited for the rapidly rising numbers of chronic stroke survivors [55].

The stress on professional manpower could be reduced by the implementation of robot-assisted rehabilitation systems, which could offer ongoing reiterative and intensive therapeutic interventions post-stroke [56]. Numerous robotic systems have been designed with feasibility tests and proven efficacious for the recovery of upper extremity motor functions, including HapticKnob [57], Haptic Master [58] and Robotic Hands [48]. Robot-assisted rehabilitation

systems, that are voluntary effort-based for chronic stroke survivors, detect the intention activities from remaining neuromuscular pathways. With the voluntary effort-based training, return of motor function could be enhanced, which was demonstrated more sustainable in comparison to passive robot-assisted interventions that lack voluntary endeavors [59, 60].

Voluntary effort can be reflected by surface electromyography (sEMG), which has sufficient sensitivity to detect muscular activities. The assistance mechanism driven by sEMG is commonly implemented in the developments of robots for stroke rehabilitation in order to promote contributions of active motions in the physical training [61, 62]. Earlier publications from our team have reported a series of robot-assisted systems driven by sEMG signal for the rehabilitation of individuals with chronic stroke, and the sEMG-driven robots have been demonstrated to facilitate the return of motor functions of the upper limb [47, 48].

To assess the rehabilitation outcome following physical training, clinical assessments should be conducted prior to and following the rehabilitation program. Several clinical scales have been widely employed for the quantitative appraisal of activities and motor functions for the upper extremity, encompassing the Action Research Arm Test (ARAT) [31], the Fugl–Meyer Assessment score (FMA) [30], the Motors Status Scale (MSS) [33], and the Modified Ashworth Scale (MAS) [32]. Among these, the most commonly utilized scales include the FMA and MAS, which provide clinical interpretations of the motor recovery and alterations in the muscle spasticity [34, 44, 63]. Such clinical measurements are regarded as the benchmark

standards for tracking the outcome of stroke rehabilitation programs [38]. However, these clinical assessments depend on professional operators conducting the measurements, which is costly in time and the manpower required. An alternative solution for managing the rapidly rising need of clinical assessments is the automated rehabilitation process, which can manage and optimize the rehabilitation quality. Taking these elements into consideration, automated assessments are necessary and desirable to monitor the effectiveness of long-term robot-aided training program for individuals with chronic stroke.

The advantages of automated assessments include a decrease of required professional manpower, a programmed method to yield rapid measures of motor recovery, and assistance in diagnostic to facilitate customized treatment. Recently, there has been considerable interest in the involvement of bioinformatic information to implement automated evaluations. Automated assessments based on the kinematic data have been designed, with the clinical scales as their development standards, and the kinematic data of upper limb captured by motion capture systems as the driving data feeding into the system. For instance, the complicated interaction between kinematic information and the clinical scales has been identified by the application of neural networks [39, 40], support vector machines [40] and extreme learning machines [64]. Nevertheless, assessments driven by kinematic data were found to have a major restriction in that they overlooked inherent muscular activity, i.e., the sEMG signals, which initiated upper limb motion [38]. More recently, multi-modal fusion systems have been designed, which

integrate kinematic data with specific muscle information, e.g., sEMG data, to track motor

recovery in the impaired upper extremity in this context of stroke from a quantitative

perspective. These multi-modal fusion automated assessments exhibited a significant

correlation between the outcomes and the routine clinical scores [41, 42]. However, a modified

scale was utilized for the outcomes of the multi-modality fusion system, which was at variance

with the clinical scale, e.g., FMA scores, so that professional therapists could hardly accept the

modified metric without additional clinical verification [38]. Additionally, clinical therapists

found it complex to operate the added devices for capturing human kinematic information, so

in reality, the temporal, financial and labor advantages of these kinematic data-driven

assessments were limited [39, 40, 42, 64].

The usage of sEMG to provide quantitative measurements on the restoration of motor functions

is a novel strategy. Previous applications of sEMG have been investigated to study the

pathophysiology [65], to monitor neuromuscular alterations [44, 45], to predict muscle force

[43], and to recognize muscle fatigue [46]. In our earlier studies, two quantitative metrics

obtained from sEMG data, i.e. the level of muscle activation reflecting muscular spasticity, and

the contraction index, CI, which could describe co-activation patterns, were used to assess

motor function recovery during sEMG-driven robot-assisted rehabilitation [44, 47-49, 62, 66].

Additionally, Fuzzy approximate entropy has been proposed as a metric to explore the

complexity of sEMG signals in the surveillance of functional motor restoration during robot-

assisted rehabilitation [67]. It was demonstrated that, for chronic stroke survivors, the sEMG

signal could offer a quantitative interpretation of the impact of sEMG-driven robot-assisted

rehabilitation intervention. However, a limitation of these sEMG-based assessments was that

only mathematical derivations from the sEMG data were used to indicate motor function

improvement; the outcomes were not directly correlated with clinical scores, which severely

restricted the clinical utilities by professional therapists. A critical impediment to the use of

sEMG by clinical personnel is the lacking of proper interpretation on sEMG signals [51].

Although multi-factor regression analysis can be explicated using a multiple linear regression

model, a more applicable method for sEMG signal analysis is the backpropagation neural

network (BPNN). The compatibility of BPNN is greater than the linear regression model when

there is significant heterogeneity among the input data, e.g., extremities, nonlinearity, and

missing values [68]. Moreover, the BPNN performed better for non-linear regression processes

in comparison to the linear regression model [69].

Regression mapping tasks related to sEMG data have been solved by BPNN, e.g. joint angle

approximation [70, 71] and sketching pattern recognition [72]; thus, it appeared promising that

BPNN could map sEMG information to clinical scales. Recently, a novel technique for the

assessment of muscular spasticity has been proposed, which mapped the sEMG information to

MAS using an adaptive neuro fuzzy inference system; notable precision was demonstrated

between the regression output and the manually assessed MAS scores [73]. Nevertheless, this

14

robotized process solely concentrated on quantified assessments of muscle tensions, neglecting the evaluation of recovery of voluntary motor functions, which was usually measured using FMA during clinical assessment. Furthermore, this strategy necessitated reiterated passive stretches carried out by physical therapists to obtain the sEMG information, therefore, it was inappropriate for an automated evaluation of the restoration of motor functions. To the best of our knowledge, the mapping relationship between sEMG information to the traditional scales, e.g., FMA and MAS, has not been studied for the robotized evaluation during robot-aided rehabilitation post-stroke.

In conclusion, this chapter aims to propose a BPNN model driven by sEMG data, to match the relationship between sEMG properties and the commonly employed clinical scores, i.e., MAS and FMA scales, during robot-aided training in individuals with chronic stroke. The configurations and framework of the BPNN model are explained in Section 2.2. The experiment results and discussion are present in Section 2.3 and 2.4, respectively. The periodic conclusion is presented in Section 2.5.

2.2 Methodology

Participants suffering from chronic stroke were enrolled in a robot-assisted intervention program comprising 20-session sEMG-based training assisted by robotic hand. This intervention program was carried out at Hong Kong Polytechnic University's neurorehabilitation laboratory. Prior to and following the intervention, clinical assessments

Table 2-1. Demographic information for participants in the pilot trial.

participant no.	Gender (female /male)	Stroke type (hemorrhagic /Ischemia)	Side of hemiparesis (left/right)	Age (years) mean±SD	Years after onset of stroke mean ± SD
29	6/23	12/17	17/12	58.7±8.3	7.1±4.0

were carried out and sEMG data in an objective evaluation was acquired. The manually acquired clinical scores and corresponding sEMG signals formed the datasets, which were further used to construct a BPNN model driven by sEMG to explore the relationship between the manually marked clinical scales and sEMG properties.

2.2.1 Recruitment of Subjects

The Hong Kong Polytechnic University's Human Subjects Ethics Committee authorized the ethical approval for this study. All subjects were provided with and signed the written informed consent before involved in this research. A total of 29 participants suffering from stroke participated in the training program, all of whom satisfied the criteria for inclusion: (i) 18-78 years of age; (ii) at least 6 months since the initial occurrence of cerebral lesion; (iii) capable for passive extension of the digit metacarpophalangeal and interphalangeal finger joints to 170°; (iv) with muscular spasticity assessed by MAS $\leqslant$ 3 at the finger, wrist and elbow articulations; (v) FMA score: 15<FMA<45, indicating moderate-severee motor deficits in the paralyzed upper limb; (vi) cognitively intact, i.e., mini-mental state examination assessment score >21;
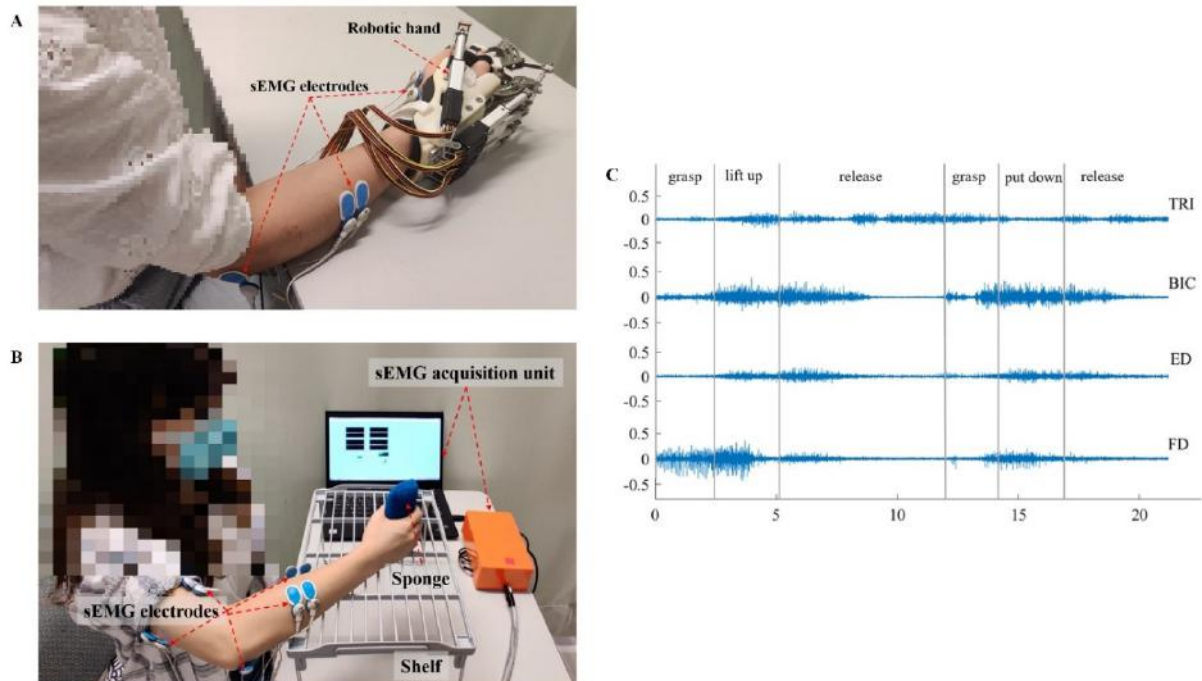
Figure 2-1. The Setup of experiments and sEMG signal samples. (a) Training assisted by the sEMG-driven robotic hand. (b) Data acquisition system in the bare hand reaching task (vertical). (c) Raw sEMG samples of four muscles, i.e., ED, TRI, FD, and BIC, within the evaluation task. The experiment operator manually marked each movement and pause periods.

and (vii) showing the presence of voluntary sEMG signals, defined as 3*standard deviations (SD) higher than mean values of sEMG signal in resting state, within the target musculature of the paretic limb, i.e., extensor digitorum (ED), triceps brachii (TRI), flexor digitorum (FD), and biceps brachii (BIC) . The participants' statistical profiles are presented in Table 2-1.

2.2.2 Intervention aided by Robotic Hand

Figure 2-1a presents an illustration of the robotic-hand triggered by sEMG employed for upper

limb training. Mechanical aid of flexion and extension at the finger joints in the paralyzed upper limb could be provided from the robotic hand. The assistance mechanism was triggered by real-time sEMG data. ED and APB (abductor pollicis brevis) muscle-derived sEMG data were exploited as voluntary intention to commence assistance from the robotic hand for the consecutive and periodical upper extremity motions, i.e., opening and clenching the hand. When the robotic hand had been initiated, the patient needed to make no further effort, which was defined as the sEMG-triggered mode. The triggering threshold for mechanical assistance was established as three times SD of the baseline sEMG signal during rest period. The detailed description of the control mechanism has been shown in our earlier studies [47, 48, 50]. All participants were assigned to the robot-assisted intervention, which consisted of 20 sessions with aids from the sEMG-triggered robotic hand, with the intensity of 3–5 sessions every week within 6 successive weeks. Individual session of robot-assisted intervention necessitated the subjects to carry out two sets of 30-minute tasks, comprising lateral and vertical upper limb grasping and reaching motions owing a 10-minute rest period in the interval of the two assignments to circumvent the muscles becoming exhausted, as discussed previously [48]. The electrodes for collecting sEMG (Blue Sensor N, Ambu Inc., 20 x 30 mm in size) were positioned on the skin in pairs with their centers 2 cm apart, which is consistent with the description published by Cram [74]. The sampling rate of the collected sEMG data (DAQ, 6218 NI DAQ card; National Instruments Corp.) was 1000 Hz. A preamplifier (INA 333; Texas

Instruments Inc.,) was used for achieving a 1000 times signal amplification and to facilitate online computation of sEMG level at the target muscles to trigger the aids from the robotic system [47].

2.2.3 Clinical Assessment

The FMA and MAS scores were used for the clinical assessment of each participant prior to and following the 20-session robot-assisted rehabilitation. In this study, primary and secondary outcomes were defined as FMA and MAS, respectively, in keeping with previous work [40], [75]. The high sensitivity and responsiveness of FMA to identify functional alterations of the upper extremity motion, making it become the primary outcome in clinical investigation of rehabilitation after stroke [30, 34]. The FMA score could be subdivided into scores for the wrist/hand (FMA-WH)and for the shoulder/elbow (FMA-SE) of 24 and 42, respectively, which summed to be a total FMA score of 66 [75]. These sub-scores provided more detailed information regarding the distal versus proximal distribution of paralysis in upper limb motor functions [76]. Independent from the FMA, the MAS score was applied for the quantification of muscular spasticity associated with the involuntary contraction of muscle post-stroke [34]. A professional therapist conducted the measurement of the passive ranges of motion for extension and flexion of the finger, wrist, and elbow articulations, with a scale of 0, 1, 1+ (represented by 1.4 in this study), 2, 3, and 4 [34, 77]. The clinical assessments of MAS and FMA were conducted by the same blinded and experienced operator who was unknown about

the purpose in this study and any details regarding the research.

2.2.4 Evaluation Tasks for sEMG Acquisition

Except for the clinical assessments of MAS and FMA, sEMG signals were recorded in evaluation tasks. For the evaluation task for collecting sEMG, four movements were studied, including finger extension and flexion, and elbow extension and flexion as the objective measurement before and after the robot-aided training [47]. During the evaluation task, the corresponding sEMG signals at the ED, TRI, FD, and BIC, were captured as objective bioinformation. It was anticipated that there would be some extent of compensatory muscle activity within the four muscles, as it is commonly observed for individuals with chronic stroke [77-79]. Supervised machine learning was employed to enter the sEMG data to the proposed BPNN model (ED, TRI, FD, and BIC), and thus, construct the mapping association between the manually marked scores and the properties of sEMG.

For each evaluation session of sEMG acquisition, the subject was invited to sit in front of a table with a distance of 0.3-0.4 meters separating their shoulder from the table surface (Figure 2-1b). Voluntary muscle contraction was observed whilst the subject carried out the bare hand assessment task. During the evaluation task, the sEMG data were captured from the targeted musculature with a sampling rate of 1k Hz. The bare hand assessment comprised grasping a 30 g sponge which was 5 cm in depth, positioning it at the center of a lower shelf, lifting it vertically for 17 cm and placing it centrally on the upper shelf. Then, the participant was

instructed to retrieve and return it to its initial point, next, to perform the bare hand reaching task with their natural and comfortable speed. Three trials were repeated separated by a 2-minute rest period to mitigate against muscular fatigue. The commencement of sEMG signal recording was the point at which the participant contacted the sponge; the recording was concluded when the participant fully put the sponge to its initial position and loosen his/her hand. These bare hand tasks were closely observed and timed by an experimental operator. Previous work has demonstrated that most chronic stroke survivors were able to take hold of the sponge but were unable to release it owing to the spasticity at flexors [47]. Ten seconds was set as the time limit, since that some individuals with chronic stroke could assist their paretic limbs to take off the sponge with the unaffected limb. Since the paralyzed upper limb could exhibit weakness and impaired coordination post-stroke, pauses and movement reiterations were permitted. During the recoding of sEMG data, the experimental operator manually marked the pause points. These pause period of sEMG signals were subsequently removed during offline post-processing. A recording sample of sEMG during the vertical evaluation task is illustrated in Figure 2-1c.

2.2.5 Data Preparation

Following manual elimination of pause periods during the assessment, the sEMG trials owned a mean length of 30.92 ± 9.93 s, with a range of $9.8 - 51.8$ s. The large deviation of the time-consuming was related to the fact that nine participants exhibited improvements in their

performance rate following the 20-session robot-assisted intervention, whereas in others, their motion speed remained unchanged. Offline processing of the sEMG data included filtering by a 10-500 Hz band-pass filter (fourth-order Butterworth filter), together with a notch filter at 50 Hz (MATLAB, 2019b). Then, the filtered data were input into the constructed model. The mapping associations of sEMG data with the FMA-SE and FMA-WH score subsets and the MAS scores (at the finger, wrist, and elbow articulations) were investigated. Additional fourth-order Butterworth lower-pass filtering with cutoff frequencies at 150, 200, 300, 400, and 500 Hz was implemented within the mapping of MAS. It was conducted to investigate the mapping performance using an efficient frequency component of sEMG, to represent the characteristics mostly associated with delayed involuntary contractures in a paralyzed muscle

with muscular tension following stroke [80].

During offline processing, sEMG data for each trial were segmented into specific time intervals, each comprising 400 ms with an overlap of 200 ms, which was consistent with the previous study [81] to generate a balance between the requisite information of sEMG data for the interpretation of muscle activities and the sEMG interval stationarity. For the individual 400 ms sEMG intervals, verification of their wide-sense stationarity was performed to ensure that the average and autocorrelation function were time-invariant [82]. The segmented sEMG signals were then used to extract features and investigate the mapping association between the manually marked clinical scales, i.e., FMA-SE, FMA-WH, and MASs (including elbow, wrist,

and finger joints) and the sEMG properties.

According to the Pareto principle, the sEMG interval data were split into two sets; In each trial, 80% and 20% of sEMG epochs were utilized as the training and testing samples, respectively [83, 84]. The sEMG epochs from a participant's sEMG trial were mapped to the manually marked scores obtained in the related assessment of the participant, i.e., prior to and following the robot-aided training. A cross-validation with 5-fold approach was utilized to make sure that each epoch was also fully used as testing samples. Then, the averaged results within testing dataset across the 5-fold was taken as general output of the model [85]. Figure 2-2a depicts the workflow of the preparation of the sEMG data and the sEMG-driven BPNN model.
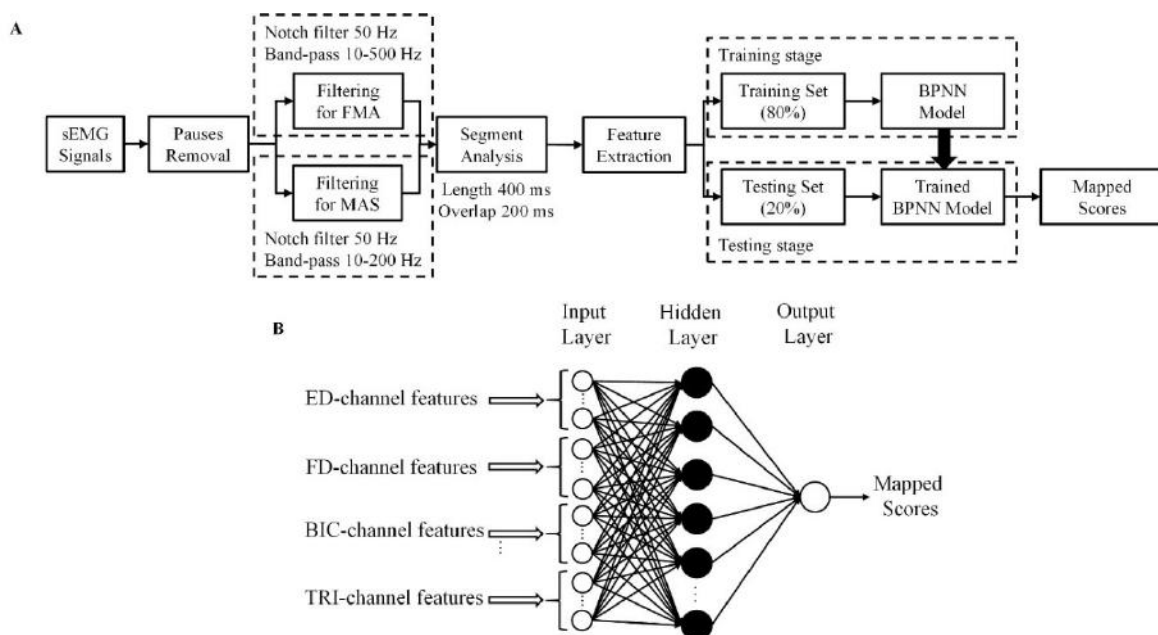
Figure 2-2. (a) Flowchart of signal processing in the proposed model. (b) Diagram of the constructed data-driven model, i.e., a backpropagation neural network (BPNN) with three layers.

23

2.2.6 The Data-driven Model based on sEMG

Based on the BPNN, an sEMG-driven model was developed following four phases: (i) sEMG feature extraction; (ii) BPNN model setup; (iii) hidden layer configurations; and (iv) selection of sEMG features.

(I) EMG Feature Extraction

The identification of dynamic muscle activity has been underpinned by a number of abstracted temporal sEMG signal characteristics [86, 87], including mean absolute value (MAV), slope sign change (SSC), wavelength (WL), root mean square (RMS), and zero crossing (ZC) are commonly utilized [88]. Among these, WL, RMS, and MAV principally reflect the sEMG amplitude intensity which varies with real-time muscle contraction [87], and is generally presumed to correlate with the force of the contraction [89]. The rate of signal variance is indicated by SSC and ZC, which represent neural firing information. Thus, SSC and ZC have been employed to estimate the firing rate of motor units in the dynamic muscle contraction [90, 91]. These characteristics can be expressed mathematically by the equations below, where $x(t)$ indicates the signal in time domain, and T reflects the number of samples in a single epoch (i.e., 400).

RMS principally represents the absolute values in magnitude of sEMG signals and can be described by:

$$RMS(x) = \sqrt{\frac{1}{T}\sum_{t=1}^{T} x^2(t)}. \tag{1}$$

Taking the absolute value of the sEMG signals $x(t)$ as the average, the MAV computation

can be obtained as given in Equation 2:

$$MAV(x) = \frac{1}{T}\sum_{t=1}^{T}|x(t)|. \tag{2}$$

The frequency of the zero axis crossing by the sEMG signal amplitude value is given by ZC,

which can be written as:

$$\begin{cases} ZC(x) = \sum_{t=1}^{T-1}(sign(x(t+1) \times x(t)) \cap |x(t) - x(t+1) \geq 0|) \\ sign(x) = \begin{cases} 1, & if \ x \geq 0 \\ 0, & else \end{cases} \end{cases}. \tag{3}$$

The frequency of sign changes in the sEMG signal slope is quantified by SSC, which can be

computed using Equation 4:

$$\begin{cases} SSC(x) = \sum_{t=2}^{T-1} f((x(t) - x(t-1)) \times (x(t) - x(t+1))) \\ f(x) = \begin{cases} 1, if \ x \geq 0 \\ 0, & else \end{cases} \end{cases}. \tag{4}$$

A cumulative parameter of the signal length, WL, is described by Equation 5:

$$WL = \frac{1}{T}\sum_{t=1}^{T-1}|x(t+1) - x(t)|. \tag{5}$$

These five features listed above were retrieved from the segmented sEMG signal of each

muscle and used as inputs for the data-driven model.

(II) BPNN Model Setup

The BPNN was constructed with a three-layer structure, i.e., output, hidden, and input layers,

respectively, as the sEMG-driven model for investigating the association between the retrieved sEMG features and the manually marked scores (Figure 2-2b). The BPPN was trained by diminishing errors within the network outputs using derivatives of error functions; iterative backpropagation was employed to update the weight factors. For each iteration, a vector of sEMG features was established for the network:$\vec{X}_k = \left[\vec{X}_{ED,k}, \vec{X}_{FD,k}, \vec{X}_{BIC,k}, \vec{X}_{TRI,k} \right]$, where k reflects the kth sEMG epoch with respect to the investigated muscles, and $\vec{X}_{m,k}$ is the sEMG feature vector of the specific muscle $m,$ according to Equations 1–5. Equation 6 defines the projection between the vectors of sEMG features and the clinical scale:

$$f(x) = W \cdot \vec{X}_k + b, \tag{6}$$

where W and b represent the respective weight matrix and bias vector of the network, respectively. Iterative updating of these two parameters was performed by the BP algorithmic error function computation [92]. During this process, activation function was assigned as the sigmoid function; the network was trained using Bayesian regularization.

The mapped scores obtained from the BPPN model comprised continuous values with decimals; in contrast, the clinical scores were formatted as integral numbers. This occurs owing to the exploited sigmoid function and the algorithmic gradient rectification. Thus, the ultimate mapped score was calculated as the average output value in the testing set for all sEMG epochs of each subject. The precision of the mapped scores was validated using Pearson correlation analysis with the manually assessed clinical scales. The correlation's significance threshold was

Table 2-2. The correlation coefficients, r, between the manually acquired and mapped FMA scores, achieved by the BPNN model with varied numbers of nodes in the hidden layer.

Number of nodes in hidden layer	*r* with FMA-SE	*r* with FMA-WH
10	0.89***	0.91***
15	**0.90*****	**0.93*****
20	0.88***	0.91***
30	0.86***	0.89***
40	0.88***	0.87***
50	0.89***	0.86***
100	0.85***	0.86***
150	0.84***	0.85***
200	0.82***	0.90***

set at 0.05, with complementary values of 0.01 and 0.001.

(III) Hidden Layer Configurations

In the phase during which the hidden layer was configured, the Pearson correlation coefficient, r, which reflected the robustness of the association between the manually acquired and the mapped scores, was assessed using a two-phase technique that used varying neuron numbers or nodes contained within the hidden layer [93]. In the configuration, a strong correlation, defined by r>0.9 [94], together with a compact number of hidden nodes, was included. The 4-channel muscles were represented by 20 nodes in the input layer (i.e., 5 features from each specific muscle). 80% of the sEMG epochs, together with the corresponding FMA-SE and

FMA-WH sub-scores prior to and following the robot-aided training, were used to train BPNN models containing 10-200 nodes in the hidden layer (Table 2-2). For the testing phase, the remaining 20% sEMG epochs were input into the model; correlation analysis in the testing set was performed on the model outputs against the manually marked scores. Since FMA was the designated primary outcome as described previously, it was used in the configuration of the model. The correlation coefficients between the manually marked and the mapped FMA sub-scores generated by the configuration models with various numbers of hidden nodes are listed in Table 2-2. A three-layer BPNN model, with a hidden layer containing 15 nodes, was utilized for the current research as the calculated correlation coefficients for FMA-SE and FMA-WH were both >0.9 (Table 2-2), which will be described detailed in the Results section. During the training phase, overfitting issues could potentially arise because of the redundant hidden nodes, which was avoided using Bayesian regularization [95].

(IV) Selection of sEMG Features

Based on the established BPNN as described previously, the optimal feature vectors were selected following the feature extraction of the sEMG data to minimize the dimensions of the input to the BPNN [96]. The five sEMG features were subdivided into two cohorts, i.e., MAV, RMS, and WL (Group I), which represented the sEMG signal magnitude, and ZC and SCC (Group II), which are indicative of the neural firing parameters. Various feature combinations from these subsets, with a minimum of one from each of the two groups, were used as BPNN

28

Table 2-3. The correlation coefficients, r, between the manually acquired and mapped FMA scores, achieved by various combinations of sEMG feature.

Feature combinations	r with FMA-SE	r with FMA-WH	Feature combinations	r with FMA-SE	r with FMA-WH
MAV	0.80***	0.61***	MAV+WL+SSC	0.86***	0.65**
ZC	0.78***	0.82***	MAV+WL+ZC	0.79***	0.88***
SSC	0.73***	0.73***	RMS+WL+SSC	0.88***	0.86***
RMS	0.71***	0.59**	RMS+WL+ZC	0.85***	0.66***
WL	0.54**	0.60***	MAV+SSC+ZC	0.82***	0.87***
MAV+SSC	0.84***	0.81***	RMS+SSC+ZC	0.62***	0.89***
MAV+ZC	0.84***	0.79***	WL+SSC+ZC	0.88***	0.76***
RMS+SSC	0.65***	0.78***	RMS+WL+SSC+ZC	0.85***	0.90***
RMS+ZC	0.83***	0.84***	MAV+WL+SSC+ZC	0.91***	0.89***
WL+SSC	0.81***	0.84***	MAV+RMS+SSC+ZC	**0.93***	**0.92***
WL+ZC	0.80***	0.83***	MAV+RMS+WL+SSC	0.89***	0.82***
MAV+RMS+SSC	0.77***	0.74***	MAV+RMS+WL+ZC	0.89***	0.88***
MAV+RMS+ZC	0.87***	0.88***	MAV+ZC+SSC+RMS +WL	0.90***	**0.93***

input vectors (Table 2-3). This facilitated the investigation of the relationship between the mapped and FMA scores. The combined temporal magnitude- and neural-firing-related features were used to seek out an optimal combination of neuromuscular characteristics with minimized redundancy. The overfitting issue, potentially redundancy arising from the decreased input node number, was circumvented with the Bayesian regularization [95]. The highest correlation coefficient for FMA-SE and FMA-WH was present using a combination of ZC, RMS, SSC and MAV (Table 2-3), which was therefore selected as the input feature vectors

in this study. The contents of Table 2-3 are described in the section of results.

2.2.7 Performance Metrics

Once the model had been configured and the features had been selected, the evaluation of the

data-driven model mapping performance was conducted in relation between the manually

marked and the mapped FMA sub-scores and MASs. The FMA scores were explored further

using the sub-datasets collected before and after the 20-session robot-aided training,

respectively, because patterns of the sEMG data differ after the intervention, as revealed in our

prior pilot trials. [47, 48]. It was probable that the results for the two subsets of data might

differ in the cross validation with 5 folds. The training set contained 80% of the sEMG epochs

in a subset of data, while the testing set contained the remaining epochs. Additionally,

mismatched test data were examined, i.e., the BPNN model was trained within the pre-

intervention dataset and tested the model with the date after the 20-session training (i.e., post-

intervention dataset) [97] to assess the heterogeneity of the two subsets of data and the

constructed data-driven model's generalization performance [98]. This mismatched approach

was also deemed to have possible output with respect to predicting the outcome of the

intervention according to the participant's situation prior to the training program. The intrinsic

generalization was measured using varying proportions of the sEMG epochs (i.e., 50%, 60%,

70%, 80%, and 90%) obtained after the intervention as the training input. Then, the

correspondingly remaining sEMG epochs (i.e., 50%, 40%, 30%, 20%, and 10%) were the

testing data. During which, the previously determined model (i.e., 16-dimension input vectors with 15 nodes in the hidden layer) was trained using five-fold cross validation.

Furthermore, the distal muscles of FD and ED, and the proximal muscles of TRI and BIC were utilized for mapping to the respective FMA-WH and FMA-SE sub-scores It was because the function of these proximal and distal muscle pairs dictated the corresponding FMA-SE and FMA-WH sub-scores, especially for unimpaired subjects [30, 77]. When only two muscles' signals were used, the BPNN was retrained since the input vectors was 8-dimension from the two sEMG channels. To avoid possible redundancy arising from the reduced input nodes, Bayesian regularization was also used to circumvent issues of overfitting [95].

Initially, the model's mapping performance, i.e., from the sEMG data to the output scores of MASs, was explored with varying low-pass cut-off frequencies, i.e., 500, 400, 300, 200, 150, and 80 Hz, with the MAS sub-score at the elbow joint obtained prior to and following the 20-session intervention. Those exhibited the most robust relationships between the output MAS and the true clinical scores, were chosen as the cutoff frequencies for continued investigation of the projection performances regarding the MAS scores at finger, wrist, and hand joints, utilizing both the datasets obtained before and after the robot-aided training.

Earlier work relating to robot-assisted rehabilitation of the upper limb motor functions demonstrated that the sEMG characteristics obtained from the bare hand assessment could identify outcomes of the rehabilitation similar to those observed in the manually assessed

scores of FMA and MAS [47] [48] [49] [50]. The amplitude of a particular muscle's sEMG

signal and the temporal relationships of the contraction within corresponding pairs of muscles

were given by the sEMG activation level and CI. Additional analysis on the activation levels

and CI for related muscle pairs was therefore conducted before and after the intervention, to

identify alternations of these sEMG characteristics at the two time points [44, 47].

The computation of a muscle's sEMG activation level during the evaluation task was performed

using Equation 7 [44]:

$$\overline{\text{EMG}} = \frac{1}{T} \int_0^T EMG_i(t) dt, \tag{7}$$

where $\overline{\text{EMG}}$ indicates the mean values of sEMG envelope at muscle i. $EMG_i(t)$ represents

the signal envelop acquired following normalization according to the value of the maximal

muscle contractions during the session, meanwhile, the signal length is represented by T.

Attenuation in spasticity could be inferred by a decline in the amplitude of the sEMG signal

quantified by the muscle activation level following the intervention [44].

Equation 8 defines the CI between a muscle pair:

$$\text{CI} = \frac{1}{T} \int_0^T A_{ij}(t) dt, \tag{8}$$

where $A_{ij}(t)$ represents the envelopes' overlapping sEMG activity at muscles j and i, and the

signal length is indicated by T. A rise or fall in the CI index indicated enhanced or diminished

muscle pair co-contraction, respectively, i.e., a wider or narrower region of imbrication [44].

For this study, the secondary outcomes were the calculated CI and activation level. The

Shapiro-Wilk test was utilized to examine whether the data was normal distributed; this

criterion was met by all sEMG measures. A paired test was then applied to the normal sEMG

parameters [48] to compare any differences between the sessions prior to and following

intervention. The value of P below 0.05 was considered significant statistically. The clinical

scale data before and after the 20-session intervention underwent identical testing for

normality; data from the FMA-WH and FMA-SE sub-scores were found to have a normal

distribution (p>0.05) but not the MAS score data. Differences between the FMA scores before

and after the intervention were therefore investigated using a paired t-test; the MAS score data

was explored with the Wilcoxon test. Statistical significance was set at a p-value of 0.05.

2.3 Results

2.3.1 Feature Selection and Model Configuration

The correlation coefficients describing the relationships between the FMA sub-scores obtained

clinically and those generated by the BPNN with varying number of hidden nodes are presented

in Table 2-2. The strongest correlation was obtained in the model of 15 hidden nodes (r=0.93

and r=0.90 for FMA-WH and FMA-SE, respectively, p<0.001). The r value diminished in trials

where the hidden nodes were either greater than or below 15.

The model's mapping performance with various combinations of input feature vectors, i.e., the

amplitude features and the features associated with neural firing, are displayed in Table 2-3. The combined features of ZC, RMS, SSC and MAV provided the maximum correlation coefficients (FMA-WH r=0.92; FMA-SE, r=0.93, p<0.05). Significant correlations between the mapped and clinically obtained FMA sub-scores were obtained with the application of all the combinations of features applied (p<0.05). The lowest correlation coefficient was when the only input feature was WL (FMA-SE, r=0.54, p<0.05). The greater the number of combined sEMG features that were entered, the better the correlation identified between the manually assessed and the mapped FMA sub-scores. However, when all five characteristics were combined together, the correlation coefficients in relation to the mapped and clinical FMA-WH and FMA-SE scores led to a correlation coefficient fall of 0.3, and a rise of 0.1, respectively, when contrasted against the highest correlation coefficient seen with the ZC, RMS, SSC, and MAV feature combination.

2.3.2 Mapping Performance for MAS and FMA

Figure 2-3 shows the correlations between the manually assessed and the mapped FMA sub-scores within the pre-intervention dataset. These reached significance for FMA-WH and FMA-SE (r=0.93 and r=0.92, respectively, p<0.05). The ranges of the mapped and clinically acquired FMA-SE scores were 6.5-32.80 and 5-30, respectively; the respective equivalent data for the MA-WH scores were 2.57-17.24 and 2-20. The correlation relationship was strong when the scores lay between 11 and 24 for FMA-SE, and between 2 and 9 for FMA-WH. The correlations
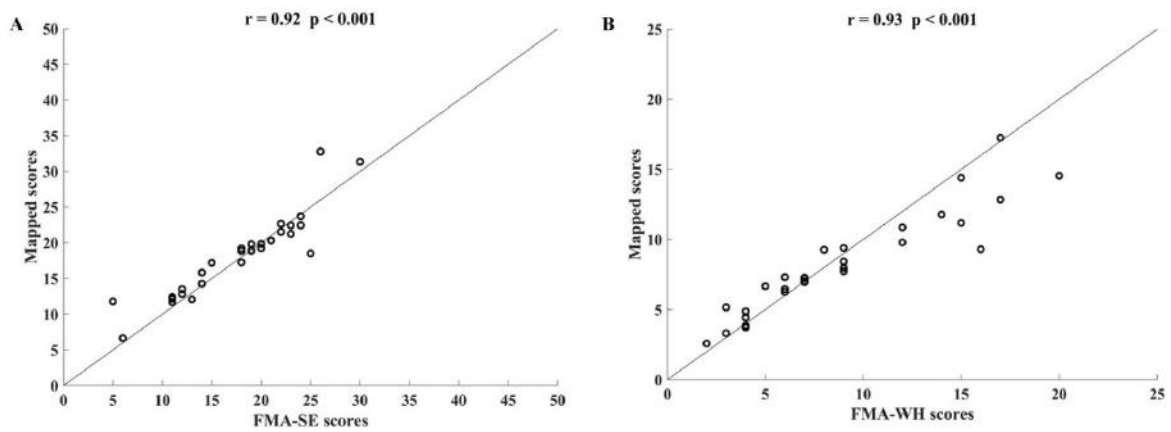
Figure 2-3. Robust correlations generated by sEMG signals from four muscles, namely BIC, ED, TRI, and FD, within the pre-intervention dataset. FMA-WH, Fugl–Meyer Assessment wrist/hand sub-score. FMA-SE, Fugl–Meyer Assessment shoulder/elbow sub-score.
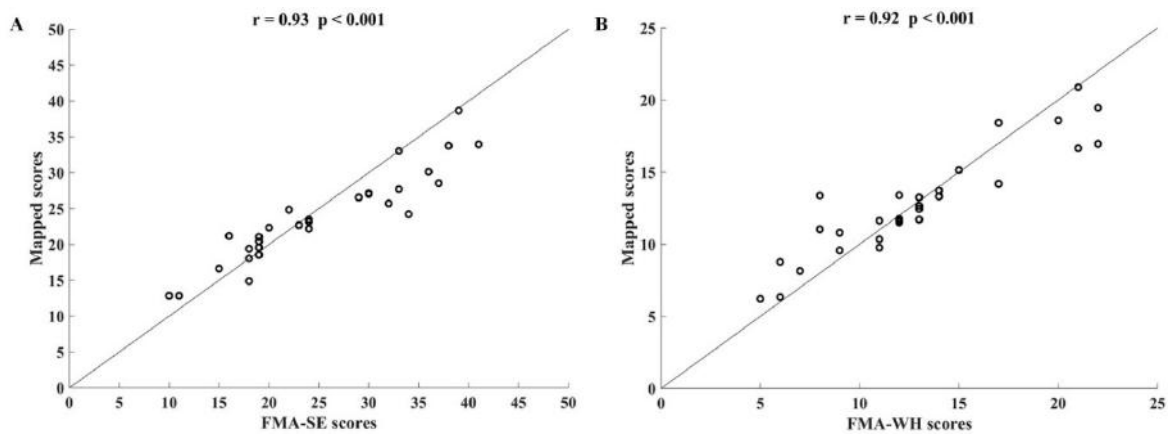
Figure 2-4. Robust correlations generated by the sEMG from the for muscles, namely TRI, ED, FD, and BIC, within the post-intervention dataset. FMA-WH, Fugl–Meyer Assessment wrist/hand sub-score. FMA-SE, Fugl–Meyer Assessment shoulder/elbow sub-score.
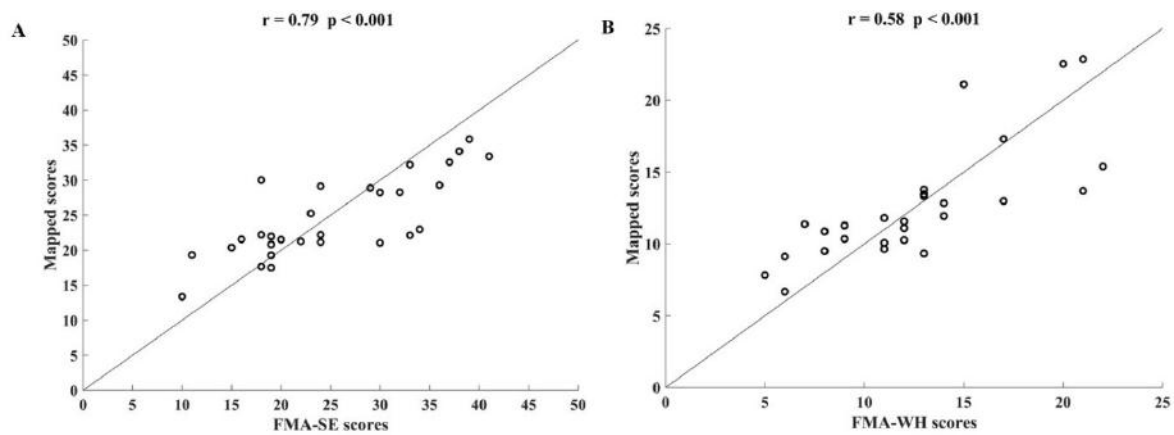
Figure 2-5. Correlations generated by the corresponding sEMG pairs after the robot-aided training, i.e., TRI and BIC for FMA-SE, ED and FD for FMA-WH. FMA-WH, Fugl–Meyer Assessment wrist/hand sub-score. FMA-SE, Fugl–Meyer Assessment shoulder/elbow sub-score.

observed between the manually acquired and the mapped FMA sub-scores after the intervention are depicted in Figure 2-4. These attained significance for FMA-WH and FMA-SE (r=0.92 and r=0.93, respectively, p<0.05). The ranges of the manually measured and the mapped FMA-SE scores were 12.84-39 and 10-41, respectively; the corresponding ranges for the FMA-WH scores were 6.22-21 and 5-22, respectively. The correlation was highest when the scores were within the range 15 and 24 for FMA-SE, and between 9 and 15 for FMA-WH. For both datasets obtained before and after the intervention, there was a high correlation between the manually assessed and the mapped FMA sub-scores.

The associations for the manually acquired and the mapped FMA sub-scores using sEMG data
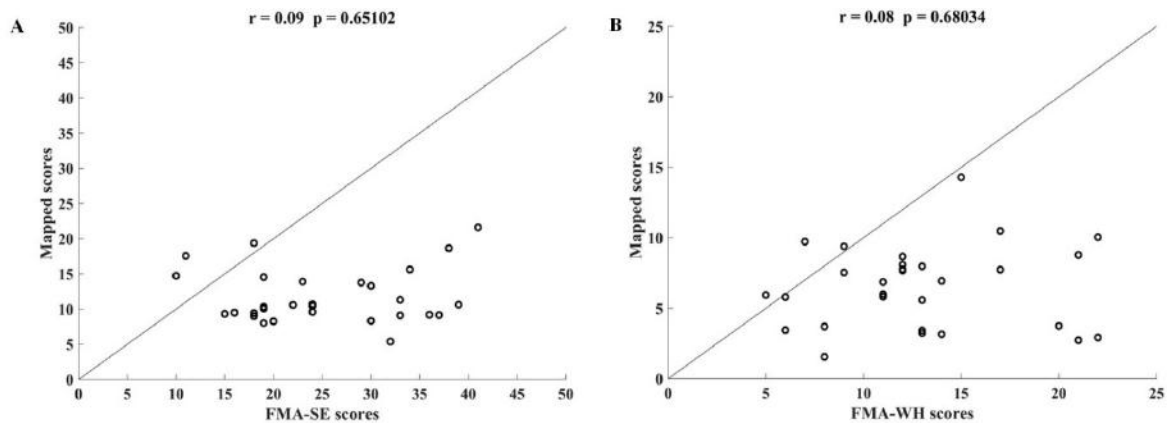
Figure 2-6. Correlations generated within the mismatched testing condition utilized the sEMG data from four muscles, i.e., BIC, FD, TRI, and ED. FMA-WH, Fugl–Meyer Assessment wrist/hand sub-score. FMA-SE, Fugl–Meyer Assessment shoulder/elbow sub-score.

from the respectively paired muscles are indicated in Figure 2-5. The corresponding muscle pairs comprised FD and ED for the FMA-WH, and TRI and BIC for the FMA-SE. The respective correlation coefficients for the clinically acquired scores and the mapped FMA-WH and FMA-SE were r=0.58 (p<0.05) and r=0.79 (p<0.05). The mapped ranges for the two scores were 13.37-35.85 and 6.67-22.87, respectively. The manually acquired scores were identical to those indicated in Figure 2-4. There was a higher correlation between the manually assessed and the mapped scores for the FMA-SE in comparison to the FMA-WH. The correlation analysis between the manually acquired and the output FMA sub-scores which were acquired with the application of the mismatched testing condition is demonstrated in Figure 2-6. No significant correlations were observed with respect to either FMA-SE or FMA-WH. The FMA-

Table 2-4. The correlation coefficients, *r*, between the manually assessed and the mapped

MAS-elbow, produced from filtered sEMG signals with various lowpass cutoff frequencies.

Cutoff frequency (Hz)	*r* with MAS-elbow
80	0.76***
150	0.89***
200	0.92***
300	0.81***
400	0.75***
500	0.42***

SE score ranges were: 5.38-21.62 (mapped scores) and 10-41 (manual scores). The equivalent

ranges for the FMA-WH scores were: 1.55-41.29 (mapped scores) and 5-22 (manual scores).

Overall, when the mismatched testing condition was applied, the output scores were lower than

those obtained clinically. Correlations between the manually assessed and the mapped FMA

sub-scores generated by the data-driven model with varying percentages data in the training set

for the evaluation of intrinsic generalization are listed in Table 2-6. The split-half technique

[99] still yielded a correlation coefficient >0.88 between mapped and clinical scores when the

training data component was diminished to 50%.

The correlation analysis output is detailed in Table 2-4 for the manual versus mapped MAS-

elbow score data when varying low-pass cutoff frequencies applied to sEMG signals. All the

relationships reached significance ($p < 0.05$). The coefficient of correlation reached the
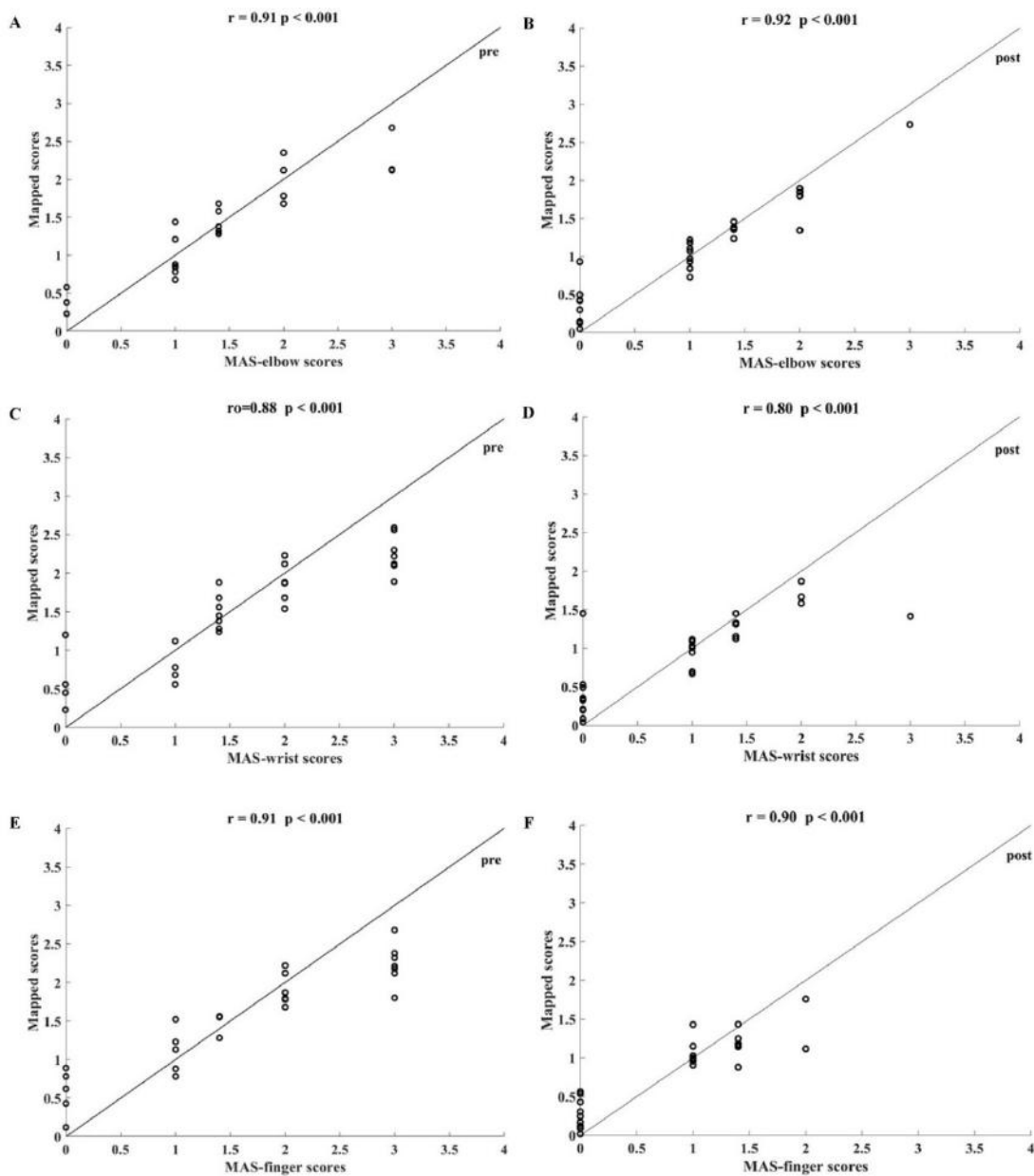
Figure 2-7. Robust correlations between the manually measured and the mapped MASs, generated by the 10-200Hz bandpass filtered sEMG signals from TRI, BIC, FD, and ED. Correlations between the manually acquired and the mapped MASs (E) at the fingers, (C) wrist, and (A) elbow joints within the pre-intervention dataset, (F) at the fingers, (D) wrist, and (B) elbow joints for post-intervention dataset.

maximum for the increased cutoff frequency values up to 200 Hz (r=0.92, p<0.05). When the cutoff frequency exceeded 200 Hz, the association between the mapped and manual scores decreased. The correlations between the mapped and the manually assessed MAS scores with respect to the use of band-pass filtered sEMG data (10-200Hz) are illustrated in Figure 2-7. Using the datasets obtained before the robot-aided training, the following correlation coefficients were calculated as: MAS-elbow, r=0.91 (p<0.05); MAS-finger, r=0.91 (p<0.05); MAS-wrist, r=0.88 (p<0.05). With the datasets collected after the intervention, the equivalent correlation coefficients comprised: MAS-elbow, r=0.92 (p<0.05); MAS-finger, r=0.90 (p<0.05); MAS-wrist, r=0.80 (p<0.05). A higher association between the manually measured and the mapped MAS sub-score (wrist joint) was found within the pre-intervention dataset, compared to that within the post-intervention dataset. For the pre-intervention dataset, while

Table 2-5a. The changes in the sEMG parameters before and after the 20-session robot-assisted rehabilitation.

	pre-intervention Mean($\pm$std)	post-intervention Mean($\pm$std)	P
BIC	0.86($\pm$0.14)	0.36($\pm$0.19)	0.000***
FD	0.93($\pm$0.07)	0.37($\pm$0.13)	0.000***
FD-BIC	0.83($\pm$0.18)	0.47($\pm$0.21)	0.000***
FD-TRI	0.85($\pm$0.15)	0.39($\pm$0.21)	0.000***
BIC-TRI	0.85($\pm$0.16)	0.32($\pm$0.13)	0.000***

Table 2-5b. The changes in the clinical scales before and after the 20-session robot-assisted rehabilitation.

	pre-intervention Mean(±std)	post-intervention Mean(±std)	P
FMA-WH	8.86(±2.49)	12.90(±2.45)	0.000***
FMA-SE	17.76(±3.03)	25.21(±4.37)	0.000***
MAS-elbow	1.52(±0.42)	0.97(±0.39)	0.001***
MAS-wrist	1.66(±0.48)	0.83(±0.41)	0.000***
MAS-finger	1.63(±0.55)	0.67(±0.35)	0.000***

Table 2-6. The correlation coefficients, *r*, between the manually measured and the mapped FMA sub-scores, produced by the BPNN model trained with varying distribution proportions of the training and testing sets.

proportion of training data	*r* with FMA-SE	*r* with FMA-WH
50%	0.89***	0.88***
60%	0.91***	0.90***
70%	0.89***	0.92***
80%	0.93***	0.92***
90%	0.87***	0.88***

the manually acquired MAS scores were graded at three and zero, the distances between the manual and the corresponding output score were >0.5. For the dataset obtained after the training, the distances within the manual and mapped scores were above 0.5 when the manually assessed MAS scores of zero, two, or three were assigned.
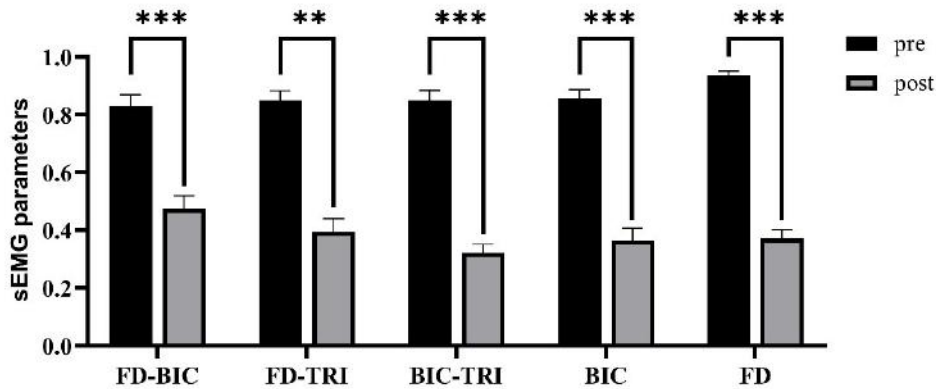
Figure 2-8. The alterations of sEMG parameters before and after the 20-session robot-aided training. The individual muscles of FD and BIC, and paired muscles, i.e., BIC-TRI, FD-TRI, and FD-BIC are indicated on the x-axis. The y-axis shows CIs of the paired muscles and the normalized activation level of the individual muscles.

2.3.3 Alterations of Clinical Scales and sEMG Parameters

The comparisons of normalized sEMG activation levels and CI prior to and following the intervention are presented in Figure 2-8. Significant changes in the normalized sEMG activation level were detected in relation to the FD and BIC (paired t-test, $P<0.05$), with the values being greater prior to the rehabilitation program. The normalized CI data also decreased significantly after the intervention in the muscle pairings, BIC-TRI, FD-TRI and FD-BIC (paired t-test, $p<0.05$). The remaining targeted musculature or paired muscle groups demonstrated no significant alterations in these sEMG measures. The changes observed
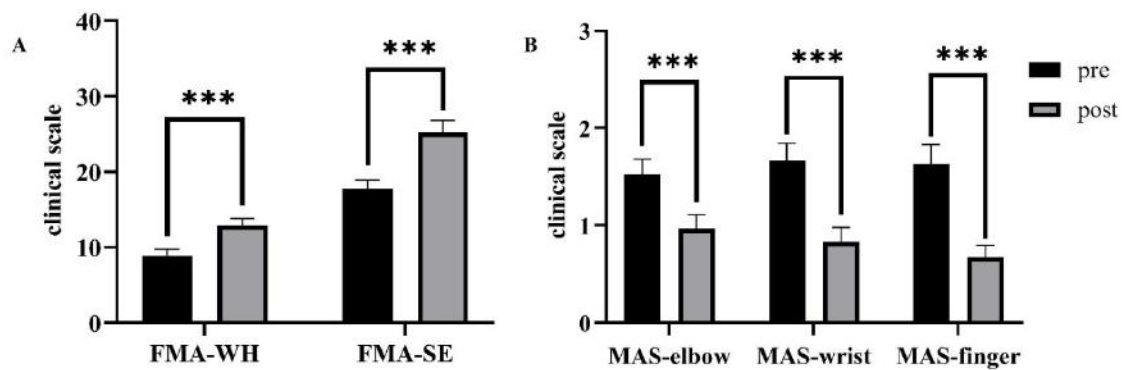
Figure 2-9. The changes of clinical scales before and after the 20-session intervention. (a) Sub-

FMA scores, (b) MASs.

between the sEMG measures before and after the intervention are demonstrated in Table 2-5a.

The comparisons of the clinical scales prior to and following the intervention are displayed in

Figure 2-9. The two FMA sub-scores increased significantly following the intervention (paired

t-test, $P<0.05$) whereas MASs significantly decreased post-intervention (Wilcoxon test,

$P<0.05$). These differences in clinical scores are also listed in Table 2-5b.

2.4 Discussion

In this study, a BPNN Model driven by sEMG data for the mapping of sEMG signals against

commonly utilized clinical scores, i.e., FMA sub-scores (FMA-WH and FMA-SE), and MASs,

was developed. Optimization of the model was carried out by adjusting the node number in the

hidden layer and by modifying the input feature vectors of the BPNN model. Strong

correlations were exhibited within the output scores yielded by the model and the scores

acquired clinically (r>0.9), for both the datasets collected prior to and following the

intervention (Figures, 2-3, 2-4, and 2-7).

2.4.1 Model Configuration

A three-layer BPNN was constructed to underpin the sEMG-data-driven model. The hidden

layer neuron count was determined using the two-step technique, and the model outputs with

varying node numbers in the middle layer, i.e., 200, 100, 50, 40, 30, 20, 15, and 10, were

evaluated. The correlations obtained from all the models between the output and manually

obtained scales were high (r>0.8), which implies that the established BPNN with three layers

is capable and adequate for projection to the FMA sub-scores acquired manually using the

sEMG data [100, 101]. The optimal model for matching the sEMG data to the FMA subscales

was the BPNN with a hidden layer containing 15 nodes, as revealed by the correlation

coefficient in Table 2-2. The hidden layer with 15 nodes was 75% of the input layer

dimensionality (20 nodes, consistent with the rule of the thumb method, which proposed that

the number of hidden nodes should be between 70% and 90% of the input feature dimension

[102]. The output of models with a higher number of hidden nodes (>15) was inferior because

of overfitting issues; complicated fitting between the misleading sEMG features and the

manual scores was potentially present in such models with excessive hidden nodes, which

diminished the precision of generalization on the testing dataset [103]. Meanwhile, the opposite

problem, i.e., underfitting, was suspected in the models with hidden nodes less than 15, leading

to insufficient plasticity in relation to the linear regression and thus diminishing the accuracy

of interpretation for the testing dataset [104].

2.4.2 Input Feature Selection

The selection of sEMG features, i.e., WL, ZC, RMS, SSC, and MAV, were tested in varying

combinations of these features as BPNN model input vectors (Table 2-3). Significant

correlations (moderate, $r \geq 0.54$) between the mapped and clinically acquired scores were

achieved using a lone sEMG feature as the model input vectors [94]. This implied that sufficient

neuromuscular information relating to the restoration of motor functions during robot-assisted

rehabilitation was encompassed within the individual sEMG features, which could be identified

by the utilized BPNN model. The performance of the models was enhanced when the sEMG

features associated with magnitudes (i.e., WL, RMS, and MAV) and neural firing information

(i.e., WL and ZC) were incorporated, indicating the necessity for the inclusion of neural-firing-

related and magnitude-related features for optimal mapping by the model. The model

performance was also promoted when the number of combined sEMG features was extended,

but interestingly, the most robust correlation between mapped and clinical scores was noted

with the combination of features ZC, SSC, RMS, and AMV, rather than all the five sEMG

features were utilized. It is possible that WL may be the superfluous feature attenuating model

output accuracy. This is substantiated by the fact that as an isolated input vector, WL gave rise

to the lowest correlation coefficient (r=0.54), suggesting its lack of efficacy for matching the

sEMG data to manually acquired scales of FMA. Thus, the BPNN input feature vector for this

study comprised the combination of ZC, RMS, SSC and MAV. This optimalization of feature

vectors was consistent with the feature reduction and selection in earlier work of sEMG signal

classification [96].

2.4.3 Relationship between the sEMG Data and FMA Sub-scores

In this work, the sEMG data on the FD, BIC, TRI, and ED muscles were projected to clinical

scores of FMA-WH and FMA-SE, yielding robust correlations prior to and following the 20-

session rehabilitation (Figures 2-3 and 2-4). The optimal regression output was observed in

relation to the average values of the manual scores, e.g., 17.76 (Figure 2-3a), which arose as in

the training datasets, the manually assessed FMA sub-scores were normally distributed (Figure

2-3a, $\mu=17.76$, $\sigma=3.03$). The training data were inadequate for model learning regarding

appropriate association within sEMG data and FMA sub-scores, since the training data were

centered on the average values, where the manually assessed scores deviated from the average

value.

Furthermore, sEMG data from two antagonistic pairs, i.e., ED and FD for distal motions, BIC

and TRI for proximal motions were projected to the manually acquired FMA-WH and FMA-

SE sub-scores using the data-driven BPNN model. These correlations within the manually

assessed and the mapped FMA sub-scores using sEMG data of the corresponding antagonistic

muscle pairs were weaker than that utilized sEMG data from the four muscles (Figure 2-5).

These observations indicate that compensatory muscular movements, particularly in the

proximal muscles, is a crucial issue in the sEMG based evaluation tasks for stroke survivors,

during the robot-aided training. During the motor recovery measurement, compensation at

proximal muscles was observed more frequently compared to that at distal muscles, which

explains the stronger correlation (Figure 2-4) within the mapped and clinically acquired FMA-

SE scores generated from the proximal TRI-BIC muscles, compared to that within the manually

assessed FMA-WH and the mapped scores from the distal FD-ED muscle pair.

2.4.4 Generalization of the Model

The mismatched testing condition, i.e., utilizing the pre-intervention dataset in the training

stage and testing the trained model with the post-intervention dataset, was applied for the

evaluation of the model generalization. The model was unable to project sEMG data to the

manually acquired FMA scores within the post-intervention data, with the model trained by the

pre-intervention dataset, which was indicated by the lack of significant correlations between

the manually marked and the mapped FMA-SE and FMA-WH scores (Figure 2-6). This finding

was further explicated by the significant differences in calculated parameters of sEMG, i.e., the

normalized and CI sEMG activation level prior to and following the intervention (Table 2-5a,

Figure 2-8). Moreover, a correlation coefficient of 0.88 was observed between the manually

marked and the mapped FMA sub-scores, despite diminishing the proportion of training data

to half (Table 2-6), this finding implied that the internal generalization of the established model

was satisfying, even with restricted samples [105].

Overall, the mapped FMA-SE and FMA-WH sub-scores had a lower value in comparison to

those acquired manually (Figure 2-6), suggesting that the motor recovery was underestimated

by the constructed model following the intervention, which was because the pre-intervention

dataset was exploited for model training, which included significantly lower values of manual

FMA sub-scores, in comparison to the post-intervention dataset (Table 2-5b, Figure 2-9). Thus,

although the constructed model could project the sEMG data to the clinically acquired FMA

sub-scores within datasets collected prior to and following the intervention (with the stable

pattern of muscle activity), it lacked the prognosis capacity to predict the FMA sub-scores after

the robot-aided training.

2.4.5 Relationship between the sEMG Data and MASs

The sEMG data-driven model was further tested for its capability of matching sEMG data to

the manual MAS scores. Thus, low-pass filtering of the sEMG data was performed, with the

cutoff frequency set based on the sEMG characteristics and according to previous studies on

the involuntary muscle contractions associated with muscular spasticity [106, 107]. When the

low-pass filter (200 Hz) was applied to the sEMG data, the best performance, i.e., the highest

correlation, was observed between the manually marked MASs and the mapped scores using

the data-driven model. This suggested that the slow and passive contraction in spastic muscles

post-stroke were efficaciously represented by the lower frequency domain of sEMG data [80]. When the cutoff frequency of the low-pass filter was set as 200 Hz, the correlation achieved a peak value, in comparison to the values of 300 and 150 Hz. This implies that for the passively tensioned muscle, the most effective frequency of sEMG data is around 200 Hz. This infers that low-frequency firing motor units are predominant within muscles affected by spasticity and supports observations found in earlier work [107]. The correlation coefficient between the manually marked and the mapped MAS scores decreased when the applied cut-off frequency was less than 200 Hz (Table 2-4), suggesting that the bio-information associated with muscular spasticity was lost in the much lower frequency band of sEMG signals.

Robust correlations within the manually acquired and the mapped MAS scales (Figure 2-7) demonstrate that the constructed model enables the projection from the sEMG data to MAS scales with a high consistency, which facilitates its potential application in estimation of passive muscle tensions for individuals with chronic stroke. Nevertheless, the model performance was less accurate for the MAS scales zero and three, with the distances separating the output and manually acquired scores greater than 0.5. This could be explained as the participants owning $0<MAS<3$ according to the inclusion criteria, which limited the model learning the characteristics of MAS grading at 0 and 3 from the restricted training data. This issue was also recognized in the previous studies [41] [73]. Moreover, the manually marked and the mapped MAS-wrist scores showed the higher correlation in the pre-intervention dataset,

in comparison to that within the post-intervention dataset. The better performance of using the pre-intervention dataset is owing to the widespread distribution of the training data. A weaker correlation was observed using the post-intervention dataset since the manual MAS-wrist scores decreased significantly after the robot-assisted training (Table 2-5b, Figure 2-9), and the training data were congregated within the lower scores.

Some limitations were identified in this study. Implemented by the mismatched testing, unsatisfactory generalization of the data-driven model was observed, which could potentially result from: (i) the limited sample size (n=29) compared to larger sample sizes in previous studies >100[108, 109]; and (ii) the marked heterogeneities in sEMG characteristics and clinical scores between the datasets collected prior to and following the intervention, as detailed in Tables 2-5a and 2-5b, and Figures 2-8 and 2-9. The insignificant correlations in the mismatched testing suggested that the sEMG information and manually acquired scores following the robot-aided training were interpreted to be fresh data by the trained model. In future work, more sEMG data and the corresponding clinical scores will be involved with additional participants, for the enhanced generalization of the constructed model on the fresh and unmarked inputs in the testing stage. Moreover, sEMG-based index, such as CI and the activation level, together with diagnostic biomarks will be integrated into the feature vectors for the enhanced robustness of the data-driven model. Additionally, interpretation of the data-driven model, i.e., non-linear mapping, would be carried out for the clinical practitioners for

future clinical applications.

2.5 Periodic Summary

In this chapter, a sEMG-driven model based on BPNN, was constructed for the mapping of sEMG data during the evaluation tasks to two commonly utilized clinical scores, i.e., FMA and MAS. The performance of the constructed model was optimized and the relatively optimal one was obtained with the sEMG feature combination of ZC, RMS, SSC, and MAV. Strong correlations were found within the manually marked and the mapped MAS scores and FMA sub-scores, indicating that the sEMG-driven model enables the measurement of the upper limb motor function with sEMG data. The promising findings suggest that once the model's extrinsic generalization being improved with enlarged samples, this data-driven model could be applied in clinical practice as an automated assessment without the need for intensive operation or supervision by a clinical professional.

CHAPTER 3

AN EXO-NEURO-MUSCULO-SKELETON WITH BALANCE SENSING FEEDBACK FOR LOWER LIMB REHABILITATION AFTER STROKE

3.1 Introduction

Stroke has been one of the primary causes of disability in adult [1]. There were around 300,000 stroke survivors in Hong Kong and over 45 million in Chinese mainland by 2019, with annually new occurrence of 4 million and an annual augment of 8% from 2009 to 2019 [2]. In contrast to the growing stroke population, resources in the rehabilitation industry (e.g., professional therapists and the length of hospital stay) are limited even in industrialized countries [4]. Restoration of locomotion for the lower limbs has a high priority in traditional early stroke rehabilitation [6]. It is because that paralysis in the affected lower limb due to post-stroke hemiplegia is easy to cause immobilization, which is a leading cause of further deterioration of the whole body. However, the current rehabilitation service of the lower limb is insufficient, particularly after discharging. Although around 60%–80% of stroke survivors could obtain some extent of independent walking, most of them suffer from long-term gait disturbances, e.g., high gait asymmetry, walking slower, cannot walk far, and more likely to fall, affecting their mobility and integration into the community [6]. More effective and easy-to-access rehabilitation services, or methods, are needed to improve the gait function of stroke survivors

with the purpose to improve their life quality.

Effective neurorehabilitation of the paretic lower limb relies on the extensive and repeated voluntary practice throughout the subacute and chronic periods [7]. Although traditional rehabilitation indicated that primary recovery of motor functions was mainly observed in the acute and subacute periods, i.e., within 6 months of the stroke occurrence [6], Some studies have found that after the first six months, i.e., during the chronic stroke period, significant returns of motor function could be achieved via rehabilitation training at the same intensity as that provided during the subacute period [8] [9]. Unfortunately, due to a shortage of skilled manpower in the existing healthcare system, discharged stroke survivors usually find it hard to obtain regular and extensive physical training. In the current inpatient lower limb rehabilitation, primary returns of lower motor function are usually exhibited in the the hip and the knee joints, i.e., the proximal joints, which could be associated with the sequence of proximal to distal joints in spontaneous motor recovery during the early periods of stroke, enhanced by the voluntary rehabilitation training during the hospital stay. However, most of the patients have not obtained enough spontaneous motor recovery at the ankle and foot joints, i.e., the distal joints, by the time of discharge, which makes voluntary physical practice at these joints difficult in early rehabilitation when they stay in the hospital. It leads to less restored ankle foot functions, contributing to the deterioration of the hemiplegic walking in later stages, e.g., muscle weakness in the paretic limb, imbalance due to asymmetry between the two limbs, high

energy consumption, and risk of fall [12] [13].

Neurorehabilitation post-stroke is a long-term relearning process of motor functions on the paralyzed limbs, which could be regained by intensive and repetitive physical practice of the desired movements with the voluntary motor effort of a patient [110]. The success of motor rehabilitation poststroke is also dependent on limb coordination practice that close to normal walking pattern, which could prevent excessive muscular compensations of both the lower limbs. Joint deformities at the ankle foot complex after stroke are consequences of muscle spasticity and muscular discoordination in the lower limb [111]. Compared to normal gait, reduced patterns of muscle synergies with muscular spasticity and compensatory synergies with learned disuse were found in stroke gait. The paralyzed foot of stroke survivors exhibited uncontrolled plantarflexion and inversion in comparison to the unimpaired foot [112], associated with the respective symptoms of foot drop and foot inversion. The foot drop has been found to be the results of weakness in the ankle dorsiflexors [11] and increased spasticity in the plantar flexors, which imposed over 50% resistance than a normal ankle [113]. The heterogeneity of dorsiflexors and plantar flexors implies that different levels of assistance are required in the target muscles during the gait training post-stroke. Long-term excessive strain on muscles of the ankle plantarflexion in stroke patients also resulted in greater weight loading on the fore and lateral regions of paretic foot, leading to foot inversion and an unstable ankle joint [17]. Both foot drop and foot inversion cause that the stroke survivors are more likely to

fall and deviate the post-stroke gait from the normal patterns [112]. In the traditional post-stroke ankle foot rehabilitation, passive ankle foot orthoses (AFO) have been widely applied to correct the foot position with a fixed joint angle at the ankle [11]. The AFO can significantly improve the plantarflexion deformity of foot drop immediately. However, it could not dynamically correct the abnormal gait pattern. Excessive use of passive AFO has been found to cause muscular disuse atrophy, since the users will gradually rely on the mechanical fixation by the AFO, rather than using their own muscular effort to stabilize and strengthen the joints [114]. More advanced ankle foot rehabilitation methods are needed to improve the muscle coordination at the ankle foot complex for a better motor restoration in the distal joints of the lower limb after stroke.

Due to the requirement of high intensity and repeatability of physical training poststroke, physical therapy is a labor-and-time consuming tasks for both the professionals and stroke survivors. Thus, different robotic skeletons powered by mechanical motors were proposed and released to assist in the extensive and repeated practices [18]. However, current exoskeletal robots for lower limb are mainly designed for paraplegia, e.g., spinal cord injured patients with permanent disabilities in both lower limbs. They are bulky, heavy, expensive, and designed for bilateral mechanical support. Strong mechanical supports with powerful motors were usually provided to the large and proximal joints, i.e., the hip and knee. In these robots, the mechanical supports to the ankle foot were usually oversimplified as a passive AFO or a mechanical joint

with one degree of freedom in the sagittal plane controlled by a single motor. The dynamic correction of the muscular discoordination on foot drop and foot inversion has not been well considered in these robots. Although the direct application of these bilateral lower limb robots to stroke rehabilitation has been proposed in the literature [19] [20], difficulties were still encountered in improving the distal joints at the ankle and foot functions. Furthermore, current bilateral lower limb robots with the original application to paraplegia provided excessive mechanical supports to both the affected and unaffected limbs of stroke survivors. It may not be an optimized rehabilitation strategy to promote post-stroke motor relearning, where support-as-necessary is required during stroke rehabilitation with the goal to ambulate without aids [13]. Although unilateral exoskeletal lower limb robots have been developed for in individuals with chronic stroke [115] [21] [22] [23], the unbalanced weight applied to the paretic lower limb has already caused the mechanical asymmetry and introduced additional load in the swing phase. There was also no significant breakthrough in the ankle foot control or mechanical design in the current unilateral exoskeletons to correct muscular discoordination, based on a direct adoption from the bilateral robots for paraplegia. Attempts have been made by using pneumatic muscles [116] [24] and Bowden cable systems [25] [26] in unilateral robot design (i.e., soft robot) for the ankle foot complex, with the main purpose to reduce the weight of the device. However, soft robots actuated by pneumatic muscles usually require gas tanks with high pressure, e.g., CO_2 cylinders [116] and pneumatic pump [24] encased in the waist belt,

which makes the whole system bulky, particularly during inflation. For the soft cable system with a weight of 0.9 kg distributed along the paretic lower limb [25], actuators were mounted around the waist of a user for dragging the cables that provide assistive torque for plantar and dorsal flexions. In both designs of the pneumatic muscle and the cable system [116] [25], correction of foot inversion at the ankle joint has not been involved. More recently, the variable stiffness pneumatic actuators [24] and the gearmotor-driven rack-and-pinions [26] were integrated in the exosuit-assisted correction of foot drop, for restricting ankle inversion by mechanical fixation at the ankle joint, however, they only demonstrated the feasibility on mechanical support in the gait, whereas the rehabilitative effects have not been reported yet. More lightweight automation systems with compact design, advanced control on muscular coordination for the correction of foot drop and foot inversion are needed for effective post-stroke gait restoration.

As one of the alternative solutions to bulk robots, neuromuscular electrical stimulation (NMES) could mimic nerve-to-muscle stimulation. Assisted by the NMES, repetitive sensorimotor experiences would be generated by cyclic stimulation on the target muscles, which could enhance the impaired muscles and activate the damaged neuroplasticity pathways. A mechanism for the therapeutic effects of NMES is that repetitive sensorimotor experiences would be produced by a periodic electrical stimulation on muscles [14]. NMES also could improve learned disuse and limb neglect after stroke through precisely stimulating on the

impaired muscles, which could elicited afferent inputs to the nervous system [14]. Therefore, one-channel NMES on the dorsiflexors of the ankle has been applied in the treatment of foot drop after stroke, with the purpose to improve the muscle force in the dorsiflexors during the swing phase of a gait cycle [16]. Furthermore, two-channel NMES on ankle plantar flexor and dorsiflexor recruitment has been suggested to improve the muscular coordination related to both push-off and foot drop in hemiparetic gait [15]. Moreover, the muscular spasticity of plantarflexors could be effectively released by applying NMES on the muscle belly of the paralyzed lower limb for half an hour [16]. However, phasic control of multi-channel NMES during dynamic gait is still challenging for stroke survivors, since difficulties could be encountered in the identification of gait events in the paretic lower limb associated with diverse patterns different from the normal patterns [111]. Furthermore, NMES alone is hard to correct the foot inversion in the ankle foot rehabilitation, due to a lack of control on foot rotation in the frontal plane and the mechanical stabilization at the ankle joint, which has been found be a main cause related to the muscle discoordination of the ankle joint [17].

In contrast to the conventional verbal reminders for correcting foot inversion by a physiotherapy [117], which requires intensive manpower, wearable devices with biofeedback, e.g., audio, visual, and tactile feedback, have great potential to improve the paretic gait of chronic stroke survivors. In a previous study, the visual kinematic feedback based on the detected ground reaction forces (GRFs) was given to the Parkinson and stroke survivors, which

has been suggested to improve symmetries in stance/swing time between two legs [27]. In our previous study, the plantar pressure could be detected by force sensitive resistors (FSRs), to provide the instant vibrotactile feedback, which could improve the plantar imbalance of stroke survivors with foot inversion [28]. However, the long-term rehabilitation effect of the tactile feedback on plantar balance has not been investigated. Moreover, most stroke survivors could not perform ankle dorsiflexion and regain muscular contraction of dorsiflexors with only the biofeedback during the gait training [13].

In this study, a multi-modal system, combining the soft pneumatic muscle, the rigid exoskeletal techniques, NMES, and vibrotactile feedback, was designed for gait restoration post-stroke, namely exoneuromusculoskeleton with balance sensing feedback (ENMS-BF). Mechanical combinations of the soft pneumatic muscle and the rigid exoskeleton, i.e., muscluloskeleton, can enable a compact size with a fast response rate, whose similar design was adopted in our previous study to provide mechanical assistance in joint extension for upper limb training after stroke [118]. Assistances from NMES and the mechanical fixation by the muscluloskeleton, together with the balance sensing feedback of vibrotactile, allow the attainment of the near-normal muscle coordination at the ankle joint with minimized compensatory movements. In addition, the FSRs under the paretic foot have been employed to capture the real-time plantar
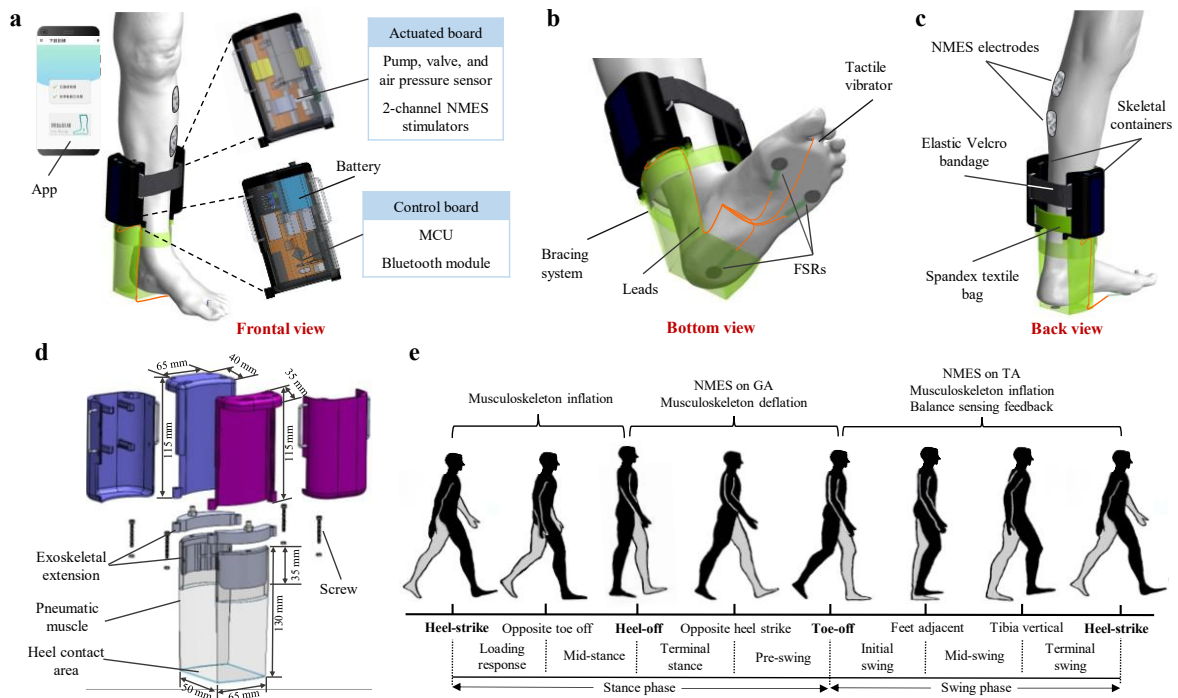
Figure 3-1. Overview of the designed ENMS-BF to restore gait functions during dynamic hemiparetic walking. (a) Frontal view, (b) bottom view, and (c) back view of the ENMS-BF worn onto the paretic lower limb. (d) Dimensions of the musculoskeleton with the exoskeletal extensions and the pneumatic muscle. (e) Illustration of dynamic assistance provided by the designed ENMS-BF during the specific gait phases in one cycle (the right side is indicated in black), adapted from [119, 120]. MCU, microprocessor-based control unit; NMES, Neuromuscular electrical stimulation; FSRs, force sensitive resistors; App, mobile application.

pressures, which can detect the dynamic gait events during the gait cycles [116] [24], to realize the phasic control of the assistance from the ENMS-BF.

This chapter aims to 1) present the designed plantar pressure driven ENMS-BF, which assists the post-stroke survivors in dynamic gait training with correction of foot drop and foot inversion; 2) assess the capability of assistance from the designed ENMS-BF on individuals with chronic stroke.

3.2 Methodology

The ENMS-BF was designed to restore gait functions after stroke by correcting the foot inversion and foot drop dynamically. It can be worn onto a stroke survivor's paralyzed lower limb with a total weight of 0.47kg (Figure 3-1a). The ENMS-BF has a soft-and-rigid musculoskeletal combination, i.e., musculoskeleton, which can provide mechanical fixation to the ankle joint in the stance phase of a gait cycle to prevent foot inversion. The musculoskeleton can be mounted onto the paretic ankle joint by an elastic bracing system with two skeletal containers located above the ankle joint bilaterally and a pneumatic muscle across the heel from the bottom of the foot (Figure 3-1a). NMES is delivered to the agonist muscles related to ankle dorsal/plantar flexion during the swing/stance phases respectively for correction of foot drop. Meanwhile, a tactile vibrator attached to the forefoot provides sensory cue to a user for self-correction of the stability in the terminal stance phase when plantar imbalance is detected by FSRs attached to the bottom of the foot. The assistive events provided by the ENMS-BF in a gait cycle is illustrated in Figure 3-1e. The ENMS-BF can be interfaced with a user via a smartphone application (APP) for easy operation (Figure 3-1a).
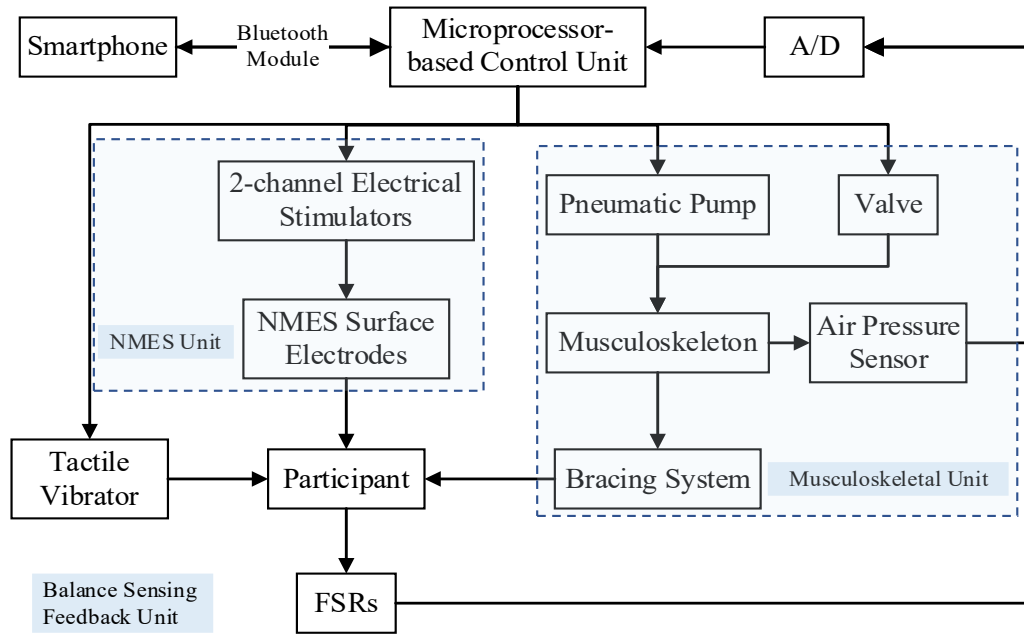
Figure 3-2. Systematic architecture of the control in the ENMS-BF. FSRs, force sensitive resistors, A/D, analog to digital convertor.

3.2.1 The ENMS-BF System Architecture

The systematic diagram of the ENMS-BF is illustrated in Figure. 3-2. The microprocessor-based control unit (MCU, STM32F103C8T6 microprocessor, STMicroelectronics Inc.) coordinates with the balance sensing feedback unit, the NMES unit, and the musculoskeletal unit and communicated with the smartphone (system of Android 10 with at least 3G network) via a Bluetooth module (HC-05, FEASYCOM. Co., Ltd). The whole system is powered by a 12-V rechargeable lithium battery for continuously working for 4 hours when fully charged. The electronic circuits of the system were separated into two flexible boards, i.e., the control

board and actuated board, which were fixed inside the two skeletal containers respectively, together with the battery (Figure 3-1a). Specifically, the actuated board contains the musculoskeletal unit and the NMES unit, and the control board includes the MCU and Bluetooth module. These two boards communicate through a miniature 20-pin flat data cable wrapped in a spandex textile bag between the two skeletal containers (Figure 3-1c).

The balance sensing feedback unit is composed of the tactile vibrator (Eccentric Rotating Mass, ERM vibration motor-E610, NFP-Motor Co., Ltd) and three FSRs (RP-C18.3-LT, LEGACT Co., Ltd) (Figure 3-1b). The vibrator is controlled by the MCU according to the inputs from the FSRs via an analog to digital (A/D) converter (Figure 3-2) with a sampling frequency of 6 Hz. The three FSRs are attached to the respective 1st, the 5th metatarsal heads, and the center of the calcaneus at the bottom of the paretic foot of a stroke survivor, with the purpose to detect the balance of plantar pressures between the medial and lateral forefoot, and to recognize dynamic gait events, e.g., heel strike, as we did previously [28]. The tactile vibrator (6.5 mm in diameter × 17.5 mm in height) can produce a constant vibration with a full magnitude (18,000 RPM with normalized amplitudes of 4.8 G) as the sensory feedback to a user when the imbalance condition is detected, and this vibration magnitude could be successfully perceived by unimpaired human subjects reported previously [121]. The vibrator is attached between the 1st and 2nd proximal phalanges, with a similar size and shape to the thorn of a flip-flop sandal, for the wearable design. Foot inversion with the reduced plantar pressure close to the 1st

metatarsal head was commonly observed in stroke survivors [122]. The position of the vibrator in this design is to give a close sensory reminder to the target plantar region of a user for self-correction during walking. Both the tactile vibrator and three FSRs are extended from the control board using fine copper leads (0.8 mm in diameter) with a miniature connector (8 × 3 × 1.5 mm) near the foot arch, whose sizes, or shapes, would not disturb gait or bring uncomfortable experience to a user when wearing the system into a sport shoe (Figure 3-4c).

There are 2 channels of electrical stimulators in the NMES unit, which interface with a user transcutaneously via surface electrodes to the target muscles for assistance of ankle dorsiflexion and plantarflexion (Figure 3-2). The 2-channel electrical stimulators can discharge symmetrical square pulse bursts with a frequency of 40 Hz, amplitude of 72V, and customized width of 0–300 μs in each pulse to vary the stimulation intensity, which is a range that can achieve effective muscular contractions in paretic muscles after stroke [123]. Two surface electrodes pairs (Axelgaard-Platinum-Electrodes-AXEG-00004, Axelgaard Manufacturing Co., Ltd. 5 × 5 cm in size) are attached to the following locations: (1) the area of common peroneal nerve (CPN) and the muscle belly of the tibialis anterior (TA), and (2) the motor points at the muscle belly of the gastrocnemius (GA). The minimal intensity of motor-level NMES will be delivered to the TA muscle for the muscular contraction of effective ankle dorsiflexion of an individual user, with an ankle joint range of motion (ROM) greater than 15° in dorsiflexion. The maximal intensity of sensory-level NMES will be applied to the GA muscle, providing sensory cue for

plantarflexion without muscular contraction. The motor-level NMES is only applied to the TA because that the extensors in lower limb, e.g., GA, commonly exhibited the involuntary muscular contraction in spasticity post-stroke, in contrast to the flexors, e.g., TA, presenting muscle weakness and discoordination post-stroke [124].

The musculoskeletal unit consists of a pneumatic pump (WP27B-6D, Micro Energy, Co., Ltd), a valve (WV110A-3A, Micro Energy, Co., Ltd), an air pressure sensor (MCP-H10, BOTLAND, Co., Ltd), and the musculoskeleton, i.e., an integration of two exoskeletal extensions at both ends of a pneumatic muscle and the two skeletal containers seated onto the respective exoskeletal extensions fixed with screws (Figure 3-1d). The inflation and deflation of the pneumatic muscle is controlled by the MCU in different gait events (Figure 3-2). The exoskeletal extensions, together with the pneumatic muscle, were wrapped into the elastic bracing system (spandex) for easy mounting to the ankle joint with a Velcro bandage. The exoskeletal extensions and the two skeletal containers were three-dimensional (3D) printed by photopolymer. The two skeletal containers can be fastened above the ankle joint bilaterally with two elastic Velcro bandages (14 × 3.5 cm), and the surface of the containers contacting the skin of the calf was designed to be curved for providing a comfortable and close contact to the curvature of the human body (Figure 3-1d). Additionally, a layer of sponge cushion (2 mm in thickness) is set between the container and the skin for comfortable wearing. The pneumatic
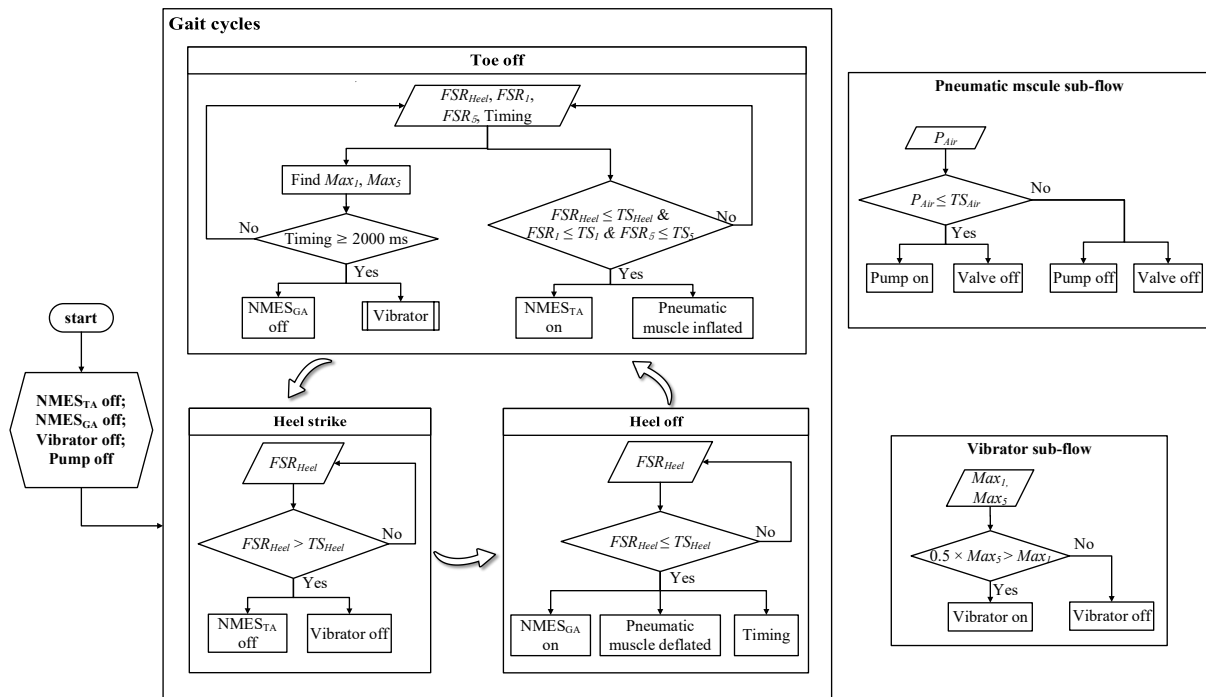
Figure 3-3. The flowchart of the plantar pressure driven control design during dynamic gait cycles.

muscle is a soft tube made by polyvinyl chloride (PVC) membrane. It was divided into two parts by compacting and sealing the PVC tube in the middle section with a length of 50 mm as the heel contact area (Figure 3-1d). The exoskeletal extensions sealed by epoxy at both ends of the PVC tube provide the connection between pneumatic muscle and the skeletal containers. The musculoskeleton can provide mechanical torque fixation from both medial and lateral sides of the ankle joint when the pneumatic muscle is inflated. In this work, we adopted two sizes of the musculoskeleton with the heights of the pneumatic muscle part of 130 mm and 115 mm, according to gender differences in anthropometrics of Asian adults [125]. The dimensional

design of the musculoskeleton is illustrated in Figure 3-1d and followed the lower limb anthropometrics [126].

The pneumatic muscle located bilaterally at the ankle joint can be inflated or deflated through an air tube with two heads connected to the pneumatic pump and the valve, sharing the same air pressure inside. Additionally, there is an air pressure sensor connected to the pneumatic muscle feeding back the real-time pressure to the MCU. The maximal air pressure inside the pneumatic muscle was preset as 50 kPa in this work, as an empirical value which could provide enough fixing torque to the ankle joint of persons after stroke and a safe value to maintain the stability of the materials in repeated usage.

3.2.2 Plantar Pressure driven Control Design

The plantar pressure captured by the three FSRs in gait cycles was adopted as the driving signal to control the ENMS-BF. The flowchart of the control design during a gait cycle is shown in Figure 3-3. Sequential assistance from the musculoskeletal, NMES, and balance sensing feedback units will be delivered to a user, according to the detected gait events of heel-off, toe-off, and heel-strike (bold in Figure 3-1e).

The assistance of the ENMS-BF was started from the heel-off event of the paretic limb detected by the real-time values of the FSRs under the respective 1st (FSR$_1$), the 5th metatarsal heads (FSR$_5$), and the center of the calcaneus (FSR$_{Heel}$) for a user after stroke, which is shown in Eq.

67

1,

$$FSR_{Heel} \leq TS_{Heel} \ and \ FSR_1 > TS_1 \ and \ \ FSR_5 > TS_5 \, , \qquad (1)$$

where FSR_{Heel}, FSR_1, and FSR_5 are the real-time values of the respective FSRs, and TS_{Heel}, TS_1, and TS_5 are the preset thresholds of the respective FSRs. Before using the ENMS-BF, the maximum values of each FSR would be measured by walking on the level ground (10-m) with a natural speed of a user when wearing the system but without any assistance. The initial threshold of each FSR was 50% of the maximum value, which was achievable for most stroke users to detect their gait events and adopted in the previous study [116]. Considering that some users after stroke could suffer from weakness of ankle plantarflexion to perform heel-off, the thresholds could be further fine-tuned for each user based on the trade-off between the false alarm or missing of the target gait events. In the heel-off event, the musculoskeleton would be deflated with the pump turned off and the valve open. Meanwhile, the sensory-level NMES to the GA muscle would be turned on for the assistance of ankle plantarflexion for 2 seconds, after which, the vibrator would be switched on until the heel-strike event was detected, if the imbalance condition was detected by the peak values of FSR_1 and FSR_5 within the 2 seconds. The vibration during the pre-swing and swing phases could be a reminder for correction of the stability in the terminal stance phase of the next gait cycle (Figure 3-3). The 2 seconds of terminal stance and pre-swing phases was set as an educational period for motor relearning of the plantarflexion, since some stroke survivors could not perform clear

plantarflexion because of the weakness at the ankle joint [13]. The imbalance condition was

recognized mathematically according to Eq. 2,

$$0.5 * Max_5 > Max_1, \tag{2}$$

where Max_5 and Max_1 are the peak values of the FSR$_5$ and FSR$_1$ during the 2 seconds, i.e., the

peak plantar force at the lateral forefoot (FSR$_5$) exceeds twice as much that at the medial

forefoot (FSR$_1$) in the 2 seconds of the terminal stance and pre-swing phases [28].

When the gait cycle entered into the toe-off event detected by the three FSRs, the

musculoskeleton would be inflated by the pump with the valve closed for the preparation of

the following stance phase, as shown in Eq. 3:

$$FSR_{Heel} \leq TS_{Heel} \ and \ FSR_1 \leq TS_1 \ and \ FSR_5 \leq TS_5, \tag{3}$$

where FSR_{Heel}, FSR_1, and FSR_5 are the real-time values of the respective FSRs, and TS_{Heel},

TS_1, and TS_5 are the preset thresholds of the respective FSRs. Meanwhile, the motor-level

NMES to the TA muscle would be turned on to evoke muscle contraction of ankle dorsiflexion

until the heel-strike event was detected. In this study, with the muscular contraction of ankle

dorsiflexion during the swing phase, heel-strike event was represented as the detection of the

three FSRs in Eq. 4,

$$FSR_{Heel} > TS_{Heel} \ and \ FSR_1 \leq TS_1 \ and \ FSR_5 \leq TS_5, \tag{4}$$

where FSR_{Heel}, FSR_1, and FSR_5 are the real-time values of the respective FSRs, and TS_{Heel},
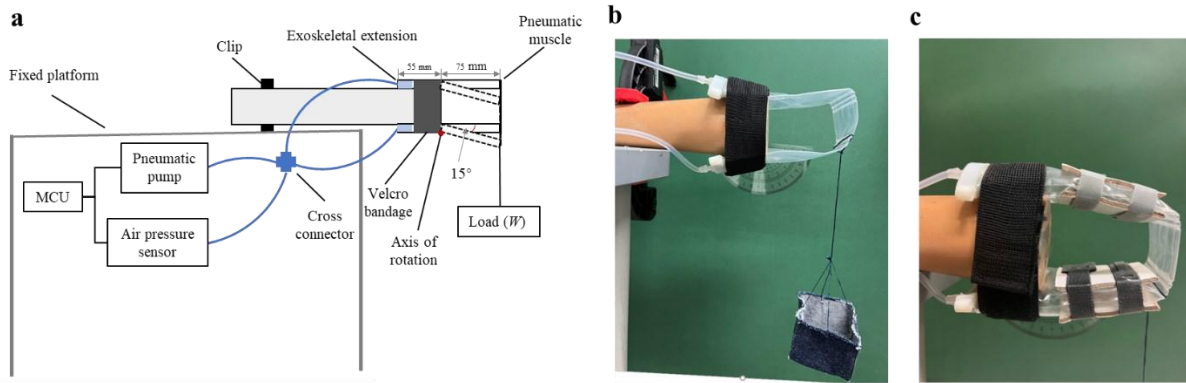
Figure 3-4. Pressure/torque transmission and assistive capability of the ENMS-BF. (a) The schematic diagram of the experimental setup for the measurement of pressure/torque properties of the musculoskeleton (b) without air volume limit and (c) with air volume limit.

TS_1, and TS_5 are the preset thresholds of the respective FSRs. Then, the vibrator, and the motor-level NMES to the TA muscle would be turned off. Meanwhile, when the air pressure inside the pneumatic muscle reached to 50 kPa, the pump would be turned off and the valve would remain closed to maintain the inner air pressure for a constant torque support to the ankle joint during the loading response and mid-stance phases, until the next heel-off event was detected.

3.2.3 Pressure-to-torque Properties of the Musculoskeleton

The musculoskeleton can convert the pressure inside the pneumatic muscle to torque support to the ankle joint together with the skeletal structures. The pressure/torque transmission properties and the response rate were measured by the experimental setup as shown in Fig. 3-

4. The pressure/torque properties were evaluated in two configurations, i.e., Fig. 3-4a&b (without air volume limitation) and Fig. 3-4c (with different air volume limitations), which simulated the scenarios of wearing the device in a shoe with different tightness. The integrated structure of the pneumatic muscle and the skeletal extensions was fastened onto a cylinder rod (65 mm in diameter), to simulate the calf above the ankle joint when wearing the musculoskeleton and was positioned on a horizontal platform for evaluation on the torque against foot inversion. Meanwhile, the pneumatic muscle part dangled away from any support with the lower edge of the Velcro bandage as the axis of rotation, and the distance from the bottom of heel and the axis of rotation was set as 75 mm (Fig. 3-4a), according to the average foot height of the ankle joint in Asian adults [126]. In the setting of Fig. 3-4c, each side of the pneumatic muscle was clamped by two splints (cardboard, 3g in each weight) with two Velcro bandages (1g). The total weight of the splints and bandages was around 15g, which would be considered in the later calculation of torque.

Then, the tolerance of the inflated musculoskeleton with varied inner pressure to different inversion torques was measured with the configuration of no limitation on the air volume first. The musculoskeleton was inflated to the preset maximum air pressure of 50 kPa (error range: ±2.5 kPa) with the valve closed, and the position of the dangling pneumatic muscle around the axis of rotation was regarded as the initial stage (i.e., 0° at the horizontal position). Next, a sandbag with variable weight was hung to the pneumatic muscle (Fig. 3-4a) to evaluate the

tolerance to torques generated by the hanging sandbag. The weight of the sandbag was increased till the inflated pneumatic muscle flexed around the rotation axis by an angle of 15° for a preset inner pressure of the pneumatic muscle. It was because that the foot inversion of 15° was typically regarded as the threshold angle to cause ankle sprains in human biomechanics [127]. The change in the rotation angle was measured by a protractor, whose midpoint was aligned with the rotation center of the dangling pneumatic muscle. Then, the air pressure inside the musculoskeleton was decreased from 50 kPa to 5kPa with a step of 5 kPa (±1 kPa) to record the weight of the sandbag and the corresponding inner air pressure. The mechanical torque was then calculated as follows,

$$torque = L \cdot W \cdot \cos 15° \tag{5}$$

where L is the distance between the rotation axis and the bottom of heel (i.e., 0.075m, Fig. 2A) and W is the weight of load (i.e., the sandbag together with the weight on the pneumatic muscle).

Then, the peak inversion torque and the associated response rate for the musculoskeleton were measured with different air volumes (Fig. 3-4c). Firstly, the maximum air volume of the fully inflated musculoskeleton (50kPa without air volume limit) was 240 milliliters (ml), which was measured by a gas-flowmeter (SFM3003, Sensirion China Co. Ltd.). Secondly, different volumes of air, i.e., 240, 210, 180, 150, 120, and 90 ml (quantified by the gas-flowmeter), were inflated into the pneumatic muscle without loading weight in the sandbag. Then, the splints were fastened to the pneumatic muscle by the adjusted Velcro bandages, to make the inner air

72

Table 3-1. Marks of Varying Assistance Schemes from the ENMS-BF.

Notation of assistance schemes	Description
N0M0V0	None of assistance
N1M0V0	Assistance from the NMES only
N0M1V0	Assistance from the musculoskeleton only
N0M0V1	Assistance from the balance sensing feedback only
N1M1V1	Assistance from the NMES, the musculoskeleton, and the balance sensing feedback

pressure reach the preset maximum of 50 kPa ($\pm$2.5 kPa). The peak inversion torque against the fully inflated musculoskeleton (with different air volumes) was measured and calculated as in Fig. 3-4a. Thirdly, with the corresponding configuration of fastened splints at different air volume limitations, the musculoskeleton was fully deflated first, and then was inflated again to 50kpa for measuring the inflation time, i.e., the response rates of different air volume. Each measurement on the pressure/torque transmission and the response rate was repeated thrice.

3.2.4 Evaluation of the Capability of Assistance from the Developed ENMS-BF

The system capability of the ENMS-BF was assessed with chronic stroke survivors, to investigate the assistive contributions of the musculoskeleton, NMES, and the tactile vibrator to ground ambulation, with five assistance schemes (Table 3-1).

After obtaining ethic approval from the Human Subjects Ethics Sub-committee of the Hong Kong Polytechnic University, ten participants with chronic stroke were recruited in the

evaluation of assistive capability, all of whom signed the informed consent before the evaluation. The inclusion criteria in this study were as follows: (1) at least 6-month following the onset of stroke; (2) without inflammatory disease or pathogenic alterations in the lower extremity joints; (3) no visual, cognitive, or attention deficits as measured by the Mini-Mental State Examination (MMSE) score >21 [128]; (4) the spasticity of the ankle joint $\leqslant 3$ as measured by the Modified Ashworth Scale (MAS) [32]; (5) mild-to-moderate motor impairment in the affected lower limb with gait abnormalities of foot drop and foot inversion, measured by the Fugl-Meyer Assessment (FMA, total score on the lower extremity) $\geqslant 16$ [30] [129], Functional Ambulatory Category (FAC) $\geqslant 3$ [37], and Berg Balance Scale (BBS) $\geqslant 40$ [36]; (6) capable of walking without manual assistance for extended periods (at least 15-min).

In an evaluation session, each participant was mounted with the ENMS-BF on the paretic lower limb and had 10 mins to get familiar with the respective assistance of NMES, musculoskeleton, and the tactile vibrator as a warm-up. Then, the participant was instructed to walk on a 6m level walkway cleared of obstacles with an assistance scheme of the ENMS-BF at a natural speed. The five assistive schemes were conducted in a random order with each scheme repeated thrice. A 5-min break was provided every three consecutive trials to avoid fatigue. In the walking, each participant used a quad cane and was followed by an experimental operator for safety.

An eight-camera motion tracking system (Vicon Nexus 2.12.1, Vicon Motion Systems Ltd.), synchronized with two force platforms (OR6, AMTI, Watertown) embedded midway on the 6-

m level walkway, sampling at 250Hz, was utilized to measure the kinematic angles at the ankle joint during ground walking with different assistance from the ENMS-BF. In the sagittal and frontal planes, dynamic angle values of the ankle joint were investigated, because of the representative poststroke foot drop and inversion mainly captured in these two planes [112]. A built-in lower body marker set, i.e., Plugin Gait Lower Body Model [130], was adopted with 16 spherical reflective markers (14 mm in diameter) bilaterally attached to at the anterior superior iliac spine, the posterior superior iliac spine, the lateral thigh, the flexion-extension axis of the knee, the lateral shanks, the lateral malleolus, the heel, and the second metatarsal head. Then, kinematic parameters i.e., peak angles of the ankle, knee, and hip joints in both stance and swing phases, and GRFs of the affected limb were calculated using the Dynamic Plugin Gait Model (low-pass filtered at 6 Hz by a 4th-order Butterworth filter) [131]. The standard deviation (SD) of ankle inversion/eversion angles (stance phase) and the peak angle of ankle dorsiflexion (swing phase) on the affected side were calculated to quantify the stability and range of motion (ROM) at the ankle joint, respectively.

In the evaluation of assistive capability of the ENMS-BF, the normality tests of the SD of ankle inversion/eversion angles and the peak angles of ankle dorsiflexion were conducted using the Shapiro-Wilk test with a significant level of 0.05[132]. The peak angles of ankle dorsiflexion followed the normal distribution, while the SD of ankle inversion/eversion angles did not obey it. Thus, one-way repeated measures analysis of variance (ANOVA) with
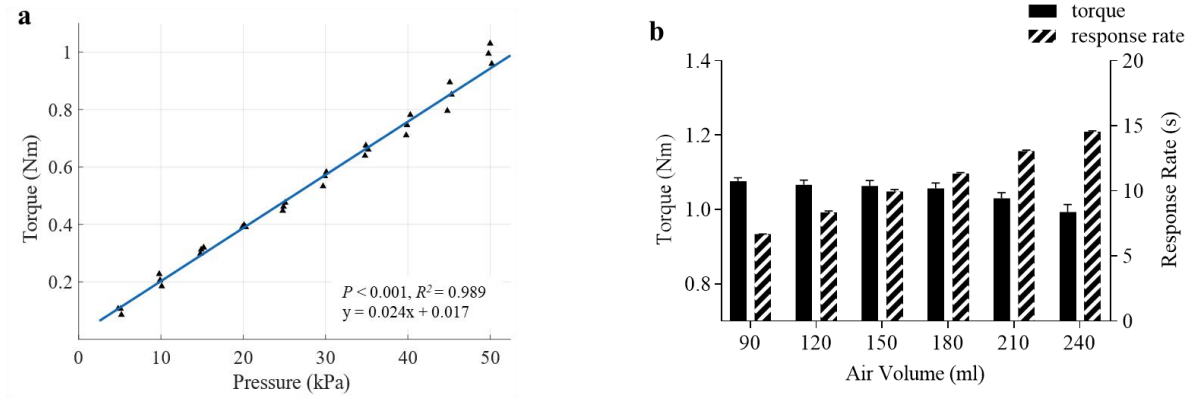
Figure 3-5. Pressure/torque transmission and assistive capability of the ENMS-BF. (a) Pressure/torque relationship of the inflated musculoskeleton without air volume limit. (b) The peak torque and response time of the fully inflated musculoskeleton (50kPa) with different air volumes.
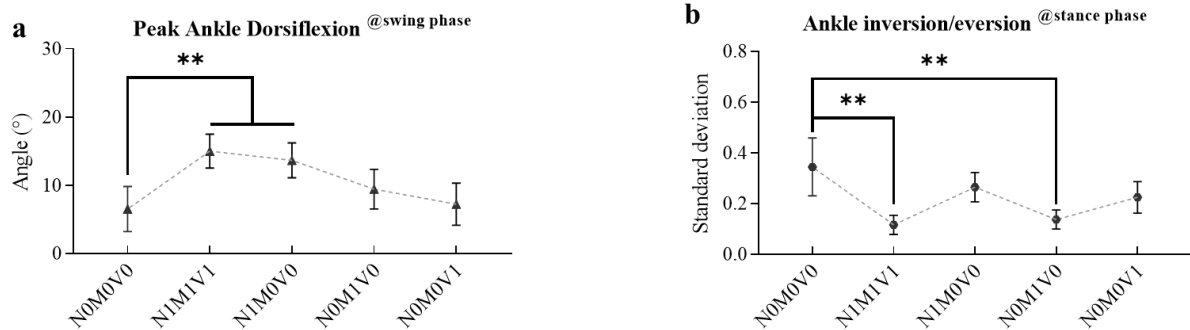
Figure 3-6. Comparisons of (a) the peak angle of ankle dorsiflexion during the swing phase and (b) the standard deviation (SD) of ankle inversion/eversion angles in the stance phase, under the five different assistance schemes for evaluation of the assistive capability of the ENMS-BF. Significant differences are indicated by "**" (P<0.01).

Bonferroni post hoc test was used to evaluate the differences of the peak angles of ankle dorsiflexion across the five assistive schemes. Friedman tests with Wilcoxon signed-rank post hoc test (Bonferroni correction), were performed to evaluate the differences in the SD of ankle inversion/eversion angles across the five assistive schemes.

3.3 Results

3.3.1 Pressure-to-torque properties of the Musculoskeleton

The pressure/torque transmission properties and the response rate of the inflated musculoskeleton is shown in Fig. 3-5. There was a significant linear relationship between the inner pressure and assistive torque of the musculoskeleton ($P<0.001$, $R2 = 0.989$) (Fig. 3-5a). The maximal inner pressure of the inflated musculoskeleton reached 50 kPa and the corresponding torque was 0.99 ± 0.03 Nm (mean $\pm$ SD), with the torque-to-weight ratio at 9.9 Nm/kg (because the weight of the musculoskeleton was 100g). Without loading weight in the sandbag, the inner air pressure of the musculoskeleton reached the maximum of 50 kPa within 14.54 ± 0.13 s (Fig. 3-5b, air volume of 240 ml). When the air volume was limited at 210, 180, 150, 120, and 90 ml, the assistive torque against the inflated musculoskeleton (50 kPa) were above 1 Nm (1.06 ± 0.03 Nm), with a minimum response rate of 6.68 ± 0.01 s, i.e., limiting the air volume to 90ml.

Table 3- 2 Means and 95% confidence intervals for the peak angle of ankle dorsiflexion (swing phase) and the SD of ankle inversion/eversion angles (stance phase) on the affected side, measured under the five assistive schemes, as well as the probabilities of the statistical analysis.

Peak angles (°) @sagittal plane	N1M1V1	N0M0V0	N1M0V0	N0M1V0	N0M0V1	One-way Repeated Measures ANOVA	
	Mean (95% confidence interval)					P (Partial η^2)	F
Ankle dorsiflexion @swing phase	14.99 (9.37–20.62)	6.52 (-0.92–13.97)	13.66 (7.90–19.41)	9.43 (2.83–16.02)	7.21 (0.22–14.20)	0.002** (0.689)	19.94
Angle standard deviation (°) @frontal plane	N1M1V1	N0M0V0	N1M0V0	N0M1V0	N0M0V1	Friedman Test	
	Mean (95% confidence interval)					P	M
Ankle inversion/eversion @stance phase	0.1161 (0.0309–0.2013)	0.3445 (0.0866–0.6025)	0.2646 (0.1345–0.3946)	0.1373 (0.0534–0.2211)	0.2244 (0.0836–0.3653)	0.000***	28.24

3.3.2 Assistive capability of the ENMS-BF

Fig. 3-6 show the peak angles of ankle dorsiflexion (swing phase) and the SD of ankle inversion/eversion angles (stance phase) on the affected side, with different assistive schemes. With the assistive schemes of N1M0V0 and N1M1V1, the peak angles of the ankle dorsiflexion were significantly higher than that without any assistance from the system (N0M0V0) (Fig. 3-6a, $P<0.01$). Under the assistive schemes of N0M1V0 and N1M1V1, the SD of ankle inversion/eversion angles was significantly lower (Fig. 3-6b, $P<0.01$), compared to no assistance from the system (N0M0V0). No significant difference was found in the peak GRFs and the other kinematic parameter, i.e., peak angles of the knee and hip joints in the sagittal and frontal plane, across the five assistance schemes. Detailed statistics of kinematics are shown in Table 3-2 .

3.4 Discussion

The plantar pressure driven ENMS-BF was designed to facilitate post-stroke gait training by dynamic corrections of foot drop and foot inversion. The pressure-to-torque properties of the proposed musculoskeleton were measured and the capability of assistance from the ENMS-BF was evaluated with varying assistance strategies of the musculoskeleton, NMES, and the tactile vibrator, on individuals with chronic stroke.

3.4.1 Design and assistive capability of the ENMS-BF

The ENMS-BF integrated the musculoskeleton, NMES, and vibrotactile feedback to correct foot drop and foot inversion in dynamic gait training post-stroke. The total weight of the designed ENMS-BF is around 0.47 kg, which is lighter in weight compared to the unilateral robotics for post-stroke gait training developed by other research groups, e.g., the soft exosuit (0.9 kg alongside the paretic limb) [25] and the robot-assisted AFO (0.5 kg to the waist and 0.5 kg at the ankle joint) [133]. Besides, the compact design of the mobile ENMS-BF (i.e., the wireless communication via Bluetooth) makes it feasible to mount the whole system on the ankle joint bilaterally. As revealed by the oral feedback from the ten stroke participants, they could walk comfortably and lightly wearing the designed ENMS-BF, without the hindrance of a power cord or data-communication cable. The calf-fit cambered skeletal container and the soft pneumatic muscle, together with the bracing system, enable a comfortable wearing experience of the ENMS-BF. No discomfort of wearing experience was reported from the ten

recruited participants in the gait training. The FSRs are attached to the specific locations under the foot sole by medical rubberized fabric, which means that the ENMS-BF can be customized for individual users during the gait training, without the limitation by shoes.

The mechanical torque from the musculoskeleton was applied to the ankle joint as the joint fixation in the frontal plane, to avoid foot inversion in the paretic gait pattern of stroke survivors, which could be caused by muscle spasticity in their ankle plantar flexors [17]. When the maximum pressure inside the musculoskeleton reached 50 kPa, the musculoskeleton provided a maximum torque of 1 Nm across the ankle joint(Figure 3-5a), which is greater compared to the peak torque of ankle inversion (i.e., 0.5 Nm) produced by the plantar flexors, e.g., the medial gastrocnemius [134]. The musculoskeleton can provide fixation (i.e., the torque of 1 Nm) to avoid foot inversion during the gait training for the chronic stroke participants in this study. Besides, five participants (amongst the ten participants) wear an AFO in their daily living, and all of them expressed that they could walk confidently with the mechanical fixation by the musculoskeleton during the ENMS-BF-assisted gait training. All the participants perceived the mechanical fixation at the ankle joint from the musculoskeleton with the inner pressure reaching 30 kPa, corresponding to the torque of 0.6 Nm at the ankle joint (Figure 3-5a), which exceed the peak ankle inversion torque of 0.5 Nm caused by plantar flexors [134] and could provide adequate mechanical fixation at the paretic ankle joint. The pressure inside the musculoskeleton could be inflated to 50 kPa within 6.68 s, when the air volume inside the

musculoskeleton was limited to 90 ml (Figure 3-5b). Moreover, for the adaptation of the educational period of relearning plantar balance and ankle plantarflexion during the ENMS-BF-assisted gait training, the participant was instructed to walk with a low speed, which enabled the air pressure inside the musculoskeleton to attain 30–50 kPa to provide the mechanical fixation, i.e., the corresponding torque of 0.6–1 Nm, at the ankle joint in the stance phase of the affected side.

Most stroke survivors suffered from foot drop and foot inversion, which causes their difficulties in ankle dorsiflexion during the swing phase and ankle stability during the stance phase [112]. Thus, assisting the ankle joint to achieve increased angle of dorsiflexion and improved is essential in poststroke rehabilitation of hemiplegic gait [17]. With the assistance from NMES (N1M0V0 and N1M1V1), the peak angle of ankle dorsiflexion in the sagittal plane was significantly higher than that measured without assistance (N0M0V0) (Figure 3-6a). This result indicated that ankle dorsiflexion was sensitive to the assistance of NMES, and the developed ENMS-BF was immediately effective for the correction of foot drop poststroke. In the frontal plane during the stance phase, the SD of ankle inversion/eversion angle when applying mechanical support (N0M1V0 and N1M1V1) was significantly lower, compared to that measured without assistance from the developed ENMS-BF (N0M0V0) (Figure 3-6b). These results implied that the ENMS-BF had immediate effects on corrections of foot drop (swing phase) and foot inversion (stance phase), which could be capable for long-term rehabilitation

after stroke. Although there was no significant difference with the assistance of balance sensing feedback (vibrator), the capability was reported in the previous study [28]. Its long-term rehabilitative effect could be investigated in the pilot trial of gait training poststroke.

3.5 Periodic Summary

A novel ENMS-BF was developed driven by plantar pressures, integrating the two-channel NMES, vibrotactile feedback, and musculoskeleton to correct foot drop and foot inversion for chronic stroke survivors with lower limb motor impairment. The developed system could be worn bilaterally above the paretic ankle joint, with a lightweight and compact design, for intensive and repetitive gait training. The results indicate that the assistive torque from the musculoskeleton could provide mechanical fixation at the ankle joint during the dynamic gait training, and the ENMS-BF was immediately effective for corrections of foot drop and foot inversion in poststroke rehabilitation of hemiplegic gait.

CHAPTER 4

INVESTIGATION OF THE FEASIBILITY AND REHABILITATION OF THE ENMS-BF WITH INDIVIDUAL AND SELF-HELP PAIRED GAIT TRAINING

4.1 Introduction

The ENMS-BF was a mobile multi-modal robot suitable for self-help training in unconventional environments, e.g., at home or outdoors, with the compact and light-weighted design of the whole system. The team designed a mobile ENMS for multi-joint coordinated training of the upper limb previously, which has been successfully applied to the self-help telerehabilitation in home environments in Hong Kong during the COVID-19 epidemic, where outpatients could continue the device-assisted upper limb training with remote professional supervision [135]. However, the remote supervision between the professional and the patient at home limited the social interactions during the training, in comparison to the scenarios in the traditional treatment rooms where one therapist coordinated a group of patients in physical practices with mutual communications and affective supports. It has been found that the social interactions besides the physical treatments are equally necessary for a person after stroke to be well motivated and committed in the long-term rehabilitation [29], as post-stroke motor restoration is a motor relearning process requiring incentive mechanism to promote persistence in acquiring motor skills [136]. Therefore, a cyber physical social system (CPSS) based paired

83

gait training with rewarding schemes was further developed in this work. It could provide a platform to facilitate 1) remote interactive social communication among different patients when their training progresses were paired together; 2) remote progress coordination by the professional on the paired patients for the rehabilitative management on multiple patients together. In the CPSS-based ENMS-BF-assisted gait training, ENMS-BF provided the physical contacts with individual patients and delivered the parameters of rehabilitative progress to the professional via the cyber network, which also built up the tele-social links among all parties. To our knowledge, self-help remote rehabilitation management based on CPSS incentives has not been well studies.

The purposes of this chapter were to 1) investigate the viability and rehabilitation effects of the designed ENMS-BF with individual gait training supervised by a professional; 2) explore the viability and training effectiveness of the self-help CPSS-based paired gait training with distanced monitoring by a professional.

4.2 Methodology

After the assistive capability evaluation of the ENMS-BF, pilot clinical trials were carried out to investigate the rehabilitative effect of the ENMS-BF on gait restoration with close supervision from a professional, which simulated the one-to-one manual practice in the conventional post-stroke services (individual training). Then, we also conducted another independent pilot trial on self-help ENMS-BF assisted gait training when participants were

Table 4-1. Demographic characteristics of the participants recruited in the individual group and CPSS group with chronic stroke.

Training Group	Gender Female/ Male	Stroke Types Hemorrhagic/Ischemic	Side of Hemiparesis Left/Right	Age (years) Mean ± SD	Years after onset of stroke Mean ± SD
Individual-	6/6	7/5	6/6	56.5 ± 11.5	7.5 ± 5.7
CPSS-	4/8	8/4	7/5	51.3 ± 10.7	7.7 ± 5.1

paired in the training progress with remote professional supervision/coordination based on a CPSS platform associated with the ENMS-BF (CPSS-based paired training). This was to evaluate the feasibility and rehabilitative effects of the remote management on the rehabilitation progresses by cyber social interactions with minimized physical contact, as in the pandemic with restricted social distances.

A total of 39 stroke survivors from local areas were screened using the same inclusion criteria as in the evaluation of the system assistive capability. Finally, twelve chronic stroke participants satisfying the inclusion criteria were recruited in the individual gait training (individual group). Then, another group of twelve participants suffering from hemiparetic gait pattern post-stroke and satisfied the criteria, conducted the CPSS-based paired gait training (CPSS group). The sample size (n=12) was estimated using G*power with the preliminary score of FMA from the previous study [133]. All the participants signed the written informed consents before the
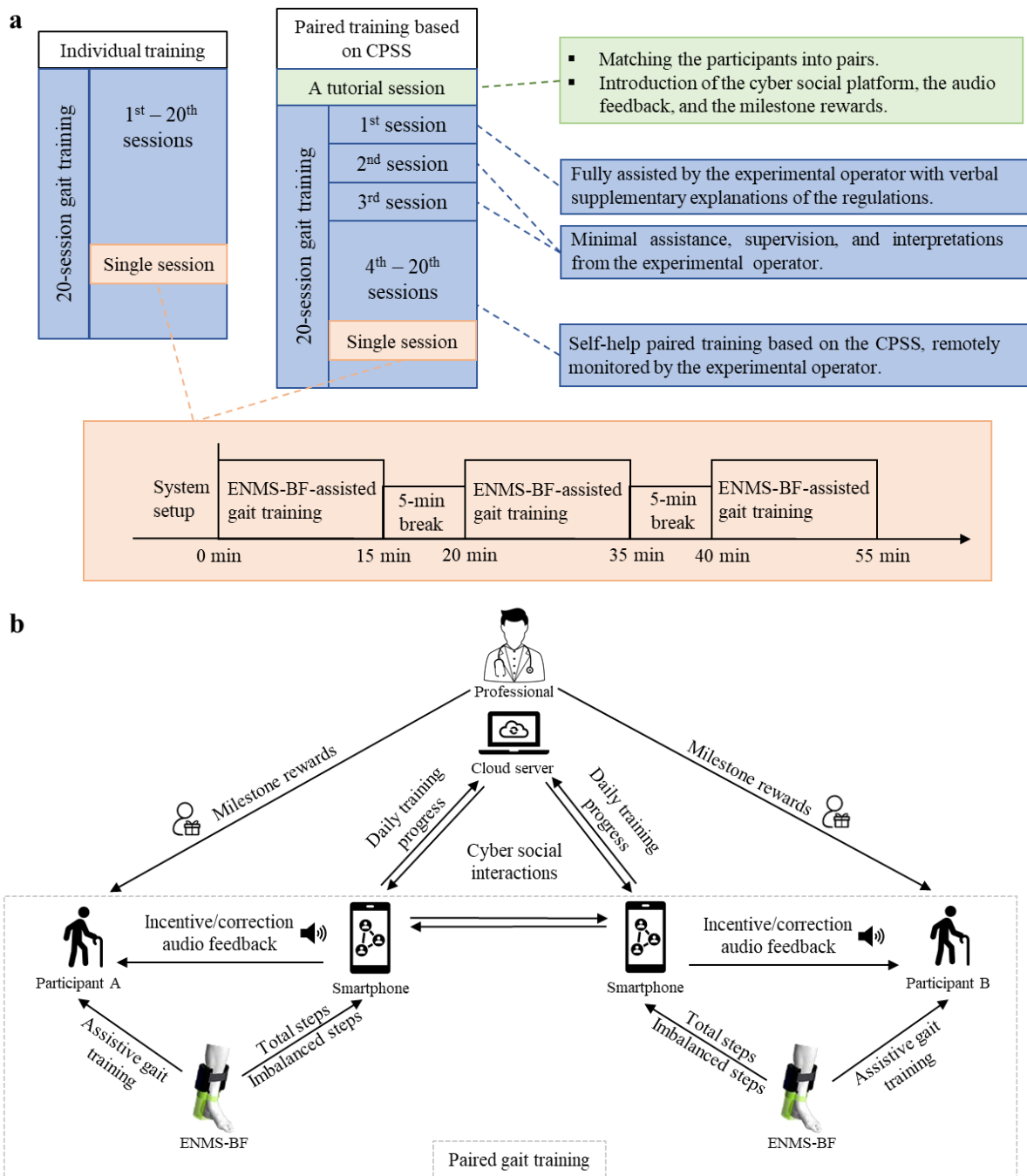
Figure 4-1. (a) The training protocol of the individual and CPSS-based paired gait training presented with timeline. (b) The systematic architecture of the CPSS-based paired training assisted by the ENMS-BF.
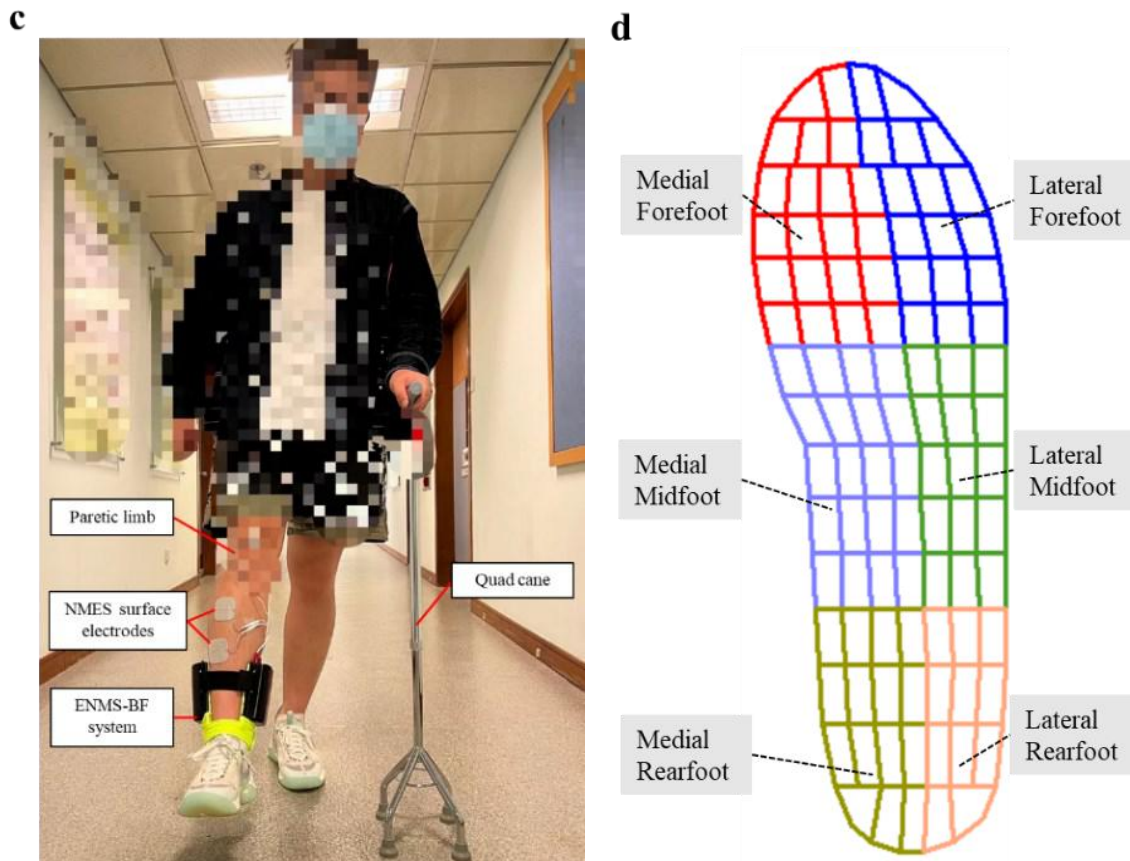
Figure 4-1. (c) The system setup of the ENMS-BF-assisted gait training in the 25-m straight corridor. (d) The schematic diagram of foot regions: Medial Rearfoot, MR; Lateral Rearfoot, LR. Medial Midfoot, MM; Lateral Midfoot, LM; Medial Forefoot, MF; Lateral Forefoot, LF.

training. Table 4-1 presents the statistical characteristics of the participants in each group. Figure 4-1a shows the training protocol of the individual and paired gait training

4.2.1 Individual Gait Training with Close Professional Supervision

All the participants in the individual group received the 20-session gait training assisted by the ENMS-BF, with a training intensity of 4–5 sessions weekly, within five successive weeks.

Before each session of gait training, an experimental operator assisted the participant in the system setup, which included wearing the ENMS-BF and calibrations of the preset parameters, i.e., thresholds of the three FSRs, the 2-channel NMES, and the maximal air pressure. Then, the participant was instructed to walk over the level ground along a straight corridor (25m long level ground) cleared of obstacles with minimal turning points for 45 minutes, with the assistance from the ENMS-BF (Figure 4-1c). The experiment operator walked alongside the participant to ensure his/her safety from falling and would provide verbal reminders to the participant to focus on the assistance from the ENMS-BF, enhancing the engagement in the gait training, particularly in the first several sessions of the training program. During the '2-second' educational period in the ENMS-BF-assistance, a participant was instructed to hold for a while from the heel-off to toe-off events of the paretic limb, the length of which should be long enough to cover the educational period, with the purpose of helping the participant to relearn the plantar balance and ankle plantarflexion. Additionally, the same quad cane was provided in the gait training for safety and a 5-min rest interval was allowed within two successive 15-min gait training to avoid fatigue.

4.2.2 Self-help CPSS-based Paired Gait Training with Cyber Social Interactions

In the CPSS group, each participant received the 20-session ENMS-BF-assisted gait training by pairing with another participant and sharing quantified training progress throughout the program based on the cyber platform. The cyber social interactive platform was established

based on the ENMS-BF-assisted training, with incentive schemes between the pair and remote communication channels among the experimental operator and the paired participants. The overview of the CPSS-based paired training is shown in Figure 4-1b, including the cyber channels for social interactions among all parties, the incentive/correction audio feedback provided based on the ENMS-BF-assisted training, and the milestone rewards along the training program.

Before the commencement of the paired training, an online tutorial session was conducted to match the 12 participants into 6 pairs, according to their baseline clinical scores of FMA, which was measured thrice before the training by the blinded assessor. A stroke participant with the FMA below 20 would own priority to pair with another participant with the FMA > 20, which was set for enhancing the complementary benefits in the paired training [137]. Meanwhile, operational rules of the CPSS-based paired gait training, including the cyber social interaction channels, incentive/correction audio feedback, and the milestone rewards, were interpreted to the participants in the tutorial session. In the first session of the CPSS-based paired gait training, the experimental operator fully assisted the participant in the system setup and supervised the gait training with supplementary explanations of the CPSS-based training regulations. In the second and third sessions of the paired training, a caregiver, who was blinded to the pilot clinical trial, assisted in the system setup of the ENMS-BF with minimum assistance, observation, and interpretation by the experimental operator. In the following CPSS-based

paired training (i.e., the 4-20th sessions), the participant completed the gait training with the caregiver assisting in the system setup and following during the training to avoid falling. The experimental operator monitored the self-help gait training with a distance away from the patient and provided help if required (e.g., the possible situation of a broken FSR lead). For safety issue in the pilot ENMS-BF-assisted dynamic gait training, all participants performed the CPSS-based paired training in the campus, with distanced monitoring from the experimental operator, to simulate the remote management in the self-help CPSS-based telerehabilitation assisted by the ENMS-BF, when the patients and caregivers were within the sight of the operator. In each session of the CPSS-based ENMS-BF-assisted paired training, a participant walked along a 25-m corridor for 45 min with the quad cane, which was same with that in the individual training. A 5-min rest interval was allowed within two successive 15-min gait training to avoid fatigue. The training intensity and frequency of each participant in the CPSS group were same as that in the individual group.

During each session of the CPSS-based training, incentive/correction audios would be fed back to a participant via the smartphone according to the real-time cumulatively total steps and imbalanced steps from the ENMS-BF. After each session of the paired gait training, the quantified daily training progress, i.e., the total steps and imbalanced steps, would be uploaded/stored in the cloud server and notified to both participants in the same pair via a common cyber social platform, i.e., WhatsApp, to establish the cyber social interactions

between the paired participants, without face-to-face physical contact. The professional would

monitor the training progresses of the paired participants and interact with the pair in the cyber

social platform, based on the log data in the cloud server. The professional also coordinated the

dialogue in the cyber communication of the paired participants, with the purpose to promote

the motivation of completing the training by the participants and encouragements between the

pair to strengthen the social link. Milestone rewards would be delivered to the participant in

the midway (i.e., the 10th session) and end of the 20-session training as the material incentives

to avoid drop out through the training program.

4.2.3 Outcome Measures

In this study, the rehabilitation effectiveness of the ENMS-BF-assisted gait training were

assessed by clinical assessments, kinematic and kinetic parameters, temporal-spatial gait

parameters, and plantar pressure distributions. These assessments were conducted before the

gait training (Pre), immediately after the 20th training session (Post), and three months after

the last training session (3-month FU), by a blinded assessor who was unknown about the

training protocols. The clinical assessment was measured thrice before the training within 2

weeks for evaluating the baseline stability.

The clinical assessment adopted in this study included: (1) the FMA for lower limb assessment

of motor function with the full score of 34 [30]; (2) the MAS at the ankle, knee, and hip joints

for the examination of joint spasticity during passive muscle stretching with 4-level scale [32];

(3) the FAC for assessing functional ambulation on the level and nonlevel surfaces with 6-level scale [37]; (4) the BBS for measuring balance ability with the full score of 56 [36]; (5) the 10-Meter Walk Test (10MWT) for measuring walking speed [35]. In this study, the FMA was recognized as the primary outcome.

These five clinical scores were supplemented by kinematic and kinetic investigation for the interpretations of the changes in spatial-temporal gait performance at the Pre, Post, and 3-month FU assessments. The same motion capturing configuration as in the evaluation of assistive capability, synchronized with two force platforms (OR6, AMTI, Watertown) embedded midway on the 6-m level walkway, was used for the investigation. After attachments of the kinematic markers to the target positions, participants were instructed to walk along the 6-m level walkway at their natural speed holding the quad cane, without wearing the ENMS-BF. At least three trials of gait cycles were selected for further investigation on the GRFs at the affected side, when the affected foot wholly located in the force platform. A 5-min rest interval was permitted every three successive trials to prevent fatigue. After low-pass filtered (4th-order Butterworth filter) of 6 Hz, all kinematic and kinetic data were analyzed using the Dynamic Plugin Gait Model [131]. Kinematic parameters of both limbs, i.e., peak angles of the ankle, knee, and hip joints in the sagittal and frontal plane, kinetic parameters of the affected limb, i.e., the peak GRFs, and temporal-spatial gait parameters of both limbs, i.e., the walking speed, stance time, swing time, and step length, were obtained from the three trials of each participant

92

as the metrics of gait performance. The peak GRFs were normalized to the body weight and all the kinematic and kinetic parameters were averaged across the repeated trials.

The plantar pressure distributions in dynamic gait of each participant were further measured utilizing an in-shoe measurement system (Novel Pedar-X system, Novel Inc.) for evaluation of the spatial-temporal gait performance and plantar balance in different portions [28] [138] [139]. In this experiment, each participant (without wearing the ENMS-BF) was instructed to walk along the level 6-m level walkway at a natural speed with the quad cane with a repletion of three trials. Parameters of both limbs, i.e., peak plantar pressures at the six regions (Figure 4-1d), i.e., medial rearfoot, MR; lateral rearfoot, LR; medial midfoot, MM; lateral midfoot, LM; medial forefoot, MF; lateral forefoot, LF, were obtained from the repeated trials as the metrics of plantar pressure distributions. Meanwhile, the spatial-temporal gait parameters of both limbs, i.e., the contact area, were further calculated from the plantar pressure measurements.

For the CPSS group, the same clinical assessment as in the individual group was conducted to investigate the rehabilitative effects. The quantified social interactions between the pairs, and the training parameters recorded by the App in each session for a participant, i.e., the total steps and imbalanced steps, were evaluated to understand the interaction between the social linkage and rehabilitation progress.

4.2.4 Statistical Analysis

Statistical Package for Social Science (SPSS, version 22.0.0.0, IBM Corp.) was used for the statistical analysis. The normality tests of the clinical scores (i.e., the BBS, FMA, and the 10MWT), kinematic and kinetic parameters, plantar pressure distribution parameters, and temporal-spatial gait parameters were conducted with the Lilliefors method with a significant level of 0.05 [132], all of which were confirmed to obey the normal distribution (P > 0.05). For the normal-distributed clinical scores and kinetic parameters of the affected limb, one-way repeated measures analysis of variance (ANOVA) was performed to investigate the intra-group differences at the three time points (i.e., Pre, Post, and 3-month FU) using Bonferroni post hoc tests. For the clinical scores of MAS and FAC, which are ordinal scales, Friedman tests were performed to assess the differences in relation to the time points using Wilcoxon signed-rank test as the post hoc test. For the kinematic parameters, plantar pressure distribution parameters, and temporal-spatial gait parameter of both sides, two-way repeated measures ANOVA was conducted to examine the main effects of time points and limbs (i.e., the affected side and the unaffected side), as well as the interaction effect within the two variables (time points × limbs). Then, the intra-group differences at the three time points and between the two limbs were evaluated by one-way repeated measures ANOVA (with Bonferroni post hoc tests) and paired t-test, respectively, as conducted in the previous studies [50] [140].

In the trial of CPSS group, the clinical scores (i.e., FMA, BBS, and 10MWT) and the total steps

followed the normal distribution, with the quantified social interactions, imbalanced steps, and the clinical scores of MAS and FAC not obeying it, after the Shapiro-Wilk test of normality. Thus, one-way repeated measures ANOVA was utilized to evaluate the differences of FMA, BBS, and 10MWT across the five time points, and to evaluate differences of the total steps across the 20 training sessions. Friedman tests with Wilcoxon signed-rank post hoc test (Bonferroni correction), were conducted to detect the differences of MAS and FAC across the three time points, and to detect the differences of the social interactions and imbalanced steps across the 20 sessions of CPSS-based paired training. In this study, Statistical Package for Social Science (SPSS, version 22.0.0.0, IBM Corp.) was utilized in the statistical analysis with 0.05 as the significant level. The significance levels of 0.01 and 0.001 were also indicated.

4.3 Results

Totally 24 participants (including the 10 participants in the system evaluation) attended the 20-session gait training assisted by the ENMS-BF, from Sep. 2021 to Sep. 2022. Two participants in the individual group lost to the 3-month FU assessment session due to the local outbreak of COVID-19. Up to now, all the 12 participants completed the individual gait training, by contrast, eight participants in the CPSS group completed the paired gait training, with 4 participants in process of the CPSS-based paired training assisted by the ENMS-BF.
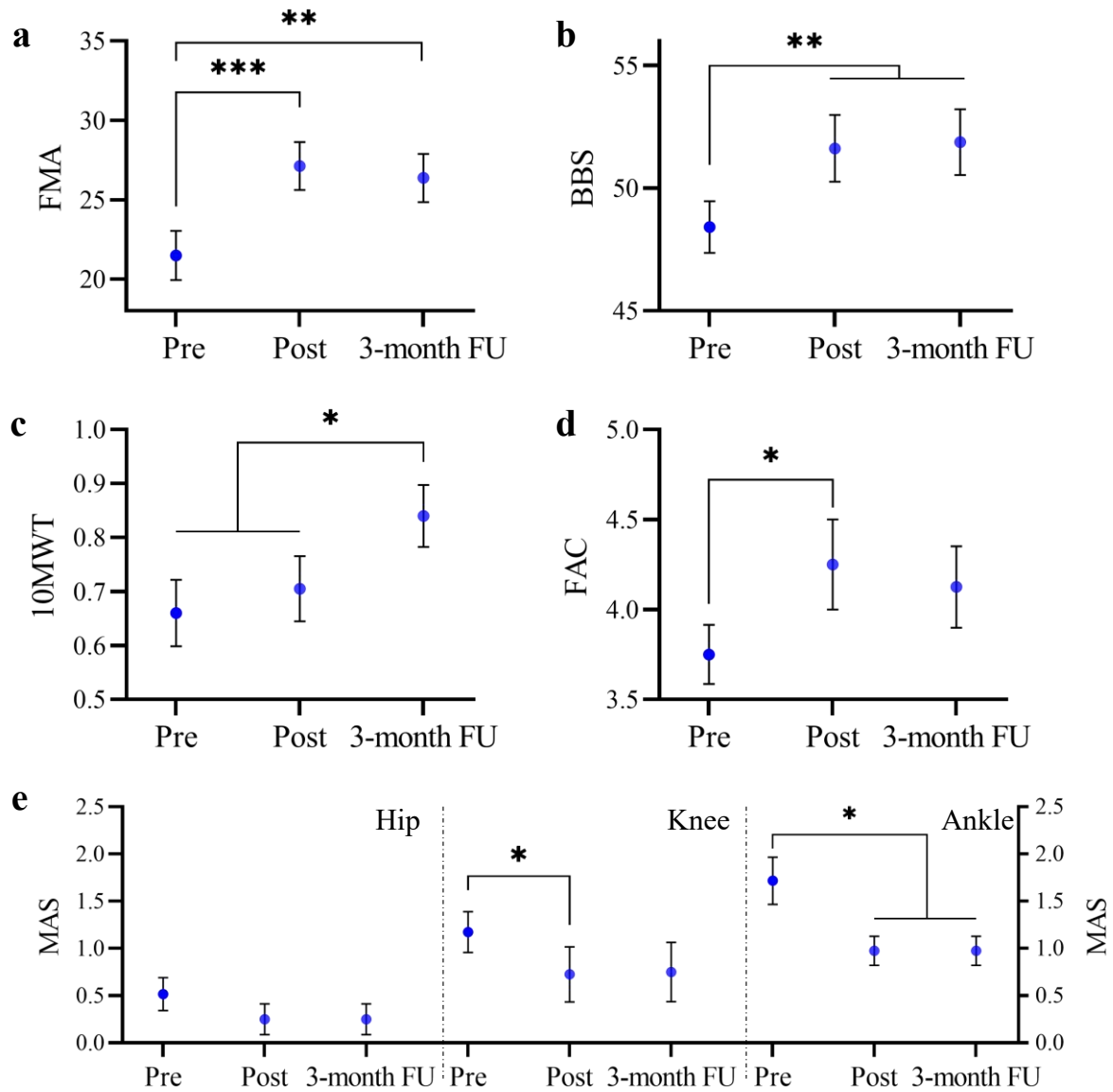
Figure 4-2. Clinical scores (mean ± SE) assessed before (Pre), immediately following (Post), 3-month following (3-month FU) the individual gaiting training: (**a**) FMA; (**b**) BBS; (**c**) 10MWT; (**d**) FAC; (**e**) MAS scores at the ankle, knee, and hip joints.

4.3.1 Training Effects for the Individual Group

All the 12 participants in the individual group completed the 20-session gait training assisted

Table 4-2. Clinical scores and the kinetic parameters measured before (Pre), immediately following (Post), and 3-month following (3-month FU) the individual gaiting training, as well as the probabilities of the statistical analysis.

Clinical assessments		Pre	Post	3-month FU	One-way Repeated Measures ANOVA	
		Mean (95% confidence interval)			P (Partial η²)	F
FMA (max. 34)		21.50 (17.84–25.16)	27.13 (23.57–30.68)	26.38 (22.77–29.98)	0.000*** (0.828)	33.58
BBS (max. 56)		48.42 (45.93–50.91)	51.63 (48.40–54.85)	51.88 (48.70–55.05)	0.000*** (0.766)	22.87
10MWT (m/s)		0.66 (0.51–0.81)	0.71 (0.56–0.85)	0.84 (0.70–0.98)	0.002** (0.600)	10.49
Clinical assessments		**Pre**	**Post**	**3-month FU**	**Friedman Test**	
		Mean (95% confidence interval)			P (X²)	W
MAS (max. 4)	-Hip	0.52 (0.10–0.93)	0.25 (0.00–0.64)	0.25 (0.00–0.64)	0.018* (8.000)	0.500
	-Knee	1.17 (0.66–1.69)	0.73 (0.04–1.41)	0.75 (0.01–1.49)	0.034* (6.741)	0.421
	-Ankle	1.68 (1.04–2.31)	0.98 (0.61–1.34)	0.98 (0.61–1.34)	0.009** (9.391)	0.587
FAC (max. 5)		3.75 (3.36–4.14)	4.25 (3.66–4.84)	4.13 (3.59–4.66)	0.039* (6.500)	0.406
GRF parameters (N/kg)		**Pre**	**Post**	**3-month FU**	**One-way Repeated Measures ANOVA**	
		Mean (95% confidence interval)			P (Partial η²)	F
Vertical Force	@loading response	8.65 (6.98–10.21)	9.73 (9.02–10.44)	9.95 (9.49–10.41)	0.105 (0.372)	3.548
Vertical Force	@terminal stance	9.13 (8.45–9.80)	9.19 (8.42–9.95)	9.22 (8.62–9.83)	0.630 (0.074)	0.481
Braking Force	@loading response	-0.67 (-0.98– -0.37)	-0.92 (-1.32– -0.52)	-0.94 (-1.38– -0.50)	0.02* (0.478)	5.500
Propulsive Force	@terminal stance	0.49 (0.32–0.67)	0.58 (0.41–0.75)	0.60 (0.42–0.79)	0.01* (0.539)	7.021

by the ENMS-BF. Participants could perform the gait training with the sequential assistance of the musculoskeleton, NMES, and the tactile vibrator. No wearing discomfort caused by the device was reported from the participants. The vulnerable point of the developed system reported from the operator was the broken leads of FSRs under foot due to the repeated tramples, which was solved by replacing a new FSRs module reinforced by the hot melt adhesive.

(I) Clinical assessments

In the individual group, the lower limb motor function measured by the clinical assessments

are depicted in Figure 4-2. There was a significant augment in FMA scores following the gaiting training (Figure 4-2a, $P < 0.001$, one-way repeated measures ANOVA with Bonferroni post hoc tests), and the increase was sustained significantly after 3-month (Figure 4-2a, $P < 0.01$, one-way repeated measures ANOVA with Bonferroni post hoc tests). The BBS significantly increased after the training and the augment was maintained in the 3-month FU assessment (Figure 4-2b, $P < 0.01$, one-way repeated measures ANOVA with Bonferroni post hoc tests). As shown in Figure 4-2c, the 10MWT parameters significantly increased 3 months after the gait training, compared to both in the pre and post assessments ($P < 0.05$, one-way repeated measures ANOVA with Bonferroni post hoc tests). There was a significant augment of the FAC scores after the gait training (($P < 0.05$, the Friedman test with the Wilcoxon signed rank post hoc test). Figure 4-2e presents the significant decreases of MASs at the knee and ankle joints after the gait training, and the decrease at the ankle joint was sustained after 3 months ($P < 0.05$, the Friedman test with the Wilcoxon signed-rank post hoc test). Table 4-2 presents the detailed clinical scores (i.e., mean $\pm$ the 95% confidence intervals as well as the one-way repeated measures ANOVA and the probabilities and estimated EFs of Friedman test) measured in this study.

(II) Kinematic and kinetic parameters

For the individual gait training, the kinematic (i.e., the peak angles of the hip, knee, and ankle joints.) and kinetic (peak GRFs) parameters are depicted in Figure 4-3. Table 4-2&3 shows the

Figure 4-3. Kinematic and kinetic parameters (mean ± SE) of the both limbs assessed before (Pre), immediately following (Post), 3-month following (3-month FU) the individual gaiting training: peak angles of (**a**) ankle dorsiflexion (sagittal plane); (**b**) ankle inversion (frontal plane); (**c**) knee varus (frontal plane); (**d**) hip abduction (frontal plane) during the swing phase, and peak ground reaction force (GRF) of (**e**) the braking force (during the loading response phase) and (**f**) the propulsive force (during the terminal stance phase).

detailed kinematic and kinetic parameters of both limbs using the two-way repeated measures

ANOVA with the probabilities and estimated EF values. Peak angles of the ankle dorsiflexion

(on the affected side) during swing phase significantly increased and the augment was

maintained after the gait training and after 3 months (Figure 4-3a, $P < 0.05$, one-way repeated

measures ANOVA with Bonferroni post hoc tests). For the unaffected side, peak ankle

dorsiflexion angles significantly increased in the 3-month FU assessment compared to those

measured in the Pre and Post assessments (Figure 4-3a, $P < 0.05$, one-way repeated measures

ANOVA with Bonferroni post hoc tests). For the peak angles of ankle eversion/inversion (i.e.,

in the frontal plane) during the swing phase, there was a significant augment following the

training and the increase was sustained after 3-month (Figure 4-3b, $P < 0.05$, one-way repeated

measures ANOVA with Bonferroni post hoc tests). Before the gait training, there was a

significant difference in peak angles of ankle eversion/inversion between the affected side and

unaffected side (unaffected side > affected side), and this significant difference reappeared 3-

month after the training (Figure 4-3b, $P < 0.05$, the paired t-test). Figure 4-3c shows a

significant decrease in peak angles of the knee varus (on the affected side) during the swing

phase following the gait training, and the significant decrease was sustained 3-month following

the training ($P < 0.05$, one-way repeated measures ANOVA with Bonferroni post hoc tests).

After the gaiting training (including the Post and 3-month FU assessment), the peak angles of

knee varus (swing phase) of the unaffected side were significantly larger than those measured

Table 4-3. Gait parameters measured of both limbs before (Pre), immediately following (Post), and 3-month following (3-month FU) the individual gaiting training, as well as the probabilities of the statistical analysis.

Gait Parameters		Pre	Post	3-month FU	Two-way Repeated Measures ANOVA		
		Mean (95% confidence interval)			Time P (Partial η²)	Limb P (Partial η²)	Time* Limb P (Partial η²)
Peak Kinematic Parameters (degree) @Sagittal plane							
Ankle dorsiflexion @stance phase	Affected side	14.09 (6.62–21.57)	13.81 (8.33–19.29)	16.28 (10.07–22.48)	0.19 (0.244)	0.000*** (0.955)	0.091 (0.329)
	Unaffected side	17.78 (12.64–22.91)	20.28 (13.16–27.40)	24.14 (16.77–31.52)			
Ankle dorsiflexion @swing phase	Affected side	3.81 (-0.38–8.01)	9.58 (3.85–15.32)	8.95 (5.55–12.35)	0.006** (0.575)	0.890 (0.003)	0.052 (0.103)
	Unaffected side	4.96 (-0.38–10.30)	8.00 (0.44–15.56)	10.53 (2.44–18.63)			
Knee extension @stance phase	Affected side	-0.53 (-10.50–9.44)	-1.90 (-9.61–5.81)	-2.62 (-8.89–3.64)	0.672 (0.064)	0.550 (0.063)	0.437 (0.129)
	Unaffected side	0.91 (-6.29–8.13)	1.57 (-4.46–7.59)	0.47 (-7.06–8.00)			
Knee flexion @swing phase	Affected side	24.14 (8.53–39.74)	25.24 (14.62–35.86)	22.70 (9.46–35.94)	0.933 (0.012)	0.011* (0.684)	0.755 (0.046)
	Unaffected side	48.35 (31.12–65.58)	50.55 (34.01–67.09)	50.74 (38.45–63.04)			
Hip extension @stance phase	Affected side	-7.04 (-14.76–0.68)	-7.92 (-15.70– -0.14)	-9.67 (-18.04– -1.30)	0.563 (0.091)	0.749 (0.018)	0.392 (0.145)
	Unaffected side	-9.20 (-15.97– -2.42)	-7.87 (-14.34– -1.41)	-10.59 (-17.12– -4.07)			
Hip flexion @swing phase	Affected side	25.95 (19.49–32.41)	27.63 (18.55–36.72)	26.02 (21.60–30.44)	0.144 (0.276)	0.019* (0.629)	0.078 (0.347)
	Unaffected side	30.32 (26.45–34.18)	36.81 (31.55–42.07)	35.23 (31.85–38.62)			
Peak Kinematic Parameters (degree) @Frontal plane							
Ankle eversion @stance phase	Affected side	2.88 (-0.23–5.99)	1.43 (-1.15–4.00)	2.72 (0.40–5.04)	0.471 (0.118)	0.005** (0.762)	0.343 (0.163)
	Unaffected side	7.10 (4.02–10.19)	8.03 (5.13–10.94)	8.64 (5.43–11.84)			
Ankle inversion @swing phase	Affected side	-3.93 (-6.97– -0.90)	2.11 (-2.00–6.21)	1.64 (-0.55–3.83)	0.001** (0.700)	0.017* (0.643)	0.142 (0.278)
	Unaffected side	1.98 (-0.72–4.68)	3.47 (0.95–6.00)	5.38 (3.33–7.43)			
Knee valgus @stance phase	Affected side	-1.78 (-7.99–4.44)	-1.43 (-6.62–3.76)	-1.90 (-8.39–4.58)	0.595 (0.083)	0.021* (0.616)	0.423 (0.134)
	Unaffected side	2.74 (-3.06–8.54)	3.38 (0.22–6.54)	4.81 (-0.74–10.35)			
Knee varus @swing phase	Affected side	26.34 (19.38–33.30)	21.84 (15.42–28.26)	22.26 (15.57–28.96)	0.201 (0.252)	0.035* (0.549)	0.785 (0.040)
	Unaffected side	38.33 (25.42–51.24)	34.42 (20.62–48.22)	37.35 (25.97–48.72)			
Hip adduction @stance phase	Affected side	4.45 (0.15–8.75)	5.01 (1.87–8.14)	2.62 (-0.53–5.77)	0.183 (0.247)	0.821 (0.009)	0.227 (0.219)
	Unaffected side	4.35 (-0.13–8.84)	3.17 (-1.98–8.31)	3.31 (-1.56–8.19)			
Hip abduction @swing phase	Affected side	-9.49 (-12.29– -6.70)	-7.04 (-10.00– -4.09)	-7.73 (-10.92– -4.54)	0.096 (0.323)	0.941 (0.001)	0.158 (0.265)
	Unaffected side	-7.97 (-12.41– -3.53)	-7.94 (-12.44– -3.43)	-7.81 (-12.64– -2.97)			
Peak Pressure (kPa)							
MF	Affected side	47.24 (31.04–63.44)	57.49 (42.04–72.95)	56.46 (40.55–72.36)	0.471 (0.096)	0.032* (0.563)	0.017* (0.610)
	Unaffected side	92.78 (70.80–114.75)	76.70 (57.95–95.46)	73.53 (53.05–94.02)			
LF	Affected side	35.93 (20.11–51.75)	40.03 (25.56–53.50)	39.91 (26.58–53.25)	0.414 (0.137)	0.088 (0.408)	0.995 (0.001)
	Unaffected side	56.10 (30.96–81.24)	59.35 (43.92–74.78)	59.99 (42.46–77.71)			
MM	Affected side	17.05 (10.75–23.35)	20.77 (16.27–25.26)	21.45 (16.60–26.30)	0.395 (0.127)	0.014* (0.661)	0.168 (0.257)
	Unaffected side	26.29 (19.53–33.04)	24.47 (18.13–30.81)	25.47 (19.50–31.45)			
LM	Affected side	44.72 (28.44–61.01)	43.05 (28.36–57.74)	46.28 (28.84–63.72)	0.898 (0.018)	0.004** (0.772)	0.914 (0.015)
	Unaffected side	67.18 (46.94–87.42)	66.03 (51.10–80.96)	65.39 (56.26–74.51)			
MR	Affected side	73.19 (52.44–93.94)	79.13 (63.06–95.20)	79.67 (62.93–96.41)	0.118 (0.299)	0.365 (0.138)	0.593 (0.056)
	Unaffected side	82.56 (74.69–94.43)	86.51 (79.50–93.52)	83.61 (77.62–89.60)			
LR	Affected side	53.02 (44.49–61.55)	63.55 (45.97–85.13)	66.92 (54.83–79.02)	0.477 (0.116)	0.040* (0.533)	0.095 (0.324)
	Unaffected side	90.13 (66.64–113.62)	86.93 (61.57–112.30)	80.01 (67.65–92.37)			

Table 4-4. Gait parameters measured of both limbs before (Pre), immediately following (Post), and 3-month following (3-month FU) the individual gaiting training, as well as the probabilities of the statistical analysis (Continued).

Gait Parameters		Pre	Post	3-month FU	Two-way Repeated Measures ANOVA		
		Mean (95% confidence interval)			Time P (Partial η^2)	Limb P (Partial η^2)	Time* Limb P (Partial η^2)
Temporal-spatial gait parameters							
Walking Speed (m/s)	Affected side	0.48 (0.25–0.71)	0.41 (0.26–0.56)	0.46 (0.28–0.63)	0.245 (0.245)	0.638 (0.048)	0.585 (0.102)
	Unaffected side	0.48 (0.26–0.70)	0.42 (0.27–0.57)	0.45 (0.28–0.63)			
Step Length (m)	Affected side	0.38 (0.25–0.51)	0.37 (0.26–0.48)	0.37 (0.27–0.48)	0.904 (0.020)	0.844 (0.009)	0.820 (0.039)
	Unaffected side	0.36 (0.27–0.46)	0.37 (0.26–0.47)	0.37 (0.26–0.47)			
Stance Time (s)	Affected side	0.78 (0.63–0.93)	1.10 (0.82–1.38)	1.09 (0.84–1.34)	0.003** (0.695)	0.093 (0.461)	0.135 (0.330)
	Unaffected side	0.95 (0.79–1.11)	1.12 (0.91–1.33)	1.09 (0.74–1.43)			
Swing Time (s)	Affected side	0.62 (0.48–0.76)	0.63 (0.53–0.74)	0.59 (0.51–0.67)	0.365 (0.167)	0.002** (0.869)	0.077 (0.401)
	Unaffected side	0.48 (0.35–0.61)	0.57 (0.48–0.66)	0.50 (0.41–0.58)			
Contact Area (cm²)	Affected side	103.44 (85.07–121.82)	117.33 (105.10–129.55)	116.93 (101.88–131.99)	0.031* (0.440)	0.003** (0.803)	0.001** (0.704)
	Unaffected side	128.55 (116.13–140.97)	129.28 (121.73–136.83)	127.10 (117.12–137.07)			

on the affected side ((Figure 4-3b, P < 0.05, the paired t-test). There were significantly larger angles of peak hip abduction (on the paretic limb) during the swing phase in the Post and 3-month FU assessment, compared to those measured in the pre assessment (Figure 4-3d, P < 0.05, one-way repeated measures ANOVA with Bonferroni post hoc tests).

For the kinetic parameters, i.e., the GRFs, of the affected limb, the absolute values of peak braking forces during the loading response increased following the gait training, and the significant augment was retained in the 3-month FU assessment (Figure 4-3e, P < 0.05, one-way repeated measures ANOVA with Bonferroni post hoc tests). Figure 4-3f shows that the peak propulsive forces (on the affected side) during the terminal stance in the Post and 3-month

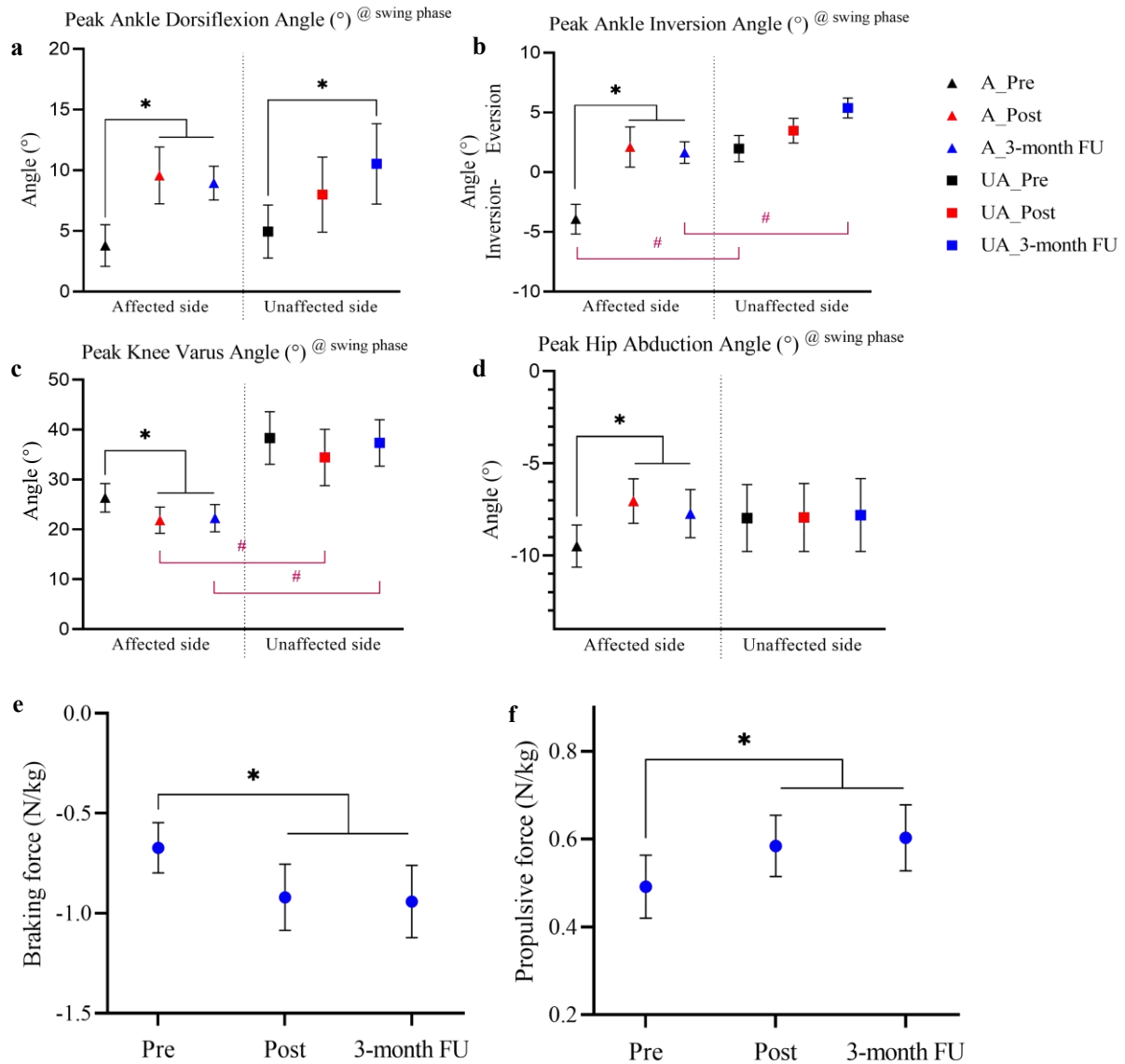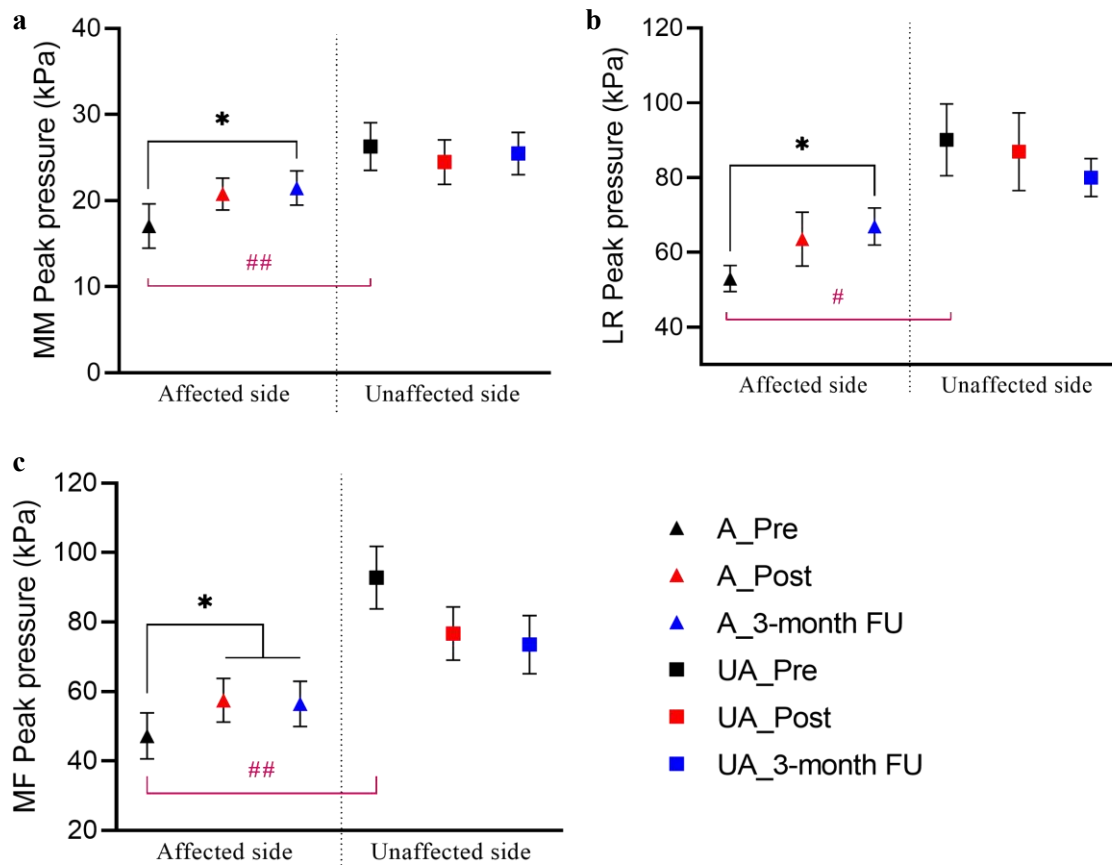**Figure 4-4.** Plantar pressure distribution parameters (mean ± SE) of both limbs assessed before (Pre), immediately following (Post), 3-month following (3-month FU) the individual gaiting training: peak averaged pressures at the regions of (**a**) medial midfoot, MM; (**b**) lateral rearfoot, LR; (**c**) medial forefoot, MF.

FU assessments, were significantly larger than those measured in the pre assessment (P < 0.05, one-way repeated measures ANOVA with Bonferroni post hoc tests). No significant differences were detected in the other kinematic (including the joint of pelvic and the kinematic parameters in the level plane) and kinetic parameters of other gait phases among the three time points.

(III) Plantar pressure distribution parameters

In the individual group of gait training, Figure. 4-4 presents the plantar pressure distribution parameters of both limbs before, after, and 3-month after the training. The two-way repeated measures ANOVA probabilities and the EFs with respect to the plantar pressure distribution parameters are integrated in Table 4-3. The peaks of the averaged plantar pressure at the MM region (the affected limb) 3-month after the gait training, were significantly greater than those measured prior to the training (Figure 4-4a, $P < 0.05$, one-way repeated measures ANOVA using Bonferroni post hoc tests). Meanwhile, before the gait training, the peaks of the averaged plantar pressure of the MM region of the paralyzed limb were significantly lower than those measured on the unaffected limb (Figure 4-4a, $P < 0.01$, the paired t-test). As shown in Figure 4-4b, the peaks of the plantar pressure at the LR region (the affected limb) in the 3-month FU assessment was significantly greater than those measured prior to the training ($P < 0.05$, one-way repeated measures ANOVA using Bonferroni post hoc tests), and they are higher on the unaffected side compared to those measured on the affected side in the pre assessment ($P < 0.05$, the paired t-test). Regarding to the peaks of the averaged plantar pressure at the MF region (the affected limb), there was a significant increase after the gait training, and the augment was maintained 3-month after the training (Figure. 4-4c, $P < 0.05$, one-way repeated measures ANOVA using Bonferroni post hoc tests). The peaks of the averaged plantar pressure (MF region) of the unaffected limb were significantly greater than those measured at the paretic
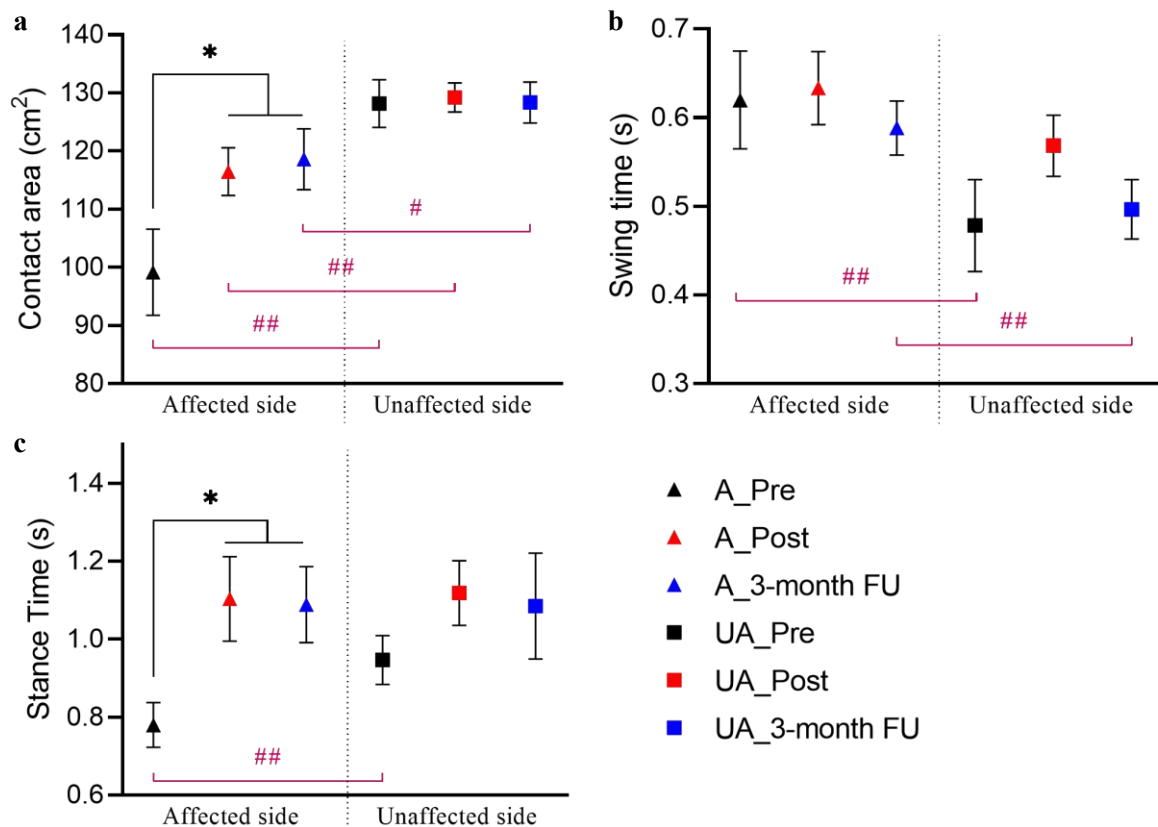
Figure 4-5. Temporal-spatial gait parameters (mean ± SE) of both limbs assessed prior to (Pre),

immediately following (Post), 3-months following (3-month FU) the individual gaiting training:

(a) foot-floor contact area; (b) swing time; (c) stance time.

limb (Figure 4-4c, $P < 0.05$, the paired t-test). No significant increase or decrease was found

among the three time points in the plantar pressure distribution parameters of other foot regions.

(IV) Temporal-spatial gait parameters

In the individual gait training, Figure 4-5 shows the temporal-spatial gait parameters, which

exhibited significant variations among the three time points and between the two limbs. The
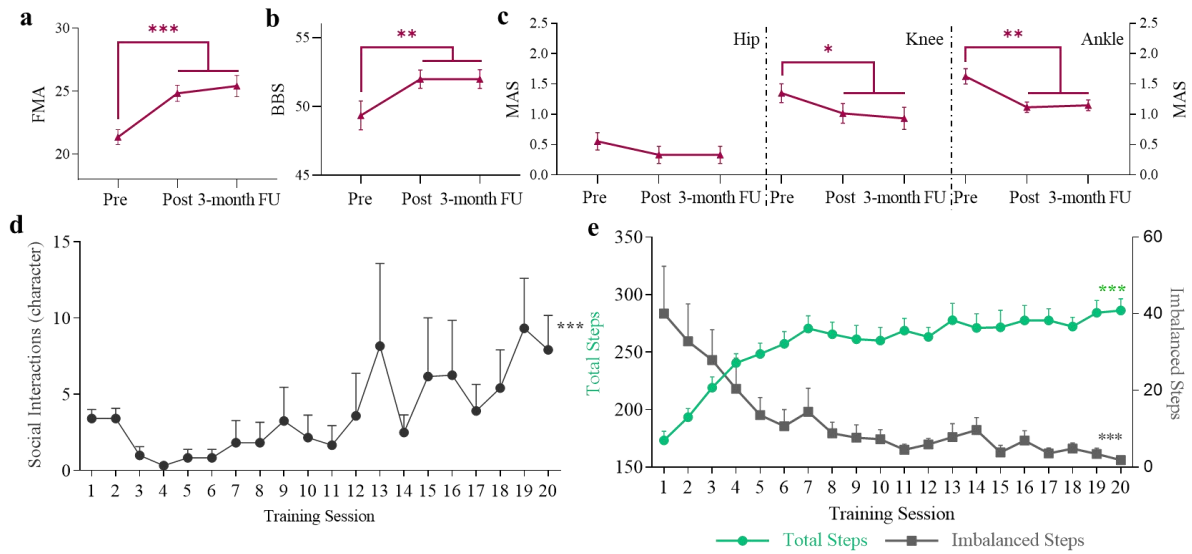
Figure 4-6. Clinical scores (mean ± SE) and the training parameters measured in the CPSS-based training: (a) FMA scores; (b) BBS scores; and (c) MAS at the ankle joint measured in the three Pre assessment, and the Post and 3-month FU assessments. The variation of daily training parameters, i.e., (d) the social interactions between the paired participants, and (e) the total steps/imbalanced steps, across the CPSS-based paired training sessions. Significant differences are indicated by "*" ($P<0.05$), "**" ($P<0.01$), and "***" ($P<0.001$).

detailed temporal-spatial gait parameters are depicted in Table 4-4, with the two-way repeated measures ANOVA probabilities and the estimated EF values. A significant increase was found in the foot-floor contact area (affected limb) following the gait training, and the augment was maintained 3-month following the training (Figure 4-5a, $P < 0.05$, one-way repeated measures ANOVA with Bonferroni post hoc tests). The foot-floor contact area of the unaffected limb was

significantly greater than that measured on the affected side before and after the gait training (Figure 4-5a, $P < 0.01$, the paired t-test). Three months after the training, the foot-floor contact area of the unaffected limb was significantly larger than that measured on the affected limb with a reduced significance (Figure 4-5a, $P < 0.05$, the paired t-test). Before the gaiting training the swing time of the paretic limb was significantly longer compared to that measured on the unaffected side (Figure 4-5b, $P < 0.01$, the paired t-test). The significantly longer swing time of the affected limb, compared to that measured on the unaffected side, reappeared 3-month after the training (Figure 4-5b, $P < 0.01$, the paired t-test). A significant augment of the stance time on the affected side was observed after the gait training (Figure 4-5c), and the significant increase was maintained in the 3-month FU assessment ($P < 0.05$, one-way repeated measures ANOVA using Bonferroni post hoc tests). Before the gait training, the stance time on the unaffected side was significantly longer than that measured of the paretic limb (Figure 4-5c, $P < 0.01$, the paired t-test). No significant differences of other temporal-spatial gait parameters were detected among the time points and between both lower limbs.

4.3.2 Training effects for the CPSS group

Twelve participants were matched into 6 pairs in the CPSS based paired training. All of them completed the 20-session training and clinical assessments at the five time points. No wearing discomfort and no complaint of the CPSS-based paired training was reported from the participants.

Table 4-5. Means and 95% confidence intervals for the clinical scores measured at Pre, Post, and 3-month FU assessments in the CPSS based paired training, as well as the probabilities of the statistical analysis.

Clinical assessments		Pre	Post	3-month FU	One-way Repeated Measures ANOVA	
		Mean (95% confidence interval)			P (Partial η^2)	F
FMA (max. 34)		20.37 (16.83–23.90)	26.20 (23.06–29.34)	25.40 (22.31–28.49)	0.000[***] (0.815)	39.54
BBS (max. 56)		49.07 (46.95–51.19)	52.20 (49.61–54.79)	52.20 (49.75–54.65)	0.000[***] (0.753)	27.46
10MWT (m/s)		0.63 (0.50–0.75)	0.66 (0.53–0.79)	0.81 (0.69–0.92)	0.000[***] (0.588)	12.83
Clinical assessments		Pre	Post	3-month FU	Friedman Test	
		Mean (95% confidence interval)			P (X^2)	W
MAS (max. 4)	-Hip	0.59 (0.14–1.04)	0.20 (0.00–0.50)	0.30 (0.00–0.65)	0.009[**] (9.500)	0.475
	-Knee	1.32 (0.87–1.76)	0.78 (0.26–1.30)	0.84 (0.26–1.42)	0.007[**] (10.059)	0.503
	-Ankle	1.75 (1.27–2.22)	1.02 (0.73–1.31)	1.02 (0.73–1.31)	0.001[**] (13.241)	0.662
FAC (max. 5)		3.80 (3.50–4.10)	4.20 (3.75–4.65)	4.10 (3.69–4.51)	0.039[*] (6.500)	0.325

Fig. 4-6a-c summarizes the clinical scores measured at five different time points in the CPSS group. Significant increases were observed in the FMA scores (Fig. 6a, $P<0.01$) and BBS (Fig. 6b, $P<0.05$) after the CPSS-based paired training, and these increases were maintained 3-month after the paired training. As shown in Fig. 6c, the MAS declined significantly at the ankle ($P<0.01$) joint and the knee joint ($P<0.05$) after the paired training, and it was maintained for 3 months. No significant difference was found in the clinical scores of FAC, 10MWT and MASs (hip joint) among the five time points. Detailed statistics of the clinical scores are summarized in Table 4-5.

Fig. 6d&e presents differences of the total steps, imbalanced steps, and the quantified social interactions between the pairs, across the 20-session CPSS-based paired training.

Accompanying with the significant increases of social interactions (Fig. 6d, P<0.001), the count of total steps increased significantly (Fig. 6e, P<0.001), and the imbalanced steps significantly declined (Fig. 6e, P<0.001) across the 20-session paired training.

4.4 Discussion

Pilot clinical trials were also carried out to validate the viability and effects of the individual and CPSS-based paired gait training, respectively, both of which were fully assisted by the ENMS-BF.

4.4.1 The ENMS-BF-assisted Individual Gait Training

The feasibility of the proposed ENMS-BF-assisted individual gait training was measured, and all the 12 participants finished the 20-session training with close supervision from the experimental operator. No accident of falling or other side effects was reported during the individual gait training. All the participants could wear the ENMS-BF with assistance from the experimental operator. Three of the twelve participants with chronic stroke encountered the problem of missing detection of heel-off event at the beginning training session, which was caused by the muscular discoordination of the plantar flexors in chronic stroke [141]. Verbal cues from the experimental operator (mainly in the first three sessions of gait training), together with the sensory-level NMES, could remind the participants focusing on the dynamic assistance from the ENMS-BF and performing heel-off event, which was similar to the

biofeedback in the intervention of plantar flexors post-stroke [142]. Supervised by the experimental operator, all the participants could complete the 45min ENMS-BF-assisted gait training with all the three gait events, i.e., heel-off, toe-off, and heel-strike, recognized successfully based on the real-time plantar pressures captured by the FSRs.

Clinical scores at the Pre, Post, and 3-month FU assessment sessions showed that the ENMS-BF-assisted gait training enhanced motor function of the paralyzed lower limb and released the muscular spasticity at the ankle, knee, and hip joints. The paretic limb's motor recovery was demonstrated by the significant augment in the FMA at Post assessment (i.e., FMA + 5.63), and the improvement was maintained at the 3-month after the gait training (i.e., FMA + 4.88). Both the increases at the Post and 3-month FU assessments were greater than the minimal detectable change (MDC) of 4 points in individuals with chronic stroke [143]. A significant increase was also found in the FAC at the Post assessment, which also suggested improved functional ambulation in the community. The significant increases of BBS in the Post and 3-month FU assessments indicated the improvement in balance ability, which could be associated with the assistance of NMES and vibrotactile feedback during the gait training [144] [145] [146]. Due to passive muscular tension and compensation in the paretic limb, stroke survivors usually show joint deformities [111]. Flexor spasticity was observed to be released at the knee and ankle joints following the gait training, associated with the significantly decreased MAS scores at the Post assessment. The release of muscular spasticity at the ankle joint was

maintained 3-month following the gait training. The decreases in MASs at both the knee and ankle joints also suggested the improved synergic control of muscles in the distal and proximal joints [147]. With the motor-level NMES to the extensor, i.e., TA muscle, and the sensory-level NMES to the flexor, i.e., GA muscle, the muscular spasticity at the ankle joint was effectively reduced, which indicated the improved muscle coordination within the antagonist muscle pairs in the ankle. This result was similar to those studies on post-stroke rehabilitation assisted by NMES [148] [149]. The non-significant increase in gait speed after the training could be explained by the "2-second" educational period in the gait training, which helped the participants to relearn plantarflexion and plantar balance with a slow walking speed. It is interesting to note that the gait speed significantly increased 3-month after the training, with the maintained improvements of motor function and balance ability in the lower limb and sustained release of muscle spasticity at the ankle joint. The augment of gait speed in the 3-month FU period was because the stroke participants persisted in self-training in the community with the relearned gait pattern, even without assistance from the ENMS-BF.

The 20-session individual training assisted by the ENMS-BF improved the gait pattern as indicated by the results of kinematic, kinetic, and spatial-temporal gait parameters. In the sagittal plane, the peak angle of the paretic ankle dorsiflexion during the swing phase significantly increased after the gait training indicating the improved voluntary ankle dorsiflexion, which might be related to the strengthened dorsiflexor and the reduced spasticity

of plantar flexor benefiting from the NMES [124] [150] [151]. In the frontal plane, the peak angle of ankle inversion during the swing phase increased significantly after the gait training, which suggested the relief of ankle varus by the vibrotactile feedback [28]. The improvement of foot inversion could also be related to the improved postural balance, as revealed by the increase of BBS after the gait training. The difference of the peak ankle inversion between the affected and unaffected limb suggested the improved spatial asymmetry after the gait training, which could also be revealed by the swing time (Figure 4-5b). The improvements of asymmetry could be explained by the improved pattern of temporal asymmetry characterized by a shorter stance time of the affected limb [152] [153], which increased significantly after the gait training (Figure 4-5c). The improvements of spatial and temporal gait asymmetry could also be related to the relief of spasticity of the affected ankle plantar flexors [154], which was reduced with the assistance of NMES in this study. However, this asymmetry of both limbs on peak foot inversion/eversion and swing time reappeared in the 3-month FU assessment in this study, which might be related to the long-term gait adaptability of the chronic stroke participants to various environmental characteristics in their daily living [13]. The peak angles of knee varus and hip abduction of the paretic limb decreased significantly during the swing phase, which might be associated with the reduced commentary motions of hip circumduction [155]. The reduced compensatory movement of the isolated joint was consistent with those interventions that assisted with NMES for chronic stroke survivors [150, 156]. In the stance phase of the

affected side, the absolute peaks of braking force and propulsive force increased significantly after the ENMS-BF-assisted gait training, which might be correlated to the muscular activity of ankle dorsiflexion and plantarflexion assisted by NMES from the ENMS-BF [157]. The improvements in braking and propulsive force on the paretic limb indicated that the participants could gain confidence in standing on the paralyzed limb with better walking capability [158], which was also supported by the significantly increased stance time and foot-floor contact area of the paralyzed limb following the ENMS-BF-assisted gait training (Figure 4-5a&c). After the gait training, the stance time of the affected side increased without significant changes in the walking speed assessed by the motion capture system, which also indicated that the improvements in the hemiparetic gait pattern were not due to the intentional changes in walking speed during the assessments [155].

The improvements in plantar balance during the stance phase were indicated by the changes in plantar pressure distributions and foot-floor contact areas of both sides. The significant increases of peak pressure at the MF and MM regions of the affected limb indicated the improved plantar balance of the paretic foot on the medial side. This improvement of plantar balance at the affected limb could also be related to the improved postural balance and reduced foot inversion in the swing phase [159]. Meanwhile, the increase of peak pressure at the LR region after the gait training could be related to the increased braking and propulsive forces, together with the increased foot-floor contact area in the stance phase after the training, which

also indicated the improved walking capability with confidence on the affected limb. The inter-limb asymmetry of plantar pressure was improved at the MM, MF, and LR regions, as revealed by the changes in peak plantar pressure at the related plantar regions after the gait training, which might be related to the improved static balance [160], as also revealed by the increased clinical score of BBS after the training. This finding of improvement in plantar balance was consistent with the previous studies with the biofeedback to correct foot inversion and plantar imbalance [28] [161]. It was found that the haptic feedback potentially to enhance proprioception for stroke survivors [162] [163]. In this study, the vibrotactile feedback came from the tactile vibrator, which was placed nearby the imbalanced region of the paretic foot sole to enhance the interaction effect of afferent vibrotactile and proprioceptive feedback. In the self-correction of plantar imbalance and foot inversion during the dynamic gait training, the afferent feedback of the vibrotactile, together with the proprioceptive stimulation under the foot sole, might contribute to the strengthened plastic changes in the relearned gait pattern, which were demonstrated in the previous study of neural plasticity [164].

4.4.2 The CPSS-based ENMS-BF-assisted Paired Gait Training

Eight participants fully completed the self-help ENMS-BF-assisted paired gait training based on the CPSS incentive mechanism, with monitoring by a distanced professional, suggesting the integration of the CPSS and ENMS-BF is feasible for the gait training post-stroke without temporal and spatial restrictions. Meanwhile, as revealed from the feedback of the participants

during the gait training, both the incentive/correction audio feedback and milestone rewards could enhance the motivation and engagement in the self-help ENMS-BF-assisted gait training, without close supervision from the professional, which was also found in the previous studies of rehabilitation post-stroke using goal setting [165] and serious games [166]. The recovery of voluntary motor function and posture balance in the lower limb was revealed by the significantly increased clinical scores of FMA and BBS after the 20-session CPPS-based paired training. The release of muscular spasticity at the knee and ankle flexors were indicated by the significantly decreased MAS, which also suggested improved muscular coordination and synergic activities between the distal and proximal joint [15]. The significant increasement of total steps and decrease in the imbalance steps, together with the significantly increased social interactions across the 20-session training, indicated that the CPSS-based ENMS-BF-assisted paired training can facilitate effective motor recovery for chronic stroke with remote management and social interactions.

4.5 Periodic Summary

In conclusion, the feasibility and rehabilitation effectiveness of the developed ENMS-BF were investigated with the individual gait training supervised by a professional and the self-help CPSS-based paired training managed remotely by the professional. Participants could complete the 20-session ENMS-BF-assisted gait training in both the individual and CPSS-based paired groups. After the ENMS-BF-assisted individual gait training, all the participants showed

enhanced motor recovery, release of involuntary muscle tension of the paretic limb, together with the improved gait pattern and plantar balance. Based on the CPSS-based incentive mechanism, participants completed the self-help paired gait training assisted by the ENMS, accompanying cyber social interactions with both the professional and the paired participants. These results indicated that both the individual and CPSS-based gait training, assisted by the ENMS-BF, could facilitate efficient gait training for stroke survivors.

CHPATER 5

CONSLUSIONS

Robot-assisted training and automated assessments are the two crucial issues in automated rehabilitation for stroke patients. Rehabilitation robots could assist in the repetitive and intensive physical training during the motor recovery of the paralyzed limb, meanwhile, the automated assessment could monitor the training effects and facilitate the customized training strategy assisted by the robot. Three experiments were carried out in this study to 1) explore the sEMG data-driven model for the robotized assessment of training effects in the robot-aided training, 2) develop and verify the capacity of a novel exo-neuro-musculo-skeleton with balance sensing feedback (ENMS-BF) for lower limb motor recovery, 3) investigate the feasibility and rehabilitation effectiveness of using the developed ENMS-BF for both the individual training and the self-help paired training with cyber physical interactions.

In the first experiment, a three-layer BPNN model driven by the sEMG data was established for the projection of the sEMG characteristics to the FMA and MASs, which are the commonly used clinical scores during the upper limb motor recovery post-stroke. Significant correlations ($P<0.05$) were observed within the manually marked and mapped scores of FMA and MAS, suggesting that the data-driven model enables measurements of upper limb motor functions and muscular spasticity for chronic stroke survivors. The constructed model could potentially

facilitate the automated assessment of motor functions with minimum assistance and supervision from the professionals, during the robot-assisted rehabilitation after stroke.

In the second section, an ENMS-BF driven by plantar pressures was designed for the dynamic correction of foot drop and foot inversion in lower limb motor recovery post-stroke. The ENMS-BF combined the pneumatic muscle, exoskeleton, NMES, and vibrotactile feedback, which was immediately effective for ankle dorsiflexion and correction of foot inversion during dynamic gait. The lightweight and compact design of the ENMS enable it to be worn bilaterally above the ankle joint of the paralyzed foot with a comfortable experience.

In the third experiment, the feasibility and rehabilitation effects of the ENMS-BF were investigated with two training strategies, i.e., the individual training supervised by an experimental operator, and the self-help CPSS-based paired training with remote management and peer interactions. All participants completed the individual gait training assisted by the developed ENMS-BF, with improved motor function, reduced muscular spasticity, and enhanced gait pattern and plantar balance of the paralyzed lower limb after the 20-session training. Eight participants completed the self-help CPSS-based paired training with cyber interactions with peers and remote monitoring from the professional, accompanying improved motor functions after the paired gait training. These results suggested that both the ENMS-BF alone, and integration with the CPSS incentive mechanism, could facilitate effective motor recovery of the lower limb for individuals with chronic stroke.

In conclusion, this study proposed the potential solution of automated assessment for post-stroke robot-assisted rehabilitation, which could track the training effects to customize the training strategy during the rehabilitation program. Moreover, a novel ENMS-BF with a lightweight and compact design was developed for the motor recovery of the paretic lower limb after stroke. The developed ENMS-BF, together with the CPSS incentive mechanism, could be feasible for self-help training monitored by a distanced professional, and this novel training strategy could provide effective motor recovery of the lower limb, accompanying cyber peer interactions with minimized physical contacts, during the long-term rehabilitation of stroke.

Future investigations will be carried out to (1) improve the generalization performance of the data-driven model with semi-supervised learning (e.g., transfer learning) and multi-mode feature vectors, e.g., the sEMG parameters and clinical diagnostic information; (2) explore the training effectiveness of the ENMS-BF-assisted gait training in home/community environment with randomized control trials; (3) explore the feasibility of utilizing the data-driven model for automated assessment in the lower limb ENMS-BF-assisted rehabilitation post-stroke; and (4) establish the CPSS-based platform for both upper and lower limb robot-assisted telerehabilitation.

APPENDICES

Appendices 1: Clinical Assessments for Upper Limb

1.1 Mini-mental State Examination (MMSE)

Mini-Mental State Examination (MMSE)

Patient's Name: _____   Date: _____

Instructions: Ask the questions in the order listed. Score one point for each correct response within each question or activity.

Maximum Score	Patient's Score	Questions
5		"What is the year? Season? Date? Day of the week? Month?"
5		"Where are we now: State? County? Town/city? Hospital? Floor?"
3		The examiner names three unrelated objects clearly and slowly, then asks the patient to name all three of them. The patient's response is used for scoring. The examiner repeats them until patient learns all of them, if possible. Number of trials: _____
5		"I would like you to count backward from 100 by sevens." (93, 86, 79, 72, 65, …) Stop after five answers. Alternative: "Spell WORLD backwards." (D-L-R-O-W)
3		"Earlier I told you the names of three things. Can you tell me what those were?"
2		Show the patient two simple objects, such as a wristwatch and a pencil, and ask the patient to name them.
1		"Repeat the phrase: 'No ifs, ands, or buts.'"
3		"Take the paper in your right hand, fold it in half, and put it on the floor." (The examiner gives the patient a piece of blank paper.)
1		"Please read this and do what it says." (Written instruction is "Close your eyes.")
1		"Make up and write a sentence about anything." (This sentence must contain a noun and a verb.)
1		"Please copy this picture." (The examiner gives the patient a blank piece of paper and asks him/her to draw the symbol below. All 10 angles must be present and two must intersect.)
30		TOTAL

(Adapted from Rovner & Folstein, 1987)

120

Instructions for administration and scoring of the MMSE

Orientation (10 points):
- Ask for the date. Then specifically ask for parts omitted (e.g., "Can you also tell me what season it is?"). One point for each correct answer.
- Ask in turn, "Can you tell me the name of this hospital (town, county, etc.)?" One point for each correct answer.

Registration (3 points):
- Say the names of three unrelated objects clearly and slowly, allowing approximately one second for each. After you have said all three, ask the patient to repeat them. The number of objects the patient names correctly upon the first repetition determines the score (0-3). If the patient does not repeat all three objects the first time, continue saying the names until the patient is able to repeat all three items, up to six trials. Record the number of trials it takes for the patient to learn the words. If the patient does not eventually learn all three, recall cannot be meaningfully tested.
- After completing this task, tell the patient, "Try to remember the words, as I will ask for them in a little while."

Attention and Calculation (5 points):
- Ask the patient to begin with 100 and count backward by sevens. Stop after five subtractions (93, 86, 79, 72, 65). Score the total number of correct answers.
- If the patient cannot or will not perform the subtraction task, ask the patient to spell the word "world" backwards. The score is the number of letters in correct order (e.g., dlrow=5, dlorw=3).

Recall (3 points):
- Ask the patient if he or she can recall the three words you previously asked him or her to remember. Score the total number of correct answers (0-3).

Language and Praxis (9 points):
- Naming: Show the patient a wrist watch and ask the patient what it is. Repeat with a pencil. Score one point for each correct naming (0-2).
- Repetition: Ask the patient to repeat the sentence after you ("No ifs, ands, or buts."). Allow only one trial. Score 0 or 1.
- 3-Stage Command: Give the patient a piece of blank paper and say, "Take this paper in your right hand, fold it in half, and put it on the floor." Score one point for each part of the command correctly executed.
- Reading: On a blank piece of paper print the sentence, "Close your eyes," in letters large enough for the patient to see clearly. Ask the patient to read the sentence and do what it says. Score one point only if the patient actually closes his or her eyes. This is not a test of memory, so you may prompt the patient to "do what it says" after the patient reads the sentence.
- Writing: Give the patient a blank piece of paper and ask him or her to write a sentence for you. Do not dictate a sentence; it should be written spontaneously. The sentence must contain a subject and a verb and make sense. Correct grammar and punctuation are not necessary.
- Copying: Show the patient the picture of two intersecting pentagons and ask the patient to copy the figure exactly as it is. All ten angles must be present and two must intersect to score one point. Ignore tremor and rotation.

(Folstein, Folstein & McHugh, 1975)

Interpretation of the MMSE

Method	Score	Interpretation
Single Cutoff	<24	Abnormal
Range	<21	Increased odds of dementia
	>25	Decreased odds of dementia
Education	21	Abnormal for 8th grade education
	<23	Abnormal for high school education
	<24	Abnormal for college education
Severity	24-30	No cognitive impairment
	18-23	Mild cognitive impairment
	0-17	Severe cognitive impairment

Sources:

- Crum RM, Anthony JC, Bassett SS, Folstein MF. Population-based norms for the mini-mental state examination by age and educational level. *JAMA*. 1993;269(18):2386-2391.
- Folstein MF, Folstein SE, McHugh PR. "Mini-mental state": a practical method for grading the cognitive state of patients for the clinician. *J Psychiatr Res*. 1975;12:189-198.
- Rovner BW, Folstein MF. Mini-mental state exam in clinical practice. *Hosp Pract*. 1987;22(1A):99, 103, 106, 110.
- Tombaugh TN, McIntyre NJ. The mini-mental state examination: a comprehensive review. *J Am Geriatr Soc*. 1992;40(9):922-935.

Adapted from: http://www.heartinstitutehd.com/Misc/Forms/MMSE.1276128605.pdf

1.2 Modified Ashworth Scores (MAS)

Modified Ashworth Scale Instructions

General Information (derived Bohannon and Smith, 1987):

- Place the patient in a supine position
- If testing a muscle that primarily flexes a joint, place the joint in a maximally flexed position and move to a position of maximal extension over one second (count "one thousand one")
- If testing a muscle that primarily extends a joint, place the joint in a maximally extended position and move to a position of maximal flexion over one second (count "one thousand one")
- Score based on the classification below

Scoring (taken from Bohannon and Smith, 1987):

0   No increase in muscle tone

1   Slight increase in muscle tone, manifested by a catch and release or by minimal resistance at the end of the range of motion when the affected part(s) is moved in flexion or extension

1+   Slight increase in muscle tone, manifested by a catch, followed by minimal resistance throughout the remainder (less than half) of the ROM

2   More marked increase in muscle tone through most of the ROM, but affected part(s) easily moved

3   Considerable increase in muscle tone, passive movement difficult

4   Affected part(s) rigid in flexion or extension

Patient Instructions:
The patient should be instructed to relax.

Adopted from: https://www.sralab.org/sites/default/files/2017-

06/Modified%20Ashworth%20Scale%20Instructions.pdf

1.3 Fugl-Meyer Assessment for Upper Extremity (FMA-UE)

FUGL-MEYER ASSESSMENT
UPPER EXTREMITY (FMA-UE)
Assessment of sensorimotor function

ID:
Date:
Examiner:

Fugl-Meyer AR, Jaasko L, Leyman I, Olsson S, Steglind S: The post-stroke hemiplegic patient. A method for evaluation of physical performance. Scand J Rehabil Med 1975, 7:13-31.

A. UPPER EXTREMITY, sitting position

I. Reflex activity		none	can be elicited	
Flexors: biceps and finger flexors (at least one)		0	2	
Extensors: triceps		0	2	
Subtotal I (max 4)				

II. Volitional movement within synergies, without gravitational help			none	partial	full
Flexor synergy: Hand from contralateral knee to ipsilateral ear. From extensor synergy (shoulder adduction/ internal rotation, elbow extension, forearm pronation) to flexor synergy (shoulder abduction/ external rotation, elbow flexion, forearm supination).	Shoulder	retraction	0	1	2
		elevation	0	1	2
		abduction (90°)	0	1	2
		external rotation	0	1	2
	Elbow	flexion	0	1	2
	Forearm	supination	0	1	2
Extensor synergy: Hand from ipsilateral ear to the contralateral knee	Shoulder	adduction/internal rotation	0	1	2
	Elbow	extension	0	1	2
	Forearm	pronation	0	1	2
Subtotal II (max 18)					

III. Volitional movement mixing synergies, without compensation		none	partial	full
Hand to lumbar spine hand on lap	cannot perform or hand in front of ant-sup iliac spine	0		
	hand behind ant-sup iliac spine (without compensation)		1	
	hand to lumbar spine (without compensation)			2
Shoulder flexion 0°- 90° elbow at 0° pronation-supination 0°	immediate abduction or elbow flexion	0		
	abduction or elbow flexion during movement		1	
	flexion 90°, no shoulder abduction or elbow flexion			2
Pronation-supination elbow at 90° shoulder at 0°	no pronation/supination, starting position impossible	0		
	limited pronation/supination, maintains starting position		1	
	full pronation/supination, maintains starting position			2
Subtotal III (max 6)				

IV. Volitional movement with little or no synergy		none	partial	full
Shoulder abduction 0 - 90° elbow at 0° forearm neutral	immediate supination or elbow flexion	0		
	supination or elbow flexion during movement		1	
	abduction 90°, maintains extension and pronation			2
Shoulder flexion 90° - 180° elbow at 0° pronation-supination 0°	immediate abduction or elbow flexion	0		
	abduction or elbow flexion during movement		1	
	flexion 180°, no shoulder abduction or elbow flexion			2
Pronation/supination elbow at 0° shoulder at 30°- 90° flexion	no pronation/supination, starting position impossible	0		
	limited pronation/supination, maintains start position		1	
	full pronation/supination, maintains starting position			2
Subtotal IV (max 6)				

V. Normal reflex activity assessed only if full score of 6 points is achieved in part IV; compare with the unaffected side		hyper	lively	normal
Biceps, triceps, finger flexors	2 of 3 reflexes markedly hyperactive	0		
	1 reflex markedly hyperactive or at least 2 reflexes lively		1	
	maximum of 1 reflex lively, none hyperactive			2
Subtotal V (max 2)				

Total A (max 36)	

B. WRIST support may be provided at the elbow to take or hold the starting position, no support at wrist, check the passive range of motion prior testing		none	partial	full
Stability at 15° dorsiflexion elbow at 90°, forearm pronated shoulder at 0°	less than 15° active dorsiflexion dorsiflexion 15°, no resistance tolerated maintains dorsiflexion against resistance	0	1	2
Repeated dorsifexion / volar flexion elbow at 90°, forearm pronated shoulder at 0°, slight finger flexion	cannot perform volitionally limited active range of motion full active range of motion, smoothly	0	1	2
Stability at 15° dorsiflexion elbow at 0°, forearm pronated slight shoulder flexion/abduction	less than 15° active dorsiflexion dorsiflexion 15°, no resistance tolerated maintains dorsiflexion against resistance	0	1	2
Repeated dorsifexion / volar flexion elbow at 0°, forearm pronated slight shoulder flexion/abduction	cannot perform volitionally limited active range of motion full active range of motion, smoothly	0	1	2
Circumduction elbow at 90°, forearm pronated shoulder at 0°	cannot perform volitionally jerky movement or incomplete complete and smooth circumduction	0	1	2
Total B (max 10)				

C. HAND support may be provided at the elbow to keep 90° flexion, no support at the wrist, compare with unaffected hand, the objects are interposed, active grasp		none	partial	full
Mass flexion from full active or passive extension		0	1	2
Mass extension from full active or passive flexion		0	1	2
GRASP				
a. Hook grasp flexion in PIP and DIP (digits II-V), extension in MCP II-V	cannot be performed can hold position but weak maintains position against resistance	0	1	2
b. Thumb adduction 1-st CMC, MCP, IP at 0°, scrap of paper between thumb and 2-nd MCP joint	cannot be performed can hold paper but not against tug can hold paper against a tug	0	1	2
c. Pincer grasp, opposition pulpa of the thumb against the pulpa of 2-nd finger, pencil, tug upward	cannot be performed can hold pencil but not against tug can hold pencil against a tug	0	1	2
d. Cylinder grasp cylinder shaped object (small can) tug upward, opposition of thumb and fingers	cannot be performed can hold cylinder but not against tug can hold cylinder against a tug	0	1	2
e. Spherical grasp fingers in abduction/flexion, thumb opposed, tennis ball, tug away	cannot be performed can hold ball but not against tug can hold ball against a tug	0	1	2
Total C (max 14)				

D. COORDINATION/SPEED, sitting, after one trial with both arms, eyes closed, tip of the index finger from knee to nose, 5 times as fast as possible		marked	slight	none
Tremor		0	1	2
Dysmetria	pronounced or unsystematic slight and systematic no dysmetria	0	1	2
		≥ 6s	**2 - 5s**	**< 2s**
Time start and end with the hand on the knee	6 or more seconds slower than unaffected side 2-5 seconds slower than unaffected side less than 2 seconds difference	0	1	2
Total D (max 6)				

TOTAL A-D (max 66)	

Adopted from: https://www.gu.se/en/neuroscience-physiology/fugl-meyer-assessment

1.4 Action Research Arm Test (ARAT)

ACTION RESEARCH ARM TEST

Patient Name: _____

Rater Name: _____

Date: _____

Instructions

There are four subtests: Grasp, Grip, Pinch, Gross Movement. Items in each are ordered so that:

- if the subject passes the first, no more need to be administered and he scores top marks for that subtest;

- if the subject fails the first *and* fails the second, he scores zero, and again no more tests need to be performed in that subtest;

- otherwise he needs to complete all tasks within the subtest

Activity	Score

Grasp

1. Block, wood, 10 cm cube (If score = 3, total = 18 and to Grip)
   Pick up a 10 cm block _____

2. Block, wood, 2.5 cm cube (If score = 0, total = 0 and go to Grip)
   Pick up 2.5 cm block _____

3. Block, wood, 5 cm cube _____

4. Block, wood, 7.5 cm cube _____

5. Ball (Cricket), 7.5 cm diameter _____

6. Stone 10 x 2.5 x 1 cm _____

Coefficient of reproducibility = 0.98

Coefficient of scalability = 0.94

Grip

1. Pour water from glass to glass (If score = 3, total = 12, and go to Pinch) _____

2. Tube 2.25 cm (If score = 0, total = 0 and go to Pinch) _____

3. Tube 1 x 16 cm _____

4. Washer (3.5 cm diameter) over bolt _____

Coefficient of reproducibility = 0.99

Coefficient of scalability = 0.98

Pinch

1. Ball bearing, 6 mm, 3rd finger and thumb (If score = 3, total = 18 and go to Grossmt) _____
2. Marble, 1.5 cm, index finger and thumb (If score = 0, total = 0 and go to Grossmt) _____
3. Ball bearing 2nd finger and thumb _____
4. Ball bearing 1st finger and thumb _____
5. Marble 3rd finger and thumb _____
6. Marble 2nd finger and thumb _____

Coefficient of reproducibility = 0.99

Coefficient of scalability = 0.98

Grossmt (Gross Movement)

1. Place hand behind head (If score = 3, total = 9 and finish) _____
2. (If score = 0, total = 0 and finish) _____
3. Place hand on top of head _____
4. Hand to mouth _____

Coefficient of reproducibility = 0.98

Coefficient of scalability = 0.97

Adopted from: https://www.physio-pedia.com/Action_Research_Arm_Test_(ARAT)

Appendices 2: Clinical Assessments for Lower Limb

2.1 Functional Ambulation Category (FAC)

Appendix—Description of Functional Ambulation Category (FAC)

FAC	Ambulation Description	Definition
0	Nonfunctional ambulation	Subject cannot ambulate, ambulates in parallel bars only, or requires supervision or physical assistance from more than one person to ambulate safely outside of parallel bars
1	Ambulator-Dependent for Physical Assistance Level II	Subject requires manual contacts of no more than one person during ambulation on level surfaces to prevent falling. Manual contacts are continuous and necessary to support body weight as well as maintain balance and/or assist coordination
2	Ambulator-Dependent for Physical Assistance Level I	Subject requires manual contact of no more than one person during ambulation on level surfaces to prevent falling. Manual contact consists of continuous or intermittent light touch to assist balance or coordination
3	Ambulator-Dependent for Supervision	Subject can physically ambulate on level surfaces without manual contact of another person but for safety requires standby guarding on no more than one person because of poor judgment, questionable cardiac status, or the need for verbal cuing to complete the task.
4	Ambulator-Independent Level Surfaces only	Subject can ambulate independently on level surfaces but requires supervision or physical assistance to negotiate any of the following: stairs, inclines, or non-level surfaces.
5	Ambulator-Independent	Subject can ambulate independently on nonlevel and level surfaces, stairs, and inclines.

Adopted from: https://strokengine.ca/en/assessments/fac/

BERG BALANCE TESTS AND RATING SCALE

Patient Name _____

Date _____

Location _____

Rater _____

ITEM DESCRIPTION SCORE (0-4) Sitting to standing _____ Standing unsupported _____ Sitting unsupported _____ Standing to sitting _____ Transfers _____ Standing with eyes closed _____ Standing with feet together _____ Reaching forward with outstretched arm _____ Retrieving object from floor _____ Turning to look behind _____ Turning 360 degrees _____ Placing alternate foot on stool _____ Standing with one foot in front _____ Standing on one foot _____ TOTAL _____

GENERAL INSTRUCTIONS

Please demonstrate each task and/or give instructions as written. When scoring, please record the lowest response category that applies for each item.

In most items, the subject is asked to maintain a given position for a specific time. Progressively more points are deducted if the time or distance requirements are not met, if the subject's performance warrants supervision, or if the subject touches an external support or receives assistance from the examiner. Subjects should understand that they must maintain their balance while attempting the tasks. The choices of which leg to stand on or how far to reach are left to the subject. Poor judgment will adversely influence the performance and the scoring.

Equipment required for testing are a stopwatch or watch with a second hand, and a ruler or other indicator of 2, 5 and 10 inches (5, 12 and 25 cm). Chairs used during testing should be of reasonable height. Either a step or a stool (of average step height) may be used for item #12.

1. SITTING TO STANDING

INSTRUCTIONS: Please stand up. Try not to use your hands for support.

( ) 4 able to stand without using hands and stabilize independently

( ) 3 able to stand independently using hands

( ) 2 able to stand using hands after several tries

( ) 1 needs minimal aid to stand or to stabilize

( ) 0 needs moderate or maximal assist to stand

2. STANDING UNSUPPORTED

INSTRUCTIONS: Please stand for two minutes without holding.

( ) 4 able to stand safely 2 minutes

( ) 3 able to stand 2 minutes with supervision

( ) 2 able to stand 30 seconds unsupported

( ) 1 needs several tries to stand 30 seconds unsupported

( ) 0 unable to stand 30 seconds unassisted

If a subject is able to stand 2 minutes unsupported, score full points for sitting unsupported. Proceed to item #4.

3. SITTING WITH BACK UNSUPPORTED BUT FEET SUPPORTED ON FLOOR OR ON A STOOL
INSTRUCTIONS: Please sit with arms folded for 2 minutes.
( ) 4 able to sit safely and securely 2 minutes
( ) 3 able to sit 2 minutes under supervision
( ) 2 able to sit 30 seconds
( ) 1 able to sit 10 seconds
( ) 0 unable to sit without support 10 seconds

4. STANDING TO SITTING
INSTRUCTIONS: Please sit down.
( ) 4 sits safely with minimal use of hands
( ) 3 controls descent by using hands
( ) 2 uses back of legs against chair to control descent
( ) 1 sits independently but has uncontrolled descent
( ) 0 needs assistance to sit

5. TRANSFERS
INSTRUCTIONS: Arrange chairs(s) for a pivot transfer. Ask subject to transfer one way toward a seat with armrests and one way toward a seat without armrests. You may use two chairs (one with and one without armrests) or a bed and a chair.
( ) 4 able to transfer safely with minor use of hands
( ) 3 able to transfer safely definite need of hands
( ) 2 able to transfer with verbal cueing and/or supervision
( ) 1 needs one person to assist
( ) 0 needs two people to assist or supervise to be safe

6. STANDING UNSUPPORTED WITH EYES CLOSED
INSTRUCTIONS: Please close your eyes and stand still for 10 seconds.
( ) 4 able to stand 10 seconds safely
( ) 3 able to stand 10 seconds with supervision
( ) 2 able to stand 3 seconds
( ) 1 unable to keep eyes closed 3 seconds but stays steady
( ) 0 needs help to keep from falling

7. STANDING UNSUPPORTED WITH FEET TOGETHER
INSTRUCTIONS: Place your feet together and stand without holding.
( ) 4 able to place feet together independently and stand 1 minute safely
( ) 3 able to place feet together independently and stand for 1 minute with supervision
( ) 2 able to place feet together independently but unable to hold for 30 seconds
( ) 1 needs help to attain position but able to stand 15 seconds with feet together
( ) 0 needs help to attain position and unable to hold for 15 seconds

8. REACHING FORWARD WITH OUTSTRETCHED ARM WHILE STANDING

INSTRUCTIONS: Lift arm to 90 degrees. Stretch out your fingers and reach forward as far as you can. (Examiner places a ruler at end of fingertips when arm is at 90 degrees. Fingers should not touch the ruler while reaching forward. The recorded measure is the distance forward that the finger reaches while the subject is in the most forward lean position. When possible, ask subject to use both arms when reaching to avoid rotation of the trunk.)

( ) 4 can reach forward confidently >25 cm (10 inches)
( ) 3 can reach forward >12 cm safely (5 inches)
( ) 2 can reach forward >5 cm safely (2 inches)
( ) 1 reaches forward but needs supervision
( ) 0 loses balance while trying/requires external support

9. PICK UP OBJECT FROM THE FLOOR FROM A STANDING POSITION

INSTRUCTIONS: Pick up the shoe/slipper which is placed in front of your feet.

( ) 4 able to pick up slipper safely and easily
( ) 3 able to pick up slipper but needs supervision
( ) 2 unable to pick up but reaches 2-5cm (1-2 inches) from slipper and keeps balance independently
( ) 1 unable to pick up and needs supervision while trying
( ) 0 unable to try/needs assist to keep from losing balance or falling

10. TURNING TO LOOK BEHIND OVER LEFT AND RIGHT SHOULDERS WHILE STANDING

INSTRUCTIONS: Turn to look directly behind you over toward left shoulder. Repeat to the right. Examiner may pick an object to look at directly behind the subject to encourage a better twist turn.

( ) 4 looks behind from both sides and weight shifts well
( ) 3 looks behind one side only other side shows less weight shift
( ) 2 turns sideways only but maintains balance
( ) 1 needs supervision when turning
( ) 0 needs assist to keep from losing balance or falling

11. TURN 360 DEGREES

INSTRUCTIONS: Turn completely around in a full circle. Pause. Then turn a full circle in the other direction.

( ) 4 able to turn 360 degrees safely in 4 seconds or less
( ) 3 able to turn 360 degrees safely one side only in 4 seconds or less
( ) 2 able to turn 360 degrees safely but slowly
( ) 1 needs close supervision or verbal cueing
( ) 0 needs assistance while turning

12. PLACING ALTERNATE FOOT ON STEP OR STOOL WHILE STANDING UNSUPPORTED

INSTRUCTIONS: Place each foot alternately on the step/stool. Continue until each foot has touched the step/stool four times.

( ) 4 able to stand independently and safely and complete 8 steps in 20 seconds
( ) 3 able to stand independently and complete 8 steps in >20 seconds
( ) 2 able to complete 4 steps without aid with supervision
( ) 1 able to complete >2 steps needs minimal assist
( ) 0 needs assistance to keep from falling/unable to try

13. STANDING UNSUPPORTED ONE FOOT IN FRONT

INSTRUCTIONS: (DEMONSTRATE TO SUBJECT) Place one foot directly in front of the other. If you feel that you cannot place your foot directly in front, try to step far enough ahead that the heel of your forward foot is ahead of the toes of the other foot. (To score 3 points, the length of the step should exceed the length of the other foot and the width of the stance should approximate the subject's normal stride width)

( ) 4 able to place foot tandem independently and hold 30 seconds
( ) 3 able to place foot ahead of other independently and hold 30 seconds
( ) 2 able to take small step independently and hold 30 seconds
( ) 1 needs help to step but can hold 15 seconds
( ) 0 loses balance while stepping or standing

14. STANDING ON ONE LEG

INSTRUCTIONS: Stand on one leg as long as you can without holding.

( ) 4 able to lift leg independently and hold >10 seconds
( ) 3 able to lift leg independently and hold 5-10 seconds
( ) 2 able to lift leg independently and hold = or >3 seconds
( ) 1 tries to lift leg unable to hold 3 seconds but remains standing independently
( ) 0 unable to try or needs assist to prevent fall

TOTAL SCORE (Maximum = 56: _____

*References

Wood-Dauphinee S, Berg K, Bravo G, Williams JI: The Balance Scale: Responding to clinically meaningful changes. Canadian Journal of Rehabilitation, 10: 35-50,1997.

Berg K, Wood-Dauphinee S, Williams JI: The Balance Scale: Reliability assessment for elderly residents and patients with an acute stroke. Scand J Rehab Med, 27:27-36, 1995.

Berg K, Maki B, Williams JI, Holliday P, Wood-Dauphinee S: A comparison of clinical and laboratory measures of postural balance in an elderly population. Arch Phys Med Rehabil, 73: 1073-1083, 1992.

Berg K, Wood-Dauphinee S, Williams JI, Maki, B: Measuring balance in the elderly: Validation of an instrument. Can. J. Pub. Health, July/August supplement 2:S7-11, 1992.

Berg K, Wood-Dauphinee S, Williams JI, Gayton D: Measuring balance in the elderly: Preliminary development of an instrument. Physiotherapy Canada, 41:304-311, 1989.

Adopted from: http://www.chiropractic.on.ca/wp-content/uploads/fp-berg-balance-scale.pdf

2.3 Modified Ashworth Scale (MAS)

Modified Ashworth Scale Instructions

<u>General Information (derived Bohannon and Smith, 1987):</u>
- Place the patient in a supine position
- If testing a muscle that primarily flexes a joint, place the joint in a maximally flexed position and move to a position of maximal extension over one second (count "one thousand one")
- If testing a muscle that primarily extends a joint, place the joint in a maximally extended position and move to a position of maximal flexion over one second (count "one thousand one")
- Score based on the classification below

<u>Scoring (taken from Bohannon and Smith, 1987):</u>

0 No increase in muscle tone

1 Slight increase in muscle tone, manifested by a catch and release or by minimal resistance at the end of the range of motion when the affected part(s) is moved in flexion or extension

1+ Slight increase in muscle tone, manifested by a catch, followed by minimal resistance throughout the remainder (less than half) of the ROM

2 More marked increase in muscle tone through most of the ROM, but affected part(s) easily moved

3 Considerable increase in muscle tone, passive movement difficult

4 Affected part(s) rigid in flexion or extension

<u>Joints:</u>

Hip:

Knee:

Ankle:

Adopted from: https://www.sralab.org/sites/default/files/2017-

06/Modified%20Ashworth%20Scale%20Instructions.pdf

2.4 Fugl-Meyer Assessment for Lower Extremity (FMA-LE)

FMA-LE PROTOCOL

FUGL-MEYER ASSESSMENT
LOWER EXTREMITY (FMA-LE)
Assessment of sensorimotor function

Fugl-Meyer AR, Jaaszko L, Leyman I, Olsson S, Steglind S: The post-stroke hemiplegic patient. 1. a method for evaluation of physical performance. Scand J Rehabil Med 1975, 7:13-31.

E. LOWER EXTREMITY

I. Reflex activity, supine position		none	can be elicited	
Flexors: knee flexors		0	2	
Extensors: patellar, achilles (at least one)		0	2	
Subtotal I (max 4)				

II. Volitional movement within synergies supine position			none	partial	full
Flexor synergy: Maximal hip flexion (abduction/external rotation), maximal flexion in knee and ankle joint (palpate distal tendons to ensure active knee flexion).	Hip	flexion	0	1	2
	Knee	flexion	0	1	2
	Ankle	dorsiflexion	0	1	2
Extensor synergy: From flexor synergy to the hip extension/adduction, knee extension and ankle plantar flexion. Resistance is applied to ensure active movement, evaluate both movement and strength (compare with the unaffected side)	Hip	extension	0	1	2
		adduction	0	1	2
	Knee	extension	0	1	2
	Ankle	plantar flexion	0	1	2
Subtotal II (max 14)					

III. Volitional movement mixing synergies sitting position, knee 10cm from the edge of the chair/bed		none	partial	full
Knee flexion from actively or passively extended knee	no active motion	0		
	less than 90° active flexion, palpate tendons of hamstrings		1	
	more than 90° active flexion			2
Ankle dorsiflexion compare with unaffected side	no active motion	0		
	limited dorsiflexion		1	
	complete dorsiflexion			2
Subtotal III (max 4)				

IV. Volitional movement with little or no synergy standing position, hip at 0°		none	partial	full
Knee flexion to 90° hip at 0°, balance support is allowed	no active motion or immediate, simultaneous hip flexion	0		
	less than 90° knee flexion and/or hip flexion during movement		1	
	at least 90° knee flexion without simultaneous hip flexion			2
Ankle dorsiflexion compare with unaffected side	no active motion	0		
	limited dorsiflexion		1	
	complete dorsiflexion			2
Subtotal IV (max 4)				

V. Normal reflex activity supine position, assessed only if full score of 4 points is achieved in part IV, compare with the unaffected side		hyper	lively	normal
Reflex activity knee flexors, Patellar, Achilles,	2 of 3 reflexes markedly hyperactive	0		
	1 reflex markedly hyperactive or at least 2 reflexes lively		1	
	maximum of 1 reflex lively, none hyperactive			2
Subtotal V (max 2)				
Total E (max 28)				

F. COORDINATION/SPEED, supine, after one trial with both legs, eyes closed, heel to knee cap of the opposite leg, 5 times as fast as possible		marked	slight	none
Tremor		0	1	2
Dysmetria	pronounced or unsystematic slight and systematic no dysmetria	0 	 1 	 2
		≥ 6s	2 - 5s	< 2s
Time	6 or more seconds slower than unaffected side 2-5 seconds slower than unaffected side less than 2 seconds difference	0 	 1 	 2
Total F (max 6)				

H. SENSATION, lower extremity eyes closed, compare with the unaffected side		anesthesia	hypoesthesia or dysesthesia	normal
Light touch	leg foot sole	0 0	1 1	2 2
		less than 3/4 correct or absence	3/4 correct or considerable difference	correct 100%, little or no difference
Position small alterations in the position	hip knee ankle great toe (IP-joint)	0 0 0 0	1 1 1 1	2 2 2 2
Total H (max12)				

I. PASSIVE JOINT MOTION, lower extremity supine position, compare with the unaffected side		only few degrees (<10° hip)	decreased	normal	J. JOINT PAIN during passive motion, lower extremity pronounced pain during movement or very marked pain at the end of the movement	some pain	no pain
Hip	Flexion Abduction External rotation Internal rotation	0 0 0 0	1 1 1 1	2 2 2 2	0 0 0 0	1 1 1 1	2 2 2 2
Knee	Flexion Extension	0 0	1 1	2 2	0 0	1 1	2 2
Ankle	Dorsiflexion Plantar flexion	0 0	1 1	2 2	0 0	1 1	2 2
Foot	Pronation Supination	0 0	1 1	2 2	0 0	1 1	2 2
Total (max 20)					Total (max 20)		

E. LOWER EXTERMTY	/28
F. COORDINATION / SPEED	/6
TOTAL E-F (motor function)	/34

H. SENSATION	/12
I. PASSIVE JOINT MOTION	/20
J. JOINT PAIN	/20

Adopted from: https://www.gu.se/en/neuroscience-physiology/fugl-meyer-assessment

2.5 10 Meter Walk Test (10MWT)

Core Measure: 10 Meter Walk Test (10mWT)

Overview	• The 10mWT is used to assess walking speed in meters/second (m/s) over a short distance.
Number of Test Items	• 1 item
Scoring	• The total time taken to ambulate 6 meters (m) is recorded to the nearest hundredth of a second. 6 m is then divided by the total time (in seconds) taken to ambulate and recorded in m/s[1,2]
Equipment	• Stopwatch • A clear pathway of at least 10 m (32.8 ft) in length in a designated area over solid flooring[2,3]
Time (new clinician)	• 5 minutes or less
Time (experienced clinician)	• 5 minutes or less
Cost	• Free
Logistics-Setup	• A clear pathway of at least 10 m (32.8 ft) in length in a designated area over solid flooring is required. • Measure and mark the start and end point of a 10-m walkway. • Add a mark at 2 m and 8 m (identifying the central 6 m which will be timed). • Quiet conditions[1]

Logistics-Administration	• Comfortable walking speed:
	   o Have the patient start on the 0-m mark (start line)
	   o Instructions to patient: *"Walk at your own comfortable walking pace and stop when you reach the far mark."*
	• Fast walking speed:
	   o Have the patient start on the 0-m mark (start line)
	   o Instructions to patient: *"Walk as fast as you can safely walk and stop when you reach the far mark."*
	• Two trials are administered at the patient's comfortable walking speed, followed by 2 trials at his/her fast walking speed, per the below instructions. The 2 trials, for each speed, are averaged and the 2 gait speeds are documented in meters/second.[1]
	• Patients may use any assistive device or bracing that they are currently using. The type of device and/or bracing must be documented.
	• When administering the test, do not walk in front of or directly beside the patient, as this may "pace" the patient and influence the speed and distance they walk. Instead, walk at least a half step behind the patient.

	- If a patient requires assistance, only the minimum amount of assistance required for a patient to complete the task should be provided. The level of assistance documented, however, should reflect the greatest amount of assistance provided during the test. For example, if a patient required minimum assistance for the majority of the test but required moderate assistance for stability on one occasion, the patient should be rated as requiring moderate assistance. Assistance should be provided to prevent a fall or collapsing (i.e. knee buckling, trunk collapse, etc). Assistance should <u>not</u> be provided for limb swing, or any other manner in which the assistance is propelling the patient forward. - The level of physical assistance documented using an ordinal 7-point scale is described below. 1 = *total assistance* [patient performs 0%-24% of task]* 2 = *maximum assistance* [patient performs 25%-49% of task] 3 = *moderate assistance* [patient performs 50%-74% of task] 4 = *minimum assistance* [patient performs 75%-99% of task] 5 = *supervision* [patient requires stand-by or set-up assistance; no physical contact is provided] 6 = *modified independent* [patient requires use of assistive devices or bracing, needs extra time, mild safety issues] 7 = *independent* ***Note:** if your patient requires *total assistance*, a score of 0 should be documented
Logistics-Scoring	- The time is measured for the middle 6 m to allow for patient acceleration and deceleration.[1,4] - The time is started when any part of the leading foot crosses the plane of the 2-m mark. - The time is stopped when any part of the leading foot crosses the plane of the 8-m mark.[1] - <u>Document the time to walk the middle 6m, the level of assistance, and type of assistive device and/or bracing used.</u> - If a patient requires *total assistance* or is unable to ambulate at all, a score of 0 m/s should be documented.
Additional Recommendations	- Patients should not talk during the test, as this depletes their respiratory reserves. Exceptions to this are if the patient requests to stop the test or needs to report any symptoms (e.g. pain, dizziness). - The person administering the test also should not talk. Talking during the test can distract the patient and affect their score on the test. - For patients who are unable to walk, but have a goal and the capacity to achieve walking, a baseline score of 0 meters/second should be documented. - To track change, it is recommended that this measure is administered a minimum of two times (admission and discharge), and when feasible, between these periods, under the same test conditions for the patient.

	Recommend review of this standardized procedure and, on an annual basis, establish consistency within and among raters using the tool.

Adopted from: https://www.sralab.org/rehabilitation-measures/10-meter-walk-test

Appendices 3: Consent Form

3.1 Consent Form for Chapter 3 and Chapter 4

THE HONG KONG
POLYTECHNIC UNIVERSITY
香港理工大學

Consent form

I, _____ (name of subject), hereby consent to participate as a subject for the project entitled "Exo-neuro-musculo-skeleton with balance sensing feedback for ankle-foot rehabilitation after stroke".

- I have understood the experimental procedures presented to me.
- I have given an opportunity to ask questions about the experiment, and these have been answered to my satisfaction.
- I have understood the information presented in the information sheet.
- I realize the experiment will possibly benefit my lower limb motor functions.
- The testing should not result in any undue discomfort, I realize that I can discontinue the experiment with no reasons given and no penalty received during the experiment.
- I realize that the results of this experiment may be published, but that my own results will be kept confidential.
- I realize that the results of this experiment are the properties of The Hong Kong Polytechnic University.
- I agree that the PI and the project research members, who obtained the authorization from the PI, can use my experimental data for this project study.

Subject name: _____   Signature: _____   Date: _____

Witness: _____   Signature: _____   Date: _____

Investigator: _____   Signature: _____   Date: _____

同意書

我, _____(受試者姓名), 在此同意作為受試者參加 "用於踝足復康的智感平衡外神經肌骨系統"。

- 我已明白到該測試的步驟。
- 我已給予機會詢問有關該測試的問題, 並已獲得滿意的回答。
- 我已明白在資料單張上所寫的所有內容
- 我已明白這個實驗有可能可以改善我的下肢運動功能
- 此實驗不會給您帶來不適, 我已明白在實驗中我可以終止測試而無需給予任何理由, 或由此而受到任何懲罰。
- 我已知道這個測試的結果可被發表, 但有關我個人的結果將獲得保密。
- 我已知道這個測試的結果屬香港理工大學。
- 我同意本項目負責人及其受權的項目研究人員使用我的實驗記錄以作此項目的研究。

受試者姓名_____   簽署_____   日期_____

作證人姓名_____   簽署_____   日期_____

研究員姓名_____   簽署_____   日期_____

138

REFERENCES

1. Tsao, C.W., et al., *Heart Disease and Stroke Statistics—2022 Update: A Report From the American Heart Association.* Circulation, 2022. **145**(8): p. e153-e639.

2. Wang, Y.-J., et al., *China Stroke Statistics: an update on the 2019 report from the National Center for Healthcare Quality Management in Neurological Diseases, China National Clinical Research Center for Neurological Diseases, the Chinese Stroke Association, National Center for Chronic and Non-communicable Disease Control and Prevention, Chinese Center for Disease Control and Prevention and Institute for Global Neuroscience and Stroke Collaborations.* Stroke and Vascular Neurology, 2022: p. svn-2021-001374.

3. Feigin, V.L., et al., *World Stroke Organization (WSO): Global Stroke Fact Sheet 2022.* Int J Stroke, 2022. **17**(1): p. 18-29.

4. Virani, S.S., et al., *Heart Disease and Stroke Statistics-2021 Update: A Report From the American Heart Association.* Circulation, 2021. **143**(8): p. e254-e743.

5. Kwakkel, G., et al., *Probability of regaining dexterity in the flaccid upper limb: impact of severity of paresis and time since onset in acute stroke.* Stroke, 2003. **34**(9): p. 2181-6.

6. Hendricks, H.T., et al., *Motor recovery after stroke: A systematic review of the literature.* Archives of Physical Medicine and Rehabilitation, 2002. **83**(11): p. 1629-1637.

7. Horn, S.D., et al., *Stroke Rehabilitation Patients, Practice, and Outcomes: Is Earlier and More Aggressive Therapy Better?* Archives of Physical Medicine and Rehabilitation, 2005. **86**(12, Supplement): p. 101-114.

8. Duncan, P.W., et al., *Body-Weight–Supported Treadmill Rehabilitation after Stroke.* New England Journal of Medicine, 2011. **364**(21): p. 2026-2036.

9. Hung, C.-s., et al., *The Effects of Combination of Robot-Assisted Therapy With Task-Specific or Impairment-Oriented Training on Motor Function and Quality of Life in Chronic Stroke.* PM&R, 2016. **8**(8): p. 721-729.

10. Hospital Authority Statistical Report, 2016. **http://www.ha.org.hk/visitor/ha_index.asp?Lang=CHIB5**.

11. Alam, M., I.A. Choudhury, and A.B. Mamat, *Mechanism and design analysis of articulated ankle foot orthoses for drop-foot.* The Scientific World Journal, 2014. **2014**.

12. Tyson, S.F., et al., *Distribution of weakness in the upper and lower limbs post-stroke.* Disability and Rehabilitation, 2006. **28**(11): p. 715-719.

13. Beyaert, C., R. Vasa, and G.E. Frykberg, *Gait post-stroke: Pathophysiology and rehabilitation strategies.* Neurophysiologie Clinique/Clinical Neurophysiology, 2015. **45**(4): p. 335-355.

14. Chae, J., et al., *Delay in initiation and termination of muscle contraction, motor impairment, and physical disability in upper limb hemiparesis.* Muscle & Nerve, 2002. **25**(4): p. 568-575.

15. Allen, J.L., L.H. Ting, and T.M. Kesar, *Gait Rehabilitation Using Functional Electrical Stimulation Induces Changes in Ankle Muscle Coordination in Stroke Survivors: A Preliminary Study.* Frontiers in Neurology, 2018. **9**.

16. Mahmood, A., et al., *Effect of Transcutaneous Electrical Nerve Stimulation on Spasticity in Adults With Stroke: A Systematic Review and Meta-analysis.* Archives of Physical Medicine and Rehabilitation, 2019. **100**(4): p. 751-768.

17. Jang, G.U., et al., *A study of structural foot deformity in stroke patients.* Journal of Physical Therapy Science, 2015. **27**(1): p. 191-194.

18. Lin, I.H., et al., *Effectiveness and Superiority of Rehabilitative Treatments in Enhancing Motor Recovery Within 6 Months Poststroke: A Systemic Review.* Archives of Physical Medicine and Rehabilitation, 2019. **100**(2): p. 366-378.

19. Nilsson, A., et al., *Gait training early after stroke with a new exoskeleton – the hybrid assistive limb: a study of safety and feasibility.* Journal of NeuroEngineering and Rehabilitation, 2014. **11**(1): p. 92.

20. Bruni, M.F., et al., *What does best evidence tell us about robotic gait rehabilitation in stroke patients: A systematic review and meta-analysis.* Journal of Clinical Neuroscience, 2018. **48**: p. 11-17.

21. Yeung, L.F., et al. *Design of an exoskeleton ankle robot for robot-assisted gait training of stroke patients.* in *2017 International Conference on Rehabilitation Robotics (ICORR).* 2017.

22. Kwon, J., et al., *A Soft Wearable Robotic Ankle-Foot-Orthosis for Post-Stroke Patients.* IEEE Robotics and Automation Letters, 2019. **4**(3): p. 2547-2552.

23. Puyuelo-Quintana, G., et al., *A new lower limb portable exoskeleton for gait assistance in neurological patients: a proof of concept study.* Journal of NeuroEngineering and Rehabilitation, 2020. **17**(1): p. 60.

24. Thalman, C.M., et al. *Design of a Soft Ankle-Foot Orthosis Exosuit for Foot Drop Assistance.* in *2019 International Conference on Robotics and Automation (ICRA).* 2019.

25. Awad, L.N., et al., *A soft robotic exosuit improves walking in patients after stroke.* Sci Transl Med, 2017. **9**(400).

26. Xia, H., et al. *Design of A Multi-Functional Soft Ankle Exoskeleton for Foot-Drop Prevention, Propulsion Assistance, and Inversion/Eversion Stabilization*. in *2020 8th IEEE RAS/EMBS International Conference for Biomedical Robotics and Biomechatronics (BioRob)*. 2020.

27. Byl, N., et al., *Clinical impact of gait training enhanced with visual kinematic biofeedback: Patients with Parkinson's disease and patients stable post stroke.* Neuropsychologia, 2015. **79**(Pt B): p. 332-43.

28. Ma, C.Z., Y.P. Zheng, and W.C. Lee, *Changes in gait and plantar foot loading upon using vibrotactile wearable biofeedback system in patients with stroke.* Top Stroke Rehabil, 2018. **25**(1): p. 20-27.

29. Ballester, B.R., S.B.i. Badia, and P.F.M.J. Verschure, *Including Social Interaction in Stroke VR-Based Motor Rehabilitation Enhances Performance: A Pilot Study.* Presence, 2012. **21**(4): p. 490-501.

30. Fugl-Meyer, A.R., et al., *The post-stroke hemiplegic patient. 1. a method for evaluation of physical performance.* Scandinavian journal of rehabilitation medicine, 1975. **7**(1): p. 13.

31. Lyle, R.C., *A performance test for assessment of upper limb function in physical rehabilitation treatment and research.* International journal of rehabilitation research, 1981. **4**(4): p. 483-492.

32. Ashworth, B., *Preliminary Trial of Carisoprodol in Multiple Sclerosis.* Practitioner, 1964. **192**: p. 540-2.

33. Aisen, M., et al., *3, 4-diaminopyridine as a treatment for amyotrophic lateral sclerosis.* Journal of the neurological sciences, 1995. **129**(1): p. 21-24.

34. Wei, X.J., K.Y. Tong, and X.L. Hu, *The responsiveness and correlation between Fugl-Meyer Assessment, Motor Status Scale, and the Action Research Arm Test in chronic stroke with upper-extremity rehabilitation robotic training.* International Journal of Rehabilitation Research, 2011. **34**(4): p. 349-356.

35. Bohannon, R.W., *Comfortable and maximum walking speed of adults aged 20-79 years: reference values and determinants.* Age Ageing, 1997. **26**(1): p. 15-9.

36. Blum, L. and N. Korner-Bitensky, *Usefulness of the Berg Balance Scale in Stroke Rehabilitation: A Systematic Review.* Physical Therapy, 2008. **88**(5): p. 559-566.

37. Holden, M.K., K.M. Gill, and M.R. Magliozzi, *Gait Assessment for Neurologically*

Impaired Patients: Standards for Outcome Assessment. Physical Therapy, 1986. **66**(10): p. 1530-1539.

38.   Simbaña, E.D.O., et al., *Review of automated systems for upper limbs functional assessment in neurorehabilitation.* IEEE Access, 2019. **7**: p. 32352-32367.

39.   Kim, W.-S., et al., *Upper extremity functional evaluation by Fugl-Meyer assessment scoring using depth-sensing camera in hemiplegic stroke patients.* PloS one, 2016. **11**(7): p. e0158640.

40.   Otten, P., J. Kim, and S.H. Son, *A framework to automate assessment of upper-limb motor function impairment: A feasibility study.* Sensors, 2015. **15**(8): p. 20097-20114.

41.   Zhang, X., et al., *A regression-based framework for quantitative assessment of muscle spasticity using combined EMG and inertial data from wearable sensors.* Frontiers in Neuroscience, 2019. **13**: p. 398.

42.   Wang, C., et al., *Quantitative Assessment of Upper-Limb Motor Function for Post-Stroke Rehabilitation Based on Motor Synergy Analysis and Multi-Modality Fusion.* IEEE Transactions on Neural Systems and Rehabilitation Engineering, 2020. **28**(4): p. 943-952.

43.   Xu, L., et al., *Feasibility study of advanced neural networks applied to sEMG-based force estimation.* Sensors, 2018. **18**(10): p. 3226.

44.   Hu, X., et al., *Quantitative evaluation of motor functional recovery process in chronic stroke patients during robot-assisted wrist training.* Journal of Electromyography and Kinesiology, 2009. **19**(4): p. 639-650.

45.   Li, X., et al., *Examination of hand muscle activation and motor unit indices derived from surface EMG in chronic stroke.* IEEE Transactions on Biomedical Engineering, 2014. **61**(12): p. 2891-2898.

46.   Campanini, I., et al., *Surface EMG in clinical assessment and neurorehabilitation: barriers limiting its use.* Frontiers in Neurology, 2020. **11**.

47.   Hu, X., et al., *The effects of post-stroke upper-limb training with an electromyography (EMG)-driven hand robot.* Journal of Electromyography and Kinesiology, 2013. **23**(5): p. 1065-1074.

48.   Nam, C., et al., *The effects of upper-limb training assisted with an electromyography-driven neuromuscular electrical stimulation robotic hand on chronic stroke.* Frontiers in neurology, 2017. **8**: p. 679.

49.   Qian, Q., et al., *Early stroke rehabilitation of the upper limb assisted with an electromyography-driven neuromuscular electrical stimulation-robotic arm.* Frontiers

in neurology, 2017. **8**: p. 447.

50.   Huang, Y., et al., *A comparison of the rehabilitation effectiveness of neuromuscular electrical stimulation robotic hand training and pure robotic hand training after stroke: A randomized controlled trial.* Biomedical Signal Processing and Control, 2020. **56**: p. 101723.

51.   Merletti, R., et al., *Surface Electromyography: Barriers Limiting Widespread Use of sEMG in Clinical Assessment and Neurorehabilitation.* Frontiers in Neurology, 2021. **12**.

52.   Langhorne, P., J. Bernhardt, and G. Kwakkel, *Stroke rehabilitation.* The Lancet, 2011. **377**(9778): p. 1693-1702.

53.   Dobkin, B.H., *Rehabilitation after stroke.* New England Journal of Medicine, 2005. **352**(16): p. 1677-1684.

54.   Harris, J.E. and J.J. Eng, *Strength training improves upper-limb function in individuals with stroke: a meta-analysis.* Stroke, 2010. **41**(1): p. 136-140.

55.   Woo, J., et al., *In patient stroke rehabilitation efficiency: influence of organization of service delivery and staff numbers.* BMC Health Services Research, 2008. **8**(1): p. 86.

56.   Norouzi-Gheidari, N., P.S. Archambault, and J. Fung, *Effects of robot-assisted therapy on stroke rehabilitation in upper limbs: systematic review and meta-analysis of the literature.* Journal of Rehabilitation Research & Development, 2012. **49**(4).

57.   Lambercy, O., et al., *Effects of a robot-assisted training of grasp and pronation/supination in chronic stroke: a pilot study.* Journal of neuroengineering and rehabilitation, 2011. **8**(1): p. 63.

58.   Timmermans, A.A., et al., *Effects of task-oriented robot training on arm function, activity, and quality of life in chronic stroke patients: a randomized controlled trial.* Journal of neuroengineering and rehabilitation, 2014. **11**(1): p. 45.

59.   Volpe, B.T., et al., *Robotics and other devices in the treatment of patients recovering from stroke.* Current neurology and neuroscience reports, 2005. **5**(6): p. 465-470.

60.   Hu, X.L., et al., *A comparison between electromyography-driven robot and passive motion device on wrist rehabilitation for chronic stroke.* Neurorehabilitation and neural repair, 2009. **23**(8): p. 837-846.

61.   Basteris, A., et al., *Training modalities in robot-mediated upper limb rehabilitation in stroke: a framework for classification based on a systematic review.* Journal of neuroengineering and rehabilitation, 2014. **11**(1): p. 111.

62.   Hu, X., et al., *The effects of electromechanical wrist robot assistive system with*

neuromuscular electrical stimulation for stroke rehabilitation. Journal of Electromyography and Kinesiology, 2012. **22**(3): p. 431-439.

63.   Coote, S., et al., *The effect of the GENTLE/s robot-mediated therapy system on arm function after stroke.* Clinical rehabilitation, 2008. **22**(5): p. 395-405.

64.   Yu, L., et al., *A remote quantitative Fugl-Meyer assessment framework for stroke patients based on wearable sensor networks.* Computer methods and programs in biomedicine, 2016. **128**: p. 100-110.

65.   Li, S., D.G. Kamper, and W.Z. Rymer, *Effects of changing wrist positions on finger flexor hypertonia in stroke survivors.* Muscle & Nerve: Official Journal of the American Association of Electrodiagnostic Medicine, 2006. **33**(2): p. 183-190.

66.   Chen, Y., et al., *A spasticity assessment method for voluntary movement using data fusion and machine learning.* Biomedical Signal Processing and Control, 2021. **65**: p. 102353.

67.   Sun, R., R. Song, and K.-y. Tong, *Complexity analysis of EMG signals for patients after stroke during robot-aided rehabilitation training using fuzzy approximate entropy.* IEEE Transactions on Neural Systems and Rehabilitation Engineering, 2013. **22**(5): p. 1013-1019.

68.   Uyanık, G.K. and N. Güler, *A study on multiple linear regression analysis.* Procedia-Social and Behavioral Sciences, 2013. **106**: p. 234-240.

69.   Tu, J.V., *Advantages and disadvantages of using artificial neural networks versus logistic regression for predicting medical outcomes.* Journal of clinical epidemiology, 1996. **49**(11): p. 1225-1231.

70.   Aung, Y.M. and A. Al-Jumaily, *Estimation of upper limb joint angle using surface EMG signal.* International Journal of Advanced Robotic Systems, 2013. **10**(10): p. 369.

71.   Yang, C., et al., *SEMG-based multifeatures and predictive model for knee-joint-angle estimation.* AIP Advances, 2019. **9**(9): p. 095042.

72.   Yang, Z. and Y. Chen, *Surface EMG-based sketching recognition using two analysis windows and gene expression programming.* Frontiers in neuroscience, 2016. **10**: p. 445.

73.   Yu, S., et al., *A Novel Quantitative Spasticity Evaluation Method Based on Surface Electromyogram Signals and Adaptive Neuro Fuzzy Inference System.* Frontiers in Neuroscience, 2020. **14**: p. 462.

74.   Cram, J.R., *Introduction to surface electromyography.* 1998: Aspen publishers.

75.   Krebs, H.a. and B. Volpe, *Rehabilitation robotics*, in *Handbook of clinical neurology*.

2013, Elsevier. p. 283-294.

76.   Page, S.J., P. Levine, and E. Hade, *Psychometric properties and administration of the wrist/hand subscales of the Fugl-Meyer Assessment in minimally impaired upper extremity hemiparesis in stroke.* Archives of physical medicine and rehabilitation, 2012. **93**(12): p. 2373-2376. e5.

77.   Qian, Q., et al., *Distal versus proximal-an investigation on different supportive strategies by robots for upper limb rehabilitation after stroke: a randomized controlled trial.* Journal of neuroengineering and rehabilitation, 2019. **16**(1): p. 64.

78.   Levin, M.F., J.A. Kleim, and S.L. Wolf, *What do motor "recovery" and "compensation" mean in patients following stroke?* Neurorehabilitation and neural repair, 2009. **23**(4): p. 313-319.

79.   Bakhti, K.K.A., et al., *Kinect-based assessment of proximal arm non-use after a stroke.* Journal of Neuroengineering and Rehabilitation, 2018. **15**(1): p. 104.

80.   Dromerick, A.W., *Clinical features of spasticity and principles of treatment*, in *Clinical evaluation and management of spasticity*. 2002, Springer. p. 13-26.

81.   Atzori, M. and H. Müller, *Fast signal feature extraction using parallel time windows.* Frontiers in neurorobotics, 2019. **13**: p. 74.

82.   Yates, R.D. and D.J. Goodman, *Probability and stochastic processes.* John Willey & Sons, 1999.

83.   Dobbin, K.K. and R.M. Simon, *Optimally splitting cases for training and testing high dimensional classifiers.* BMC Med Genomics, 2011. **4**(1): p. 31.

84.   Ramesh, V., et al., *Back propagation neural network based big data analytics for a stock market challenge.* Communications in Statistics-Theory and Methods, 2019. **48**(14): p. 3622-3642.

85.   Mostafavi, S.M., et al., *Robot-based assessment of motor and proprioceptive function identifies biomarkers for prediction of functional independence measures.* Journal of neuroengineering and rehabilitation, 2015. **12**(1): p. 105.

86.   Nazmi, N., et al., *A review of classification techniques of EMG signals during isotonic and isometric contractions.* Sensors, 2016. **16**(8): p. 1304.

87.   Tsai, A.-C., et al., *A comparison of upper-limb motion pattern recognition using EMG signals during dynamic and isometric muscle contractions.* Biomedical Signal Processing and Control, 2014. **11**: p. 17-26.

88.   Hudgins, B., P. Parker, and R.N. Scott, *A new strategy for multifunction myoelectric control.* IEEE transactions on biomedical engineering, 1993. **40**(1): p. 82-94.

89.   Hof, A.L. and J. Van den Berg, *EMG to force processing I: an electrical analogue of the Hill muscle model.* Journal of biomechanics, 1981. **14**(11): p. 747-758.

90.   Milner-Brown, H., R.B. Stein, and R. Yemm, *Changes in firing rate of human motor units during linearly changing voluntary contractions.* The Journal of physiology, 1973. **230**(2): p. 371.

91.   Dorfman, L.J., J.E. Howard, and K.C. McGill, *Motor unit firing rates and firing rate variability in the detection of neuromuscular disorders.* Electroencephalography and clinical neurophysiology, 1989. **73**(3): p. 215-224.

92.   LeCun, Y., et al. *A theoretical framework for back-propagation.* in *Proceedings of the 1988 connectionist models summer school.* 1988. CMU, Pittsburgh, Pa: Morgan Kaufmann.

93.   Karsoliya, S., *Approximating number of hidden layer neurons in multiple hidden layer BPNN architecture.* International Journal of Engineering Trends and Technology, 2012. **3**(6): p. 714-717.

94.   Evans, J.D., *Straightforward statistics for the behavioral sciences.* 1996: Thomson Brooks/Cole Publishing Co.

95.   Burden, F. and D. Winkler, *Bayesian regularization of neural networks.* Artificial neural networks, 2008: p. 23-42.

96.   Phinyomark, A., P. Phukpattaranont, and C. Limsakul, *Feature reduction and selection for EMG signal classification.* Expert systems with applications, 2012. **39**(8): p. 7420-7431.

97.   Li, Q. and Y. Huang, *An auditory-based feature extraction algorithm for robust speaker identification under mismatched conditions.* IEEE transactions on audio, speech, and language processing, 2010. **19**(6): p. 1791-1801.

98.   Xu, Y., et al., *An experimental study on speech enhancement based on deep neural networks.* IEEE Signal processing letters, 2013. **21**(1): p. 65-68.

99.   Steyerberg, E.W., et al., *Internal validation of predictive models: efficiency of some procedures for logistic regression analysis.* Journal of clinical epidemiology, 2001. **54**(8): p. 774-781.

100.   De Villiers, J. and E. Barnard, *Backpropagation neural nets with one and two hidden layers.* IEEE transactions on neural networks, 1993. **4**(1): p. 136-141.

101.   Freedman, D.A., *Statistical models: theory and practice.* 2009: cambridge university press.

102.   Boger, Z. and H. Guterman. *Knowledge extraction from artificial neural network*

models. in *1997 IEEE International Conference on Systems, Man, and Cybernetics. Computational Cybernetics and Simulation*. 1997.

103. Sheela, K.G. and S.N. Deepa, *Review on methods to fix number of hidden neurons in neural networks.* Mathematical Problems in Engineering, 2013. **2013**.

104. Mitchell, T.M., *Machine learning.* 1997.

105. Steyerberg, E.W. and F.E. Harrell Jr, *Prediction models need appropriate internal, internal-external, and external validation.* Journal of clinical epidemiology, 2016. **69**: p. 245.

106. Van Boxtel, A., *Optimal signal bandwidth for the recording of surface EMG activity of facial, jaw, oral, and neck muscles.* Psychophysiology, 2001. **38**(1): p. 22-34.

107. Sahrmann, S.A. and B.J. Norton, *The relationship of voluntary movement of spasticity in the upper motor neuron syndrome.* Annals of Neurology: Official Journal of the American Neurological Association and the Child Neurology Society, 1977. **2**(6): p. 460-465.

108. Kim, M.-S., et al., *Development and validation of a prediction model for home discharge in patients with moderate stroke: The Korean stroke cohort for functioning and rehabilitation study.* Topics in stroke rehabilitation, 2020. **27**(6): p. 453-461.

109. Scrutinio, D., et al., *Machine learning to predict mortality after rehabilitation among patients with severe stroke.* Scientific reports, 2020. **10**(1): p. 1-10.

110. Leuner, B. and E. Gould, *Structural plasticity and hippocampal function.* Annu Rev Psychol, 2010. **61**: p. 111-40, c1-3.

111. Peng, Q., et al., *Quantitative evaluations of ankle spasticity and stiffness in neurological disorders using manual spasticity evaluator.* J Rehabil Res Dev, 2011. **48**(4): p. 473-81.

112. Forghany, S., et al., *The effect of stroke on foot kinematics and the functional consequences.* Gait & Posture, 2014. **39**(4): p. 1051-1056.

113. Thilmann, A.F., S.J. Fellows, and H.F. Ross, *Biomechanical changes at the ankle joint after stroke.* Journal of Neurology, Neurosurgery &amp; Psychiatry, 1991. **54**(2): p. 134.

114. Geboers, J.F., et al., *Immediate and long-term effects of ankle-foot orthosis on muscle activity during walking: A randomized study of patients with unilateral foot drop.* Archives of Physical Medicine and Rehabilitation, 2002. **83**(2): p. 240-245.

115. Sánchez-Manchola, M., et al. *Development of a Robotic Lower-Limb Exoskeleton for Gait Rehabilitation: AGoRA Exoskeleton*. in *2018 IEEE ANDESCON*. 2018.

116. Park, Y.L., et al., *Design and control of a bio-inspired soft wearable robotic device for*

ankle-foot rehabilitation. Bioinspir Biomim, 2014. **9**(1): p. 016007.

117. Hesse, S., *Rehabilitation of Gait After Stroke: Evaluation, Principles of Therapy, Novel Treatment Approaches, and Assistive Devices.* Topics in Geriatric Rehabilitation, 2003. **19**(2).

118. Nam, C., et al., *An Exoneuromusculoskeleton for Self-Help Upper Limb Rehabilitation After Stroke.* Soft Robot, 2022. **9**(1): p. 14-35.

119. Rose, J., J.G. Gamble, and V.T. Inman, *Human Walking.* 1994: Williams & Wilkins.

120. Pirker, W. and R. Katzenschlager, *Gait disorders in adults and the elderly.* Wiener klinische Wochenschrift, 2017. **129**(3): p. 81-95.

121. Ki-Uk, K., et al. *Perceptual and biomechanical frequency response of human skin: implication for design of tactile displays.* in *First Joint Eurohaptics Conference and Symposium on Haptic Interfaces for Virtual Environment and Teleoperator Systems. World Haptics Conference.* 2005.

122. de Haart, M., et al., *Recovery of standing balance in postacute stroke patients: a rehabilitation cohort study11No commercial party having a direct financial interest in the results of the research supporting this article has or will confer a benefit upon the authors(s) or upon any organization with which the author(s) is/are associated.* Archives of Physical Medicine and Rehabilitation, 2004. **85**(6): p. 886-895.

123. Rong, W., et al., *A Neuromuscular Electrical Stimulation (NMES) and robot hybrid system for multi-joint coordinated upper limb rehabilitation after stroke.* Journal of NeuroEngineering and Rehabilitation, 2017. **14**(1): p. 34.

124. Sabut, S.K., et al., *Functional electrical stimulation of dorsiflexor muscle: effects on dorsiflexor strength, plantarflexor spasticity, and motor recovery in stroke patients.* NeuroRehabilitation, 2011. **29**(4): p. 393-400.

125. Lin, Y.-C., M.-J.J. Wang, and E.M. Wang, *The comparisons of anthropometric characteristics among four peoples in East Asia.* Applied Ergonomics, 2004. **35**(2): p. 173-178.

126. Goonetilleke, R.S., C.F. Ho, and R.H.Y. So. *Foot Anthropometry in Hong Kong.* 1997.

127. Ha, S.C.-W., D.T.-P. Fong, and K.-M. Chan, *Review of ankle inversion sprain simulators in the biomechanics laboratory.* Asia-Pacific Journal of Sports Medicine, Arthroscopy, Rehabilitation and Technology, 2015. **2**(4): p. 114-121.

128. Folstein, M.F., S.E. Folstein, and P.R. McHugh, *"Mini-mental state": a practical method for grading the cognitive state of patients for the clinician.* Journal of psychiatric research, 1975. **12**(3): p. 189-198.

129.   Duncan, P.W., et al., *Similar motor recovery of upper and lower extremities after stroke.* Stroke, 1994. **25**(6): p. 1181-8.

130.   Kadaba, M.P., H.K. Ramakrishnan, and M.E. Wootten, *Measurement of lower extremity kinematics during level walking.* J Orthop Res, 1990. **8**(3): p. 383-92.

131.   Davis, R.B., et al., *A gait analysis data collection and reduction technique.* Human Movement Science, 1991. **10**(5): p. 575-587.

132.   Razali, N.M. and Y.B. Wah, *Power comparisons of shapiro-wilk, kolmogorov-smirnov, lilliefors and anderson-darling tests.* Journal of statistical modeling and analytics, 2011. **2**(1): p. 21-33.

133.   Yeung, L.F., et al., *Randomized controlled trial of robot-assisted gait training with dorsiflexion assistance on chronic stroke patients wearing ankle-foot-orthosis.* J Neuroeng Rehabil, 2018. **15**(1): p. 51.

134.   Vieira, T.M.M., et al., *How much does the human medial gastrocnemius muscle contribute to ankle torques outside the sagittal plane?* Human Movement Science, 2013. **32**(4): p. 753-767.

135.   Nam, C., et al., *Home-based self-help telerehabilitation of the upper limb assisted by an electromyography-driven wrist/hand exoneuromusculoskeleton after stroke.* Journal of NeuroEngineering and Rehabilitation, 2021. **18**(1): p. 137.

136.   Chaparro, D., et al., *Home-based physical activity incentive and education program in subacute phase of stroke recovery (Ticaa'dom): study protocol for a randomized controlled trial.* Trials, 2018. **19**(1): p. 68.

137.   Davin, K.J. and R. Donato, *Student Collaboration and Teacher-Directed Classroom Dynamic Assessment: A Complementary Pairing.* Foreign Language Annals, 2013. **46**(1): p. 5-22.

138.   Putti, A.B., et al., *The Pedar in-shoe system: repeatability and normal pressure values.* Gait Posture, 2007. **25**(3): p. 401-5.

139.   Price, C., D. Parker, and C. Nester, *Validity and repeatability of three in-shoe pressure measurement systems.* Gait Posture, 2016. **46**: p. 69-74.

140.   Zhou, S., et al., *Pathway-specific cortico-muscular coherence in proximal-to-distal compensation during fine motor control of finger extension after stroke.* J Neural Eng, 2021. **18**(5).

141.   Allen, J.L., S.A. Kautz, and R.R. Neptune, *Step length asymmetry is representative of compensatory mechanisms used in post-stroke hemiparetic walking.* Gait Posture, 2011. **33**(4): p. 538-43.

142.   Luque-Moreno, C., et al., *Reinforced Feedback in Virtual Environment for Plantar Flexor Poststroke Spasticity Reduction and Gait Function Improvement.* Biomed Res Int, 2019. **2019**: p. 6295263.

143.   Hiengkaew, V., K. Jitaree, and P. Chaiyawat, *Minimal Detectable Changes of the Berg Balance Scale, Fugl-Meyer Assessment Scale, Timed "Up & Go" Test, Gait Speeds, and 2-Minute Walk Test in Individuals With Chronic Stroke With Different Degrees of Ankle Plantarflexor Tone.* Archives of Physical Medicine and Rehabilitation, 2012. **93**(7): p. 1201-1208.

144.   Paillard, T., *Neuromuscular or Sensory Electrical Stimulation for Reconditioning Motor Output and Postural Balance in Older Subjects?* Frontiers in Physiology, 2022. **12**.

145.   Mahmoudi, Z., et al., *The Effects of Electrical Stimulation of Lower Extremity Muscles on Balance in Stroke Patients: A Systematic Review of Literatures.* Journal of Stroke and Cerebrovascular Diseases, 2021. **30**(8): p. 105793.

146.   Yasuda, K., et al., *Haptic-based perception-empathy biofeedback system for balance rehabilitation in patients with chronic stroke: Concepts and initial feasibility study.* Gait & Posture, 2018. **62**: p. 484-489.

147.   Qian, Q., et al., *Distal versus proximal - an investigation on different supportive strategies by robots for upper limb rehabilitation after stroke: a randomized controlled trial.* Journal of NeuroEngineering and Rehabilitation, 2019. **16**(1): p. 64.

148.   Mesci, N., et al., *The effects of neuromuscular electrical stimulation on clinical improvement in hemiplegic lower extremity rehabilitation in chronic stroke: A single-blind, randomised, controlled trial.* Disability and Rehabilitation, 2009. **31**(24): p. 2047-2054.

149.   Knutson, J.S., et al., *Neuromuscular Electrical Stimulation for Motor Restoration in Hemiplegia.* Physical medicine and rehabilitation clinics of North America, 2015. **26**(4): p. 729-745.

150.   Bakhtiary, A.H. and E. Fatemy, *Does electrical stimulation reduce spasticity after stroke? A randomized controlled study.* Clinical Rehabilitation, 2008. **22**(5): p. 418-425.

151.   Allen, J.L. and R.R. Neptune, *Three-dimensional modular control of human walking.* Journal of Biomechanics, 2012. **45**(12): p. 2157-2163.

152.   Lewek, M.D., et al., *The relationship between spatiotemporal gait asymmetry and balance in individuals with chronic stroke.* Journal of applied biomechanics, 2014. **30**(1): p. 31-36.

153.   Patterson, K.K., et al., *Evaluation of gait symmetry after stroke: A comparison of*

current methods and recommendations for standardization. Gait & Posture, 2010. **31**(2): p. 241-246.

154. Hsu, A.-L., P.-F. Tang, and M.-H. Jan, *Analysis of impairments influencing gait velocity and asymmetry of hemiplegic patients after mild to moderate stroke11No commercial party having a direct financial interest in the results of the research supporting this article has or will confer a benefit upon the authors(s) or upon any organization with which the author(s) is/are associated.* Archives of Physical Medicine and Rehabilitation, 2003. **84**(8): p. 1185-1193.

155. Kim, C.M. and J.J. Eng, *Magnitude and pattern of 3D kinematic and kinetic gait profiles in persons with stroke: relationship to walking speed.* Gait & Posture, 2004. **20**(2): p. 140-146.

156. Yavuzer, G., et al., *Neuromuscular Electric Stimulation Effect on Lower-Extremity Motor Recovery and Gait Kinematics of Patients With Stroke: A Randomized Controlled Trial.* Archives of Physical Medicine and Rehabilitation, 2006. **87**(4): p. 536-540.

157. Turns, L.J., R.R. Neptune, and S.A. Kautz, *Relationships Between Muscle Activity and Anteroposterior Ground Reaction Forces in Hemiparetic Walking.* Archives of Physical Medicine and Rehabilitation, 2007. **88**(9): p. 1127-1135.

158. Jonkers, I., S. Delp, and C. Patten, *Capacity to increase walking speed is limited by impaired hip and ankle power generation in lower functioning persons post-stroke.* Gait & Posture, 2009. **29**(1): p. 129-137.

159. Hertel, J., M.R. Gay, and C.R. Denegar, *Differences in Postural Control During Single-Leg Stance Among Healthy Individuals With Different Foot Types.* J Athl Train, 2002. **37**(2): p. 129-132.

160. Yu, B., et al., *Impairments and Compensations of Static Balance and Plantar Load Distribution in Patients With Chronic Stroke: An Observational Study.* Journal of Manipulative and Physiological Therapeutics, 2021. **44**(9): p. 734-742.

161. Barcala, L., et al., *Visual Biofeedback Balance Training Using Wii Fit after Stroke: A Randomized Controlled Trial.* Journal of Physical Therapy Science, 2013. **25**(8): p. 1027-1032.

162. Squeri, V., et al. *Integrating proprioceptive assessment with proprioceptive training of stroke patients*. in *2011 IEEE International Conference on Rehabilitation Robotics*. 2011.

163. De Santis, D., et al., *Robot-Assisted Training of the Kinesthetic Sense: Enhancing Proprioception after Stroke.* Frontiers in Human Neuroscience, 2015. **8**.

164. Kleim Jeffrey, A. and A. Jones Theresa, *Principles of Experience-Dependent Neural Plasticity: Implications for Rehabilitation After Brain Damage.* Journal of Speech, Language, and Hearing Research, 2008. **51**(1): p. S225-S239.

165. Sugavanam, T., et al., *The effects and experiences of goal setting in stroke rehabilitation – a systematic review.* Disability and Rehabilitation, 2013. **35**(3): p. 177-190.

166. Burke, J.W., et al., *Optimising engagement for stroke rehabilitation using serious games.* The Visual Computer, 2009. **25**(12): p. 1085.